ARH-ST-149
Dist. Cat. UC-11

HANFORD PATHLINE CALCULATIONAL PROGRAM - THEORY, ERROR ANALYSIS AND APPLICATIONS

*D. R. Friedrichs
*C. R. Cole
R. C. Arnett

Research Department
Research and Engineering Division

*Water and Land Resources Department
Battelle, Pacific Northwest Laboratories
Richland, Washington

June 1977

ATLANTIC RICHFIELD HANFORD COMPANY
RICHLAND, WASHINGTON 99352

DISCLAIMER

ABSTRACT

The Hanford Pathline Calculational Program (HPCP) is a numerical model developed to predict the movement of fluid "particles" from one location to another within the Hanford or similar groundwater systems. As such it can be considered a simple transport model wherein only advective changes are considered. Application of the numerical HPCP to test cases for which semi-analytical results are obtainable showed that with reasonable time steps and the grid spacing requirements HPCP gives good agreement with the semi-analytical solution. The accuracy of the HPCP results is most sensitive in areas near steep or rapidly changing potential gradients and may require finer grid spacing in those areas than for the groundwater system as a whole.

Initial applications of HPCP to the Hanford groundwater flow regime show that significant differences (improvements) in the predictions of fluid "particle" movement are obtainable with the pathline approach (changing groundwater potential or water table surface) as opposed to the streamline approach (unchanging potential or water table surface) used in past Hanford groundwater analyses.

This report documents capability developed for estimating groundwater travel times from the Hanford high-level waste areas to the Columbia River at different water table levels. As such it satisfies in part committments made in ERDA 1538 "Final Environmental Statement - Waste Management Operations, Hanford Reservation Richland, Washington." Volume 1, page X-18.

CONTENTS

FIGURES

TABLES

ACKNOWLEDGMENTS

The authors wish to express their gratitude to R. A. Deju and R. E. Gephart of Rockwell Hanford Operations who were involved in initiating the study. The review and comments of R. G. Baca, A. G. Law, K. R. Price, and R. D. Fox of Rockwell are gratefully acknowledged.

The authors are especially indebted to H. P. Foote of Battelle and R. W. Nelson of Boeing Computer Services who Developed the analytic test cases used to test the HPCP.

The authors would also like to thank S. R. Gano who provided editorial assistance and K. A. Kiser, I. B. Daer and M. A. Eierdam who typed the drafts and final document.

HANFORD PATHLINE CALCULATIONAL PROGRAM - THEORY, ERROR ANALYSIS AND APPLICATIONS

INTRODUCTION

Since 1944 the Hanford Reservation, located in south-central Washington, has been a site for radioactive waste storage, reactor development, and chemical separation facilities for the production and purification of plutonium.[1] The radioactive waste storage and chemical separation facilities are located within the high-level radioactive waste areas labeled 200 W and 200 E on Figure 1. The plutonium production reactors (only one is currently operational) are located along the Columbia River in the 100 Areas. Laboratory facilities (300 Area), an important reactor testing facility called the Fast Flux Test Facility (FFTF), and several commercial nuclear power reactors to be operated by the Washington Public Power Supply System (WPPSS) are also located on the Reservation. Waste management practices have involved the release of some radionuclides to near-surface disposal sites with a consequent contamination of some aquifers underlying the Reservation. An extensive groundwater monitoring program conducted over the years at Hanford indicates that the movement of radioactive contaminants through the groundwater flow system toward biosphere uptake points (primarily the Columbia River) is rather limited.[2] Nevertheless, a program is being conducted to assure continued isolation of such contaminants from the biosphere both now and in the future.

From September 3, 1967 to July 1, 1977, the Atlantic Richfield Hanford Company (ARHCO) operated the waste management activities at Hanford under contract to the U.S. Atomic Energy Commission and its successor, the U.S. Energy Research and Development Administration (ERDA). Subsequent to that time the Rockwell Hanford Operations of the Atomics International Division of Rockwell International assumed responsibility. In support of the waste management activities, a Groundwater Management program has been instituted to achieve the following management goals:

(1) identify potential ways in which ground water can come in contact with high-level radioactive wastes;

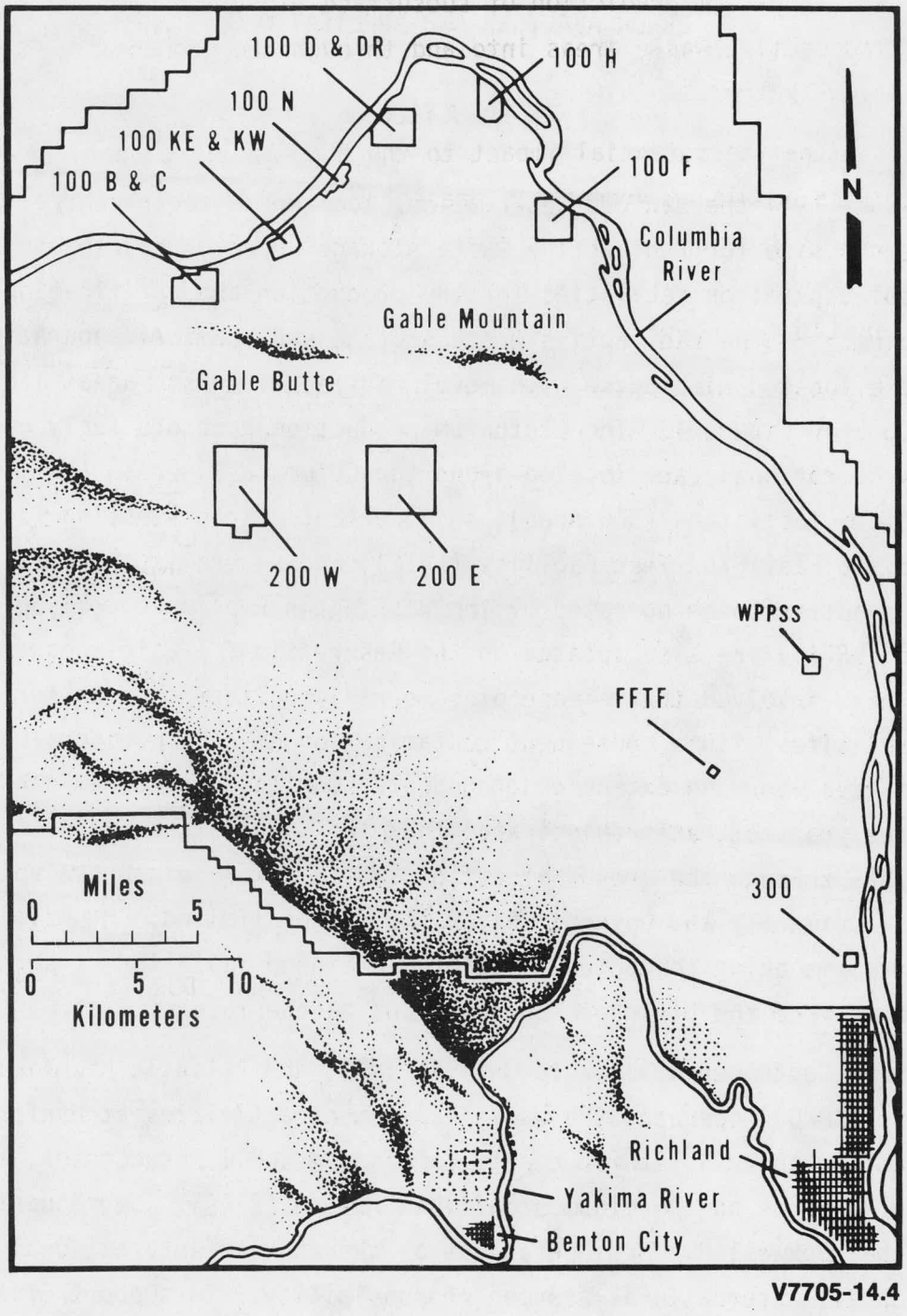

FIGURE 1

HANFORD AREA MAP

(2) assess data gathering and computer modeling capabilities needed for long-term prediction of subsurface migration from high-level radioactive waste areas into and through the groundwater flow system;

(3) examine the potential impact to the high-level radioactive waste areas resulting from past, present, and projected activities at Hanford, potentially hazardous incidents, and potential or existing water use activities adjacent to or within the Hanford Reservation; and

(4) improve the management of the Hanford flow regime and identify methods of controlling accidental contaminant releases and preventing the contaminant from reaching the biosphere.

The steps in the technical evaluation and management of the Hanford groundwater system are depicted in Figure 2. System characterization is

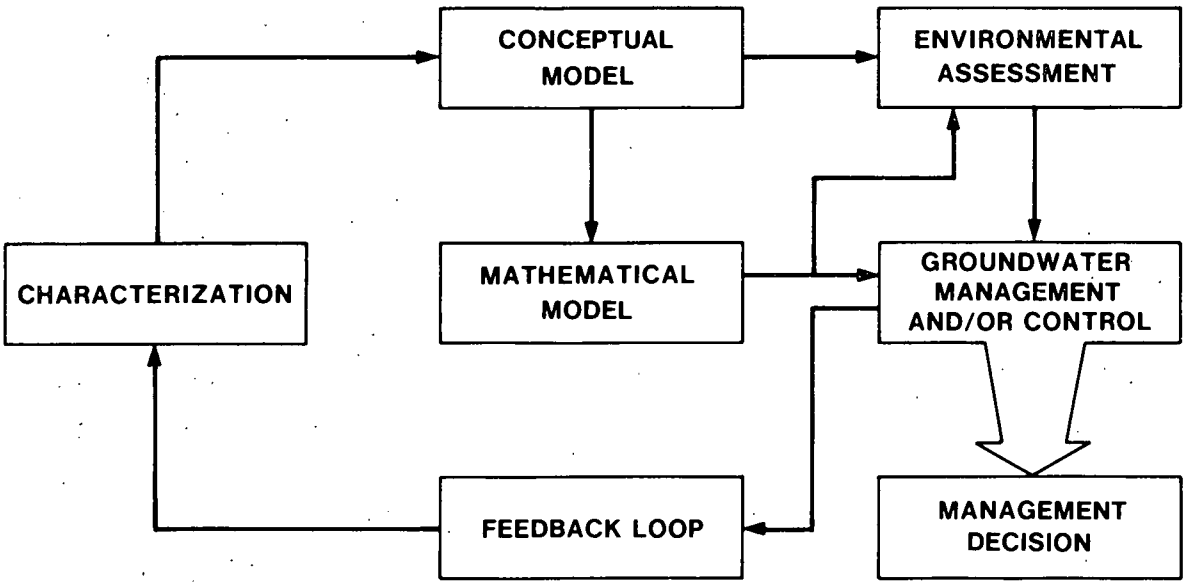

FIGURE 2

HANFORD GROUNDWATER SYSTEM
TECHNICAL EVALUATION AND MANAGEMENT PROCEDURE

established through data collection and interpretation which lead to a conceptual model of the system. Such a conceptual model may be used directly for environmental assessment and management decision purposes or it may first be translated into mathmatical form amenable to analytical or computer solution methods.

The current Hanford conceptual model is presented in detail elsewhere together with a description of a set of mathematical models and associated computer codes applicable to Hanford.[3] Briefly, a complete predictive model treatment of groundwater contaminant migration at Hanford consists of adequately simulating:

(1) the groundwater flow field, and

(2) the contaminant transport within the flow field.

PURPOSE AND SCOPE

This report presents the theory, error analysis and preliminary applications of a computer model designed to predict the movement of fluid "particles" from one location to another within the Hanford or similar groundwater system. This model is known as the Hanford Pathline Calculational Program (HPCP).

The HPCP Model can be considered a simple transport model wherein only advective changes are considered.[3] Rather than predict the movement of the entire contaminant plume as would a complete transport model, the HPCP model predicts the paths (ignoring dispersion) and travel times (ignoring sorption, chemical reaction, and radioactive decay) from a contaminant source to the groundwater discharge area, in this case the Columbia River. It is used as a rapid, economical, and convenient means of obtaining a preliminary estimate of the contaminant travel direction, travel distance, and travel times under different water table (or potential) conditions.

The contaminant travel time from source to discharge predicted by the HPCP Model is usually conservative in the sense that lateral dispersion,

chemical reaction, and decay are ignored. Ignoring longitudinal dispersion will cause the HPCP model to yield nonconservative results which would under predict the actual rate of contaminant movement. On the other hand, longitudinal dispersivities will also tend to spread the contamination and reduce its concentration at discharge.

STREAMLINES VS. PATHLINES

For a given two-dimensional representation of a groundwater potential surface, the groundwater velocity vector is perpendicular to the potential contour lines and points in the direction of lower hydraulic potential (water table elevation). Therefore, for any instantaneous groundwater potential distribution (potentiometric map in two dimensions) flow directions can be drawn illustrating the direction of groundwater movement at a specific point in time. A line which is everywhere tangent to velocity vectors is an instantaneous streamline. Such a streamline is only the path of a fluid particle as long as the potential surfaces do not change with time or is at "steady state."

A changing water table configuration or transient condition will cause that parcel of water to move always parallel to consecutive instantaneous streamlines. Its resulting path through the flow system is called a pathline. A pathline of a fluid particle is therefore the locus or path of a fluid particle through the flow system as time passes. Instantaneous streamlines in the general transient case are theoretical abstractions of limited practical usefulness only as indicators of direction of movement.

The use of streamlines is not new in the analysis of groundwater systems and some of their applications can be found in previous documents.[4,5] A pathline, the true path of a particle in a transient or changing flowfield, can only be determined if a tagged particle can be followed. Calculation of pathlines in a changing flowfield is relatively complex. Pathlines are normally determined only in closed-form mathematical solutions. The use of a series of discrete potential surfaces (water tables) is not easily adapted to pathline calculations. However, computerized groundwater flow models permit development of closely spaced consistent surfaces so that pathline calculations can be performed. The accuracy of the predicted potential surfaces, and consequently the accuracy of the pathline calculations is dependent upon the precision of the source terms and boundary conditions.

When an analytical function of a time varying potential function is available, a set of differential equations for pathlines can be solved via a numerical integration technique. In the past, many attempts were made to fit analytical functions to the Hanford groundwater potentials. However, the complexity of this system has prevented the successful application of satisfactory analytical functions.

In the Final Environmental Statement, Hanford Waste Management Operations, ERDA-1538,[5] the groundwater travel pathways and travel times from the 200 Areas to the Columbia River (Figure 1) were estimated with the streamline approach using the 1972 water table surface. In a comment letter on the draft of ERDA-1538 the following question was asked:

> "What estimated travel times are predicted for other water table conditions (i.e., higher or lower water table levels)?

The response in the final version of ERDA-1538 stated that

> "predictive capabilities are being developed for estimating travel times at higher and lower water table levels."

The capability described in this document is in partial fulfillment of the committment made in ERDA-1538.

A numerical technique must be used to predict pathlines both at discrete time steps and intervals when, as is the case with the Hanford system, all that is available is the predicted potential distribution over a fixed set of nodes. Consequently a numerical technique was developed for the HPCP to predict pathlines within the Hanford site.

Since the HPCP numerical method and the analytical method of computing pathlines are different and since the HPCP method for Hanford pathlines is more approximate, a study was required to identify and quantify possible errors due strictly to calculational technique. This study was designed to examine possible calculational errors as well as to determine the degree of improvement in contaminant movement predictions that a practical pathline approach might yield over the streamline approach.

ANALYTICAL VS. NUMERICAL SOLUTION METHODS

Since an analytical function of the time varying potential function was not available for the Hanford saturated groundwater system, it was necessary to produce a simplified comparison test function which would have characteristics similiar to those of the Hanford site. It was particularly important to produce potentials and potential gradients comparable with those from the 200 East Area to the Columbia River as this section represents one of the shortest travel times and distances from radioactive waste disposal sites to the river. Pathlines generated using this function could then be compared with the results produced by the numerical technique used in the HPCP.

Two test cases were employed in this study using the same analytical function[6] with different values for the parameters. Extensive testing was performed using both test cases to determine the comparative accuracy of the numerical method and to establish parameter values which would most closely represent the section of the Hanford Reservation from the 200 East Area to the river.

ANALYTICAL POTENTIAL FUNCTION TEST CASES

The analytical expression for the potential $\phi(x,y)$ for the test system shown in Figure 3 is given by:

$$\phi = H_o - U_o X + \frac{U_o (r_o)^2 X}{(x^2 + y^2)} - \frac{H_o}{\ln(\frac{R}{r_o})} \ln\left(\frac{\sqrt{x^2 + y^2}}{r_o}\right)$$

$$- \sum_{j=1}^{j=N} \frac{M_j}{2\pi} \ln \sqrt{\frac{(x - x_j)^2 + (y - y_j)^2}{(x_j^2 + y_j^2)}}, \quad N = 3; \qquad (1)$$

where

	Units
ϕ is the groundwater potential	FL/f
H_o is the head in the reservoir with center at x=0, y=0	L

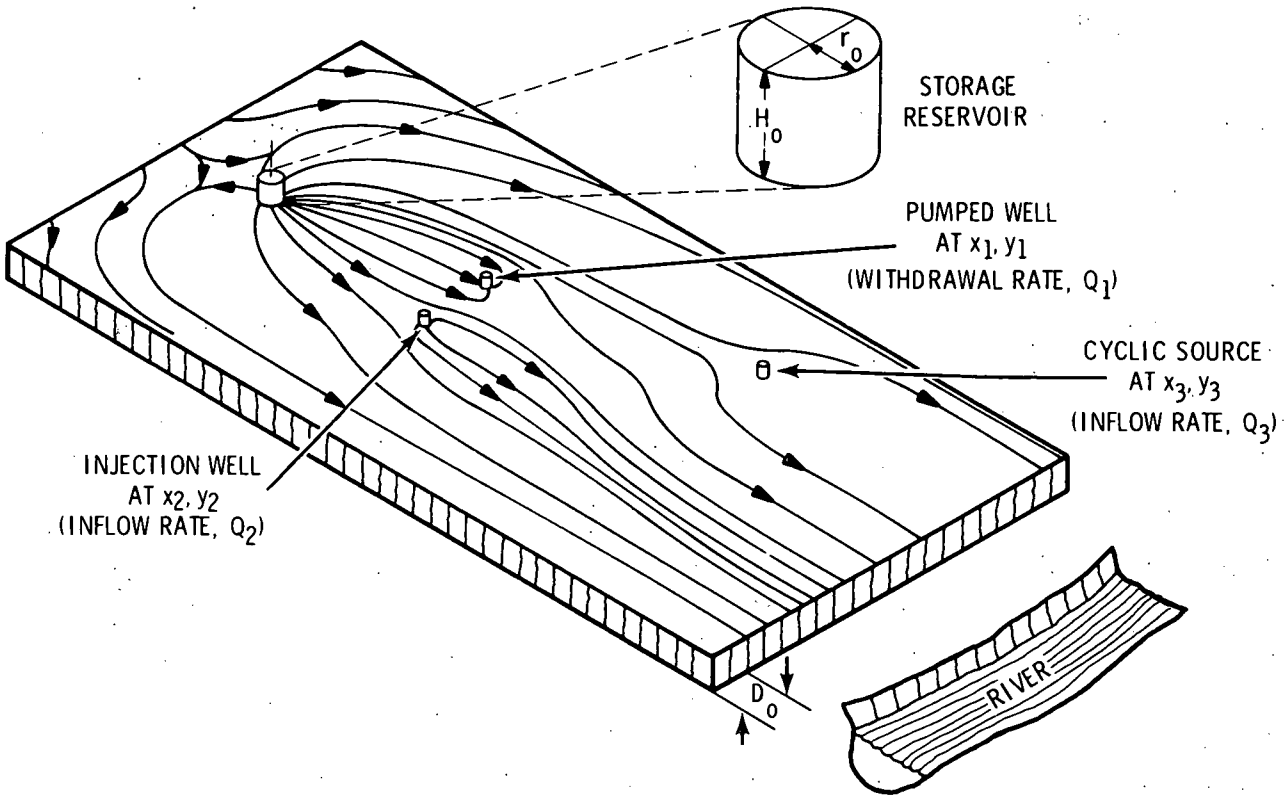

FIGURE 3

GROUNDWATER PATHLINE TEST SYSTEM

U_o is gradient of the uniform lateral flow	L/L
r_o is the radius of the cylindrical reservoir	L
R is large radial distance to the remote outer boundary	L
$M_j = \frac{Q_j}{K_o D_o}$, strength of the j^{th} pumped or injection well	$L^3/T/L^2/T$
X_j is the x coordinate of the center of the j^{th} pumped or injection well	L
y_j is the y coordinate of the center of the j^{th} pumped or injection well	L

j as an index denotes the particular well described
i.e. j = 1,2,3 — none
K_o is the uniform hydraulic conductivity value — $L^3/T/L^2$
D_o is the uniform strata thickness — L

Two flow rates at the injection/pumped wells which permit analytical solutions of the potential are the serpentine and cyclic options.

(1) Time dependent (Serpentive) well inflow (-) or well outflow (+) rate — L^3/T

Serpentine Option:

$$Q_j = Q_j(t) = Q_{o\,j} + \frac{2(Q_{m,j} - Q_{oj})\left[\frac{t}{t_{n,j}} + 1\right]}{\left[\frac{t}{t_{n,j}} + 1\right]^2 + 1}$$

(2) cyclic inflow or outflow rate — L^3/T

Cyclic Option:

$Q_j = f_j$ if $f_j > 0$

and

$Q_j = 0$ if $f_j \leq 0$

where

$$f_j = Q_{o,j} \sin \pi\left[\left(\frac{t - t_{o,j}}{t_{m,j} - t_{o,j}}\right)\right]$$

Note: ϕ has singularities at $x = 0$, $y = 0$ and at all $x = x_j$, $y = y_j$.

Except at the singularity points Equation 1 can be evaluated at discrete intervals to give ϕ values such as those produced from a numerical groundwater flow model. Thus, a consistent comparison between the analytical and numerical pathline solution methods can be obtained.

Test Case 1

The first test (Figure 4) used the following Input Parameters:

H_o = 30 ft
U_o = 0.002 ft/ft
r_o = 300 ft
R = 15840 ft
K_o = 150 ft/day
D_o = 100 ft

j = 1 (Serpentine opt)	j = 2 (Serpentine opt)	j = 3 (Cyclic opt)
x_1 = 4920 ft	x_2 = 4920 ft	x_3 = 10,520 ft
y_1 = 692 ft	y_2 = -692 ft	y_3 = 2,020 ft
$r_{o,1}$ = 200 ft	$r_{o,2}$ = 200 ft	$Q_{o,3}$ = 548,000 ft^3/day
$Q_{o,1}$ = -13,700 ft^3/day	$Q_{o,2}$ = -13,700 ft^3/day	$t_{o,3}$ = 1,440 days
$Q_{m,1}$ = -658,000 ft^3/day	$Q_{m,2}$ = 685,000 ft^3/day	$t_{m,3}$ = 5,040 days
$t_{n,1}$ = 360 days	$t_{n,2}$ = 360 days	

Test Case 2

The second test case (Figure 5) used the following Input Parameters:

H_o = 30 ft
U_o = 0.0005 ft/ft
r_o = 300 ft
R = 70,000 ft
K_o = 500 ft/day
D_o = 100 ft

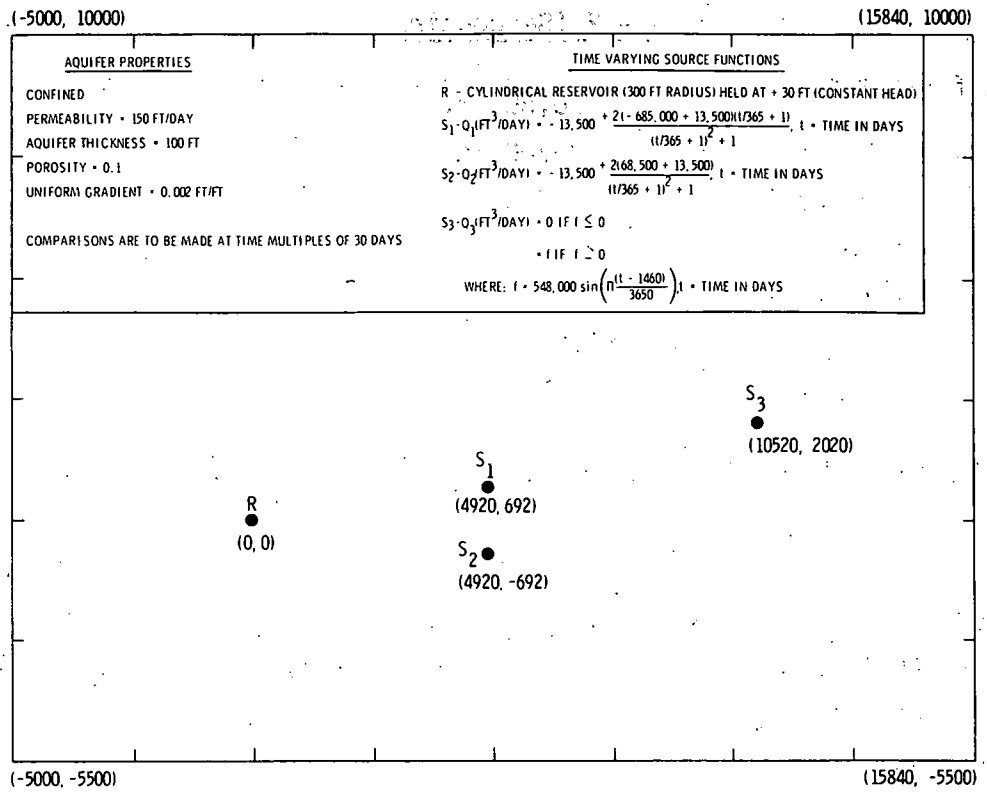

FIGURE 4

ANALYTICAL TEST CASE NUMBER 1

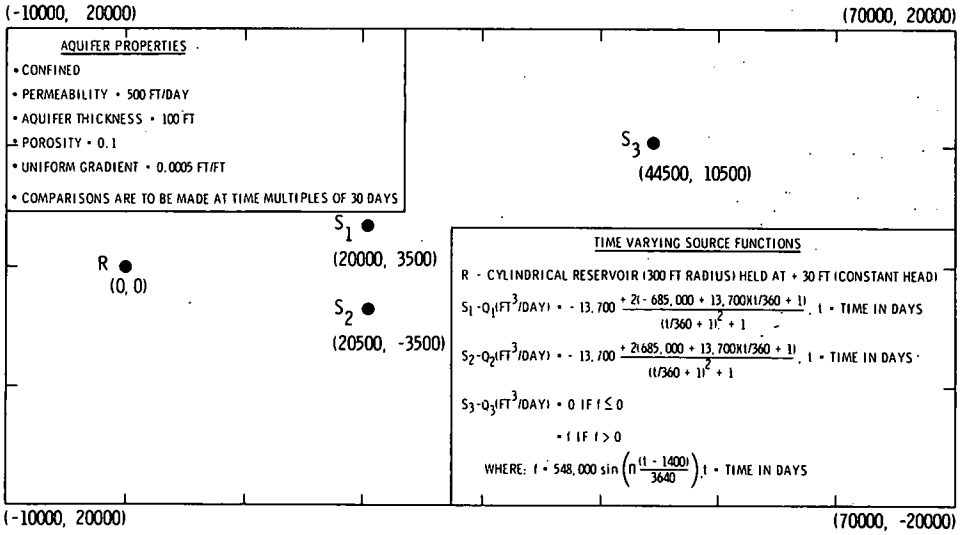

FIGURE 5

ANALYTICAL TEST CASE NUMBER 2

j = 1 (Serpentine opt)	j = 2 (Serpentine opt)	j = 3 (Cyclic opt)
x_1 = 20,500 ft	x_2 = 20,500 ft	x_3 = 44,500 ft
y_1 = 3,500 ft	y_2 = 3,500 ft	y_3 = 10,500 ft
$r_{o,1}$ = 200 ft	$r_{o,2}$ = 200 ft	$Q_{o,3}$ = 548,000 ft^3/day
$Q_{o,1}$ = -13,500 ft^3/day	$Q_{o,2}$ = -13,500 ft	$t_{o,3}$ = 1,460 days
$Q_{m,1}$ = -685,000 ft^3/day	$Q_{m,2}$ = 68,500 ft	$t_{m,3}$ = 5,110 days
$t_{n,1}$ = 365 days	$t_{n,2}$ = 365 days	

The individual velocity components are defined as:

$$\frac{dx}{dt} = -\frac{K}{\sigma}\frac{\partial \Phi}{\partial x} \qquad (2)$$

$$\frac{dy}{dt} = -\frac{K}{\sigma}\frac{\partial \Phi}{\partial y} \qquad (3)$$

where:

$\frac{dx}{dt}$ = velocity in x direction

$\frac{dy}{dt}$ = velocity in y direction

K = hydraulic conductivity

σ = effective porosity

$\frac{\partial \phi}{\partial x}$ = x gradient component calculated from analytic function

$\frac{\partial \phi}{\partial y}$ = y gradient component calculated from analytic function

A fourth order Runge Kutta method was used to integrate the above differential equations for the reference pathlines.

HANFORD PATHLINE CALCULATIONAL PROGRAM

Extensive testing was conducted on the HPCP to determine its limitations and sensitivity to input and control parameters. This included a systematic error analysis and sensitivity studies using the two analytical test surfaces described earlier. The results of these studies show that the HPCP can accurately reproduce the results of an analytical surface which closely resembles that of the Hanford unconfined aquifer. At the same time, the HPCP is sensitive in regions of high gradient or rapidly changing gradient. However, this is not a limitation if these regions can be defined and the potential distribution determined in such regions with a reduced grid spacing.

HPCP Numerical Methods

The HPCP can operate in two modes: 1) calculation of accumulated time along a pathline with a constant step size, or 2) calculation of accumulated distance along a pathline with a constant time increment. Both modes may be operated so that pathlines travel either down or up gradient.

The equations used by the Program are:

1) Constant Step Size

$$T = - \sum_{i=1}^{N} \frac{s}{v_i} \tag{4}$$

Since velocity = v_i =

$$\left(\frac{\left.\frac{\partial \Phi}{\partial s}\right|_i \; K_i}{\sigma_i} \right) \tag{5}$$

Equation (4) can be written

$$T = -s \sum_{i=1}^{N} \left(\frac{\sigma_i}{\left.\frac{\partial \Phi}{\partial s}\right|_i \; K_i} \right) \tag{6}$$

where:

T = total time
s = constant step size along pathline
σ_i = effective porosity at position i
K_i = hydraulic conductivity at position i

$\left.\frac{\partial \Phi}{\partial s}\right|_i$ = hydraulic gradient at position i.

2) Constant Time Increment

$$S = - \sum_{i=1}^{N} v_i \, t \tag{7}$$

Substituting Equation (5) into Equation (7) gives

$$S = -t \sum_{i=1}^{N} \left(\frac{\left.\frac{\partial \Phi}{\partial s}\right|_i \; K_i}{\sigma_i} \right) \tag{8}$$

where:

S = total distance along pathline
t = constant time increment.

The new coordinates are calculated as follows

$$x_{i+1} = x_i - s_i \; \frac{\left.\frac{\partial \Phi}{\partial x}\right|_i}{\left.\frac{\partial \Phi}{\partial s}\right|_i} \tag{9}$$

$$y_{i+1} = y_i - s_i \; \frac{\left.\frac{\partial \Phi}{\partial y}\right|_i}{\left.\frac{\partial \Phi}{\partial s}\right|_i} \tag{10}$$

where:

$\frac{\partial \Phi}{\partial x}_i$ = x gradient component at position i

$\frac{\partial \Phi}{\partial y}_i$ = y gradient component at position i

x_i = x coordinate at position i

y_i = y coordinate at position i

s_i = i^{th} step length along pathline.

If the program uses time plane interpolation, all of the data in two time planes are used and the above values are interpolated between these time planes.

Data Storage and Retrieval

Two data calculational methods were used by the HPCP Model. The first method calculated gradient components at each node for each calculated potential surface and stored these values in a data base for each time plane. The second method simply stored the potential values for each calculated potential surface, and the HPCP used the actual potential values to calculate the gradient components at each step as a function of the potential surface. While the results of thorough testing determined that the second method was more accurate, both methods are discussed in Appendix A.

SENSITIVITY ANALYSIS

The two test surfaces used to study the HPCP are shown in Figures 4 and 5. The test cases used on each test surface required reference pathlines or streamlines to be used as a standard for comparing the results of the HPCP. These reference lines were generated using the fourth order Runge Kutta method as mentioned earlier. All of the cases for each surface with the same pathline or streamline starting time (T_o) use the same set of reference lines. When T_o is changed a new set of reference lines is generated.

The HPCP uses a set of potential surfaces generated at even increments of time. These will be referred to as time planes. Also the coordinate positions along a pathline or streamline are generated at even increments of time, referred to as time steps. As an example, if the potential surfaces had been created at 30 day time planes and pathlines were being generated using 10 day time steps, the pathline would take three time steps using one potential surface then on the fourth step would retrieve and use a new potential surface.

The following analysis shows the effects of changing the data storage and calculational methods and various calculational parameters used by the HPCP. The resulting pathlines or streamlines produced by the HPCP after each change were then compared with the corresponding reference lines to determine the effect of the change upon the accuracy of the HPCP solution.

TEST SURFACE 1

The HPCP used stored gradients and did not interpolate between time planes on the cases run using Test Surface 1 shown in Figure 4. The gradient magnitude for this surface at time T_o = 0 days is shown in Figure 6. Figure 7 shows the line numbers assigned to each of the 15 pathlines or streamlines referred to in the following text for Test Surface 1.

Several cases, using 15 pathlines per case, were run starting at different times and traveling both up and down gradient. These cases used 10-day time steps and tick marks were plotted every 300 days. Thirty-day time planes were used by the HPCP for a period of 25 years.

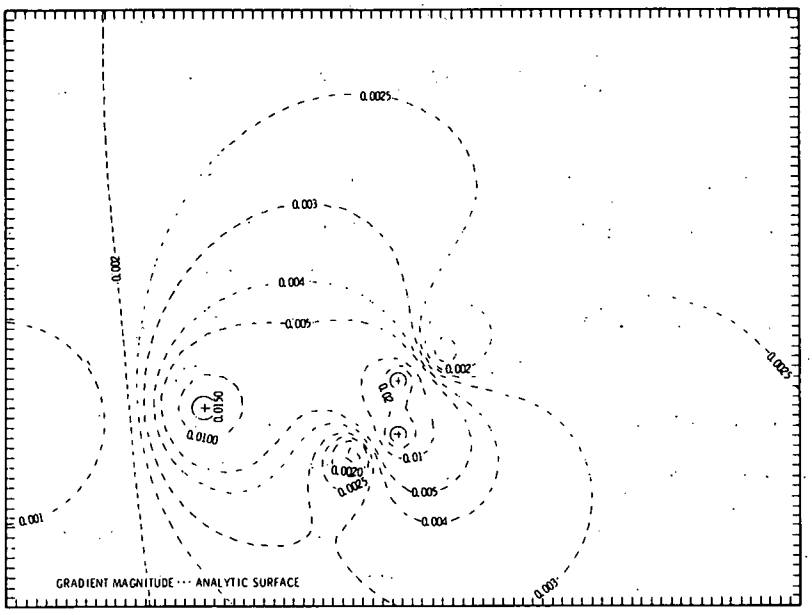

FIGURE 6

TEST SURFACE 1 GRADIENT MAGNITUDE
AT TIME T_o = 0 DAYS

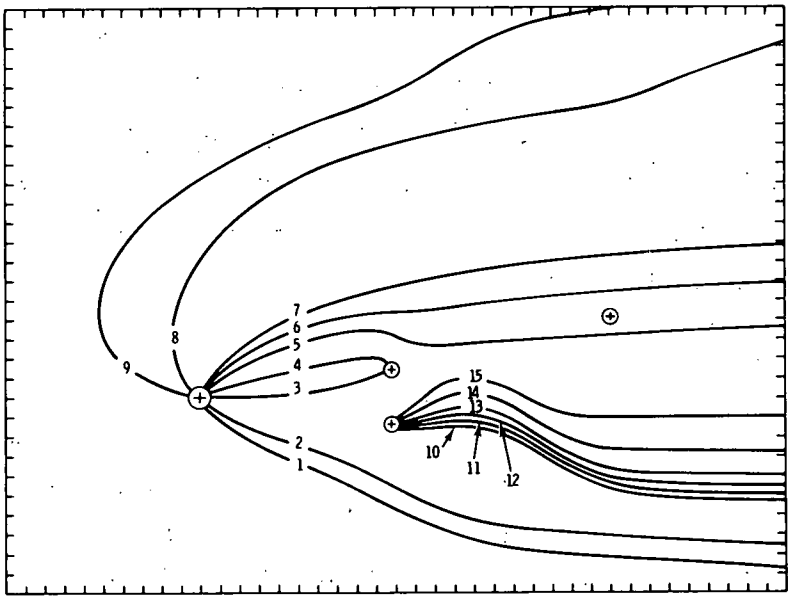

FIGURE 7

LINE NUMBERS FOR TEST SURFACE 1

Figures 8, 9 and 10 show three down gradient cases for 0, 900 and 1800 days, respectively. Up gradient cases were run in conjunction with all of the down gradient cases. The accuracy of the HPCP numerical method may be judged by comparing the semi-analytical results which are also presented in the figures. The starting x,y positions and times were taken from the reference pathline and the HPCP calculated the numerical pathline solution. A considerable improvement was noted for each up gradient case when compared to its corresponding down gradient case. Figure 11 shows a typical up gradient case which can be compared with Figure 10. It can be seen from these two figures that the pathlines calculated by the HPCP compare better with the reference pathlines in the up gradient direction (Figure 11) than they do in the down gradient direction (Figure 10). All of the up gradient cases showed the same improvements, and this was found to be true in all cases where a pathline or streamline started some distance away from an area of steep or rapidly changing gradient.

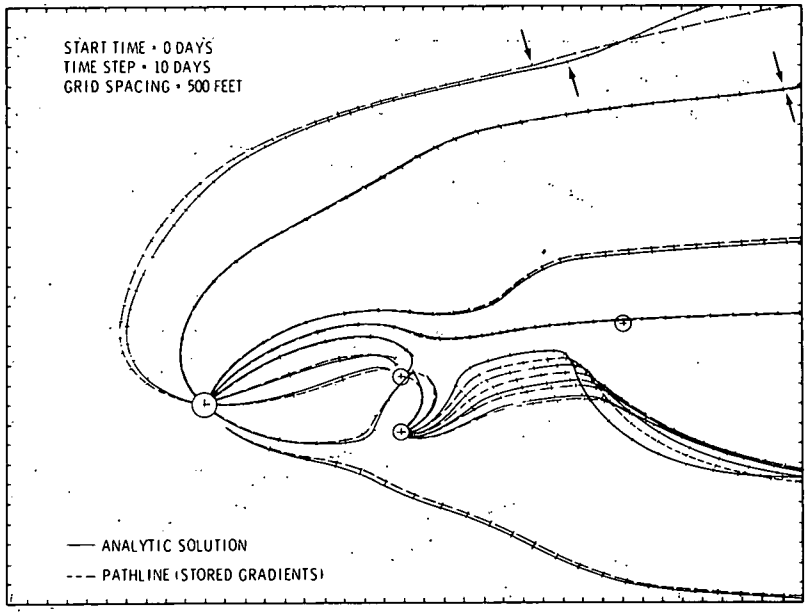

FIGURE 8

TEST SURFACE 1, DOWN GRADIENT PATHLINES
STARTING AT T_o = 0 DAYS

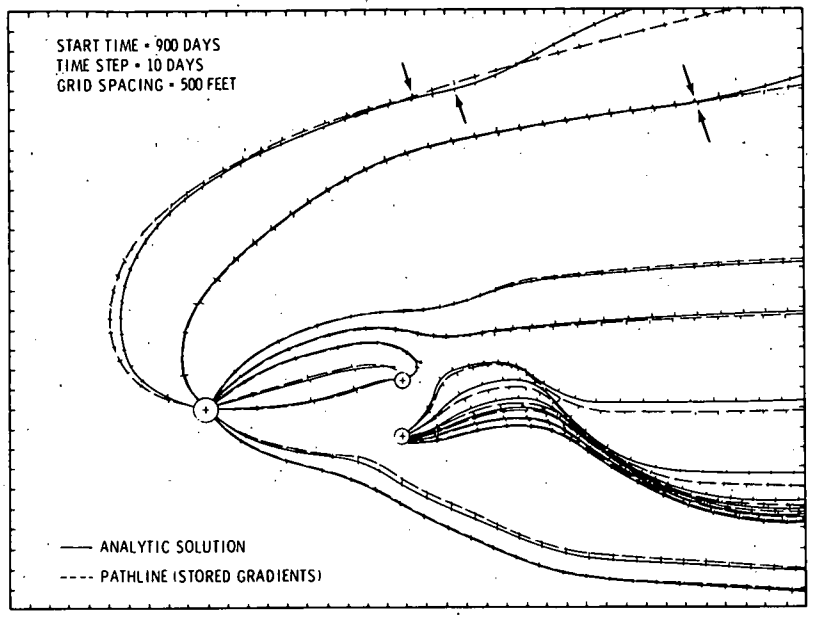

FIGURE 9

TEST SURFACE 1, DOWN GRADIENT PATHLINES STARTING AT T_o = 900 DAYS

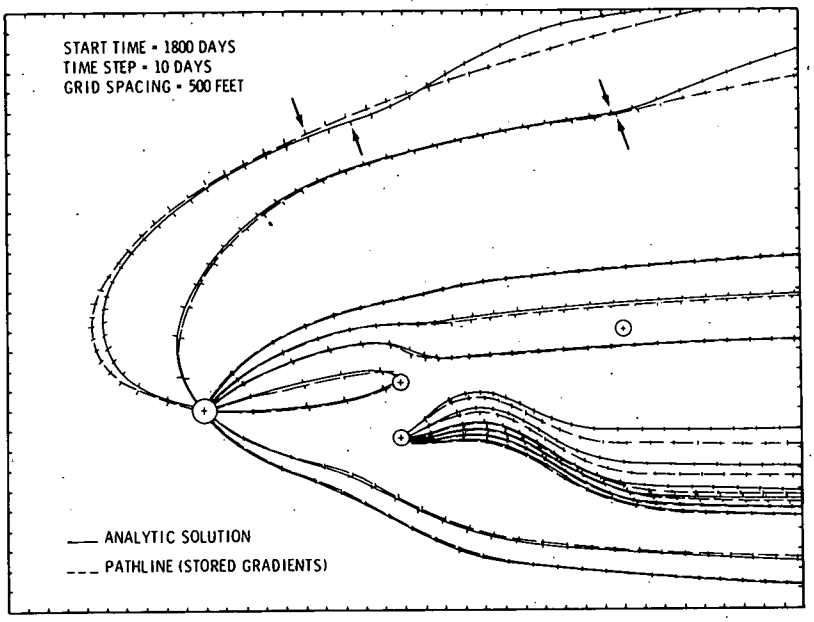

FIGURE 10

TEST SURFACE 1, DOWN GRADIENT PATHLINES STARTING AT T_o = 1800 DAYS

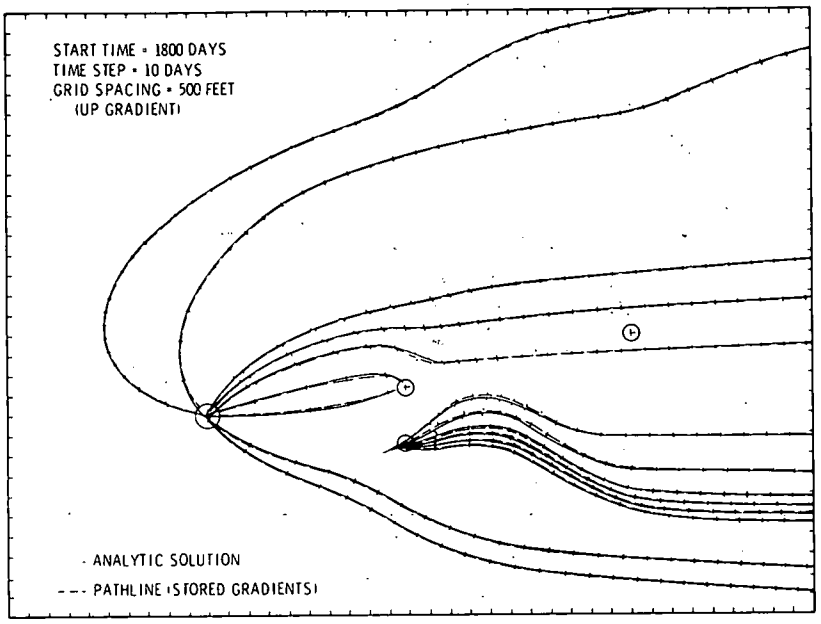

FIGURE 11

TEST SURFACE 1, UP GRADIENT PATHLINE STARTING AT T_o = 1800 DAYS

All of these cases also show that as the intensity of the cyclic source decreases over time, the pathlines near this source begin to more accurately agree with those of the analytical solution. In addition, it was found that the results agreed more closely if the starting coordinates of the pathlines were more than one nodal spacing away from a source or sink.

The arrows on Pathlines 8 and 9 shown in Figures 8, 9 and 10 indicate when pathlines have exceeded the stored time planes and have become streamlines.

In all the cases, the actual times calculated by the analytical solution and the HPCP agreed very well. This can be seen by the 300-day tick marks shown on the pathlines in Figures 8 through 11.

Several additional cases, using 15 streamlines per case, were run to show the effects of grid spacing. Figures 12 and 13 show the down and up gradient cases, respectively, using a 500-ft grid spacing for time T_o = 0 days.

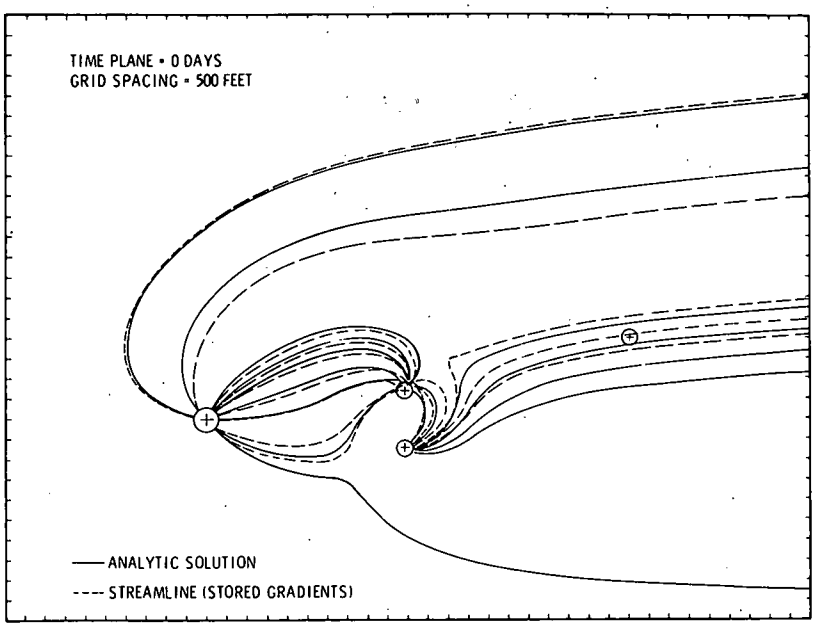

FIGURE 12

TEST SURFACE 1, DOWN GRADIENT STREAMLINES ON A LARGE GRID

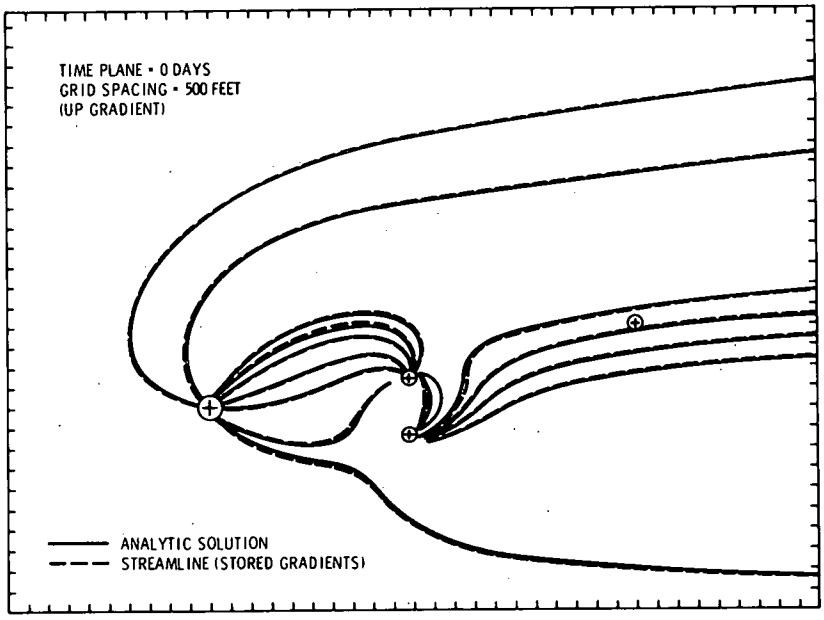

FIGURE 13

TEST SURFACE 1, UP GRADIENT STREAMLINES ON A LARGE GRID

Figures 14 and 15 show the down and up gradient cases, respectively, using a 250-ft grid spacing for the same time period (T_o = 0 days). There is a marked improvement in the cases with the smaller grid spacing; however, it should be noted that the streamlines for both the up gradient 500-ft case (Figure 13) and the up gradient 250-ft case (Figure 15) agree with the reference streamlines until the streamlines approach areas of rapidly changing gradient. When this happens the smaller grid produces more accurate results.

When comparing the two down gradient cases (Figures 12 and 14), the streamlines produced using the 250-ft grid spacing (Figure 14) show a much closer agreement with the reference streamlines than those produced using the 500-ft grid (Figure 12). This is because the streamlines are started very close to the sources where the higher gradients occur. The larger grid spacing is unable to produce accurate enough gradient components required at the start to keep the streamlines on the true path.

Finally, the gradient magnitude of Test Surface 1 (Figure 6) can be compared with the September 1973 Hanford gradient magnitude shown in Figure 16. This comparison shows that the average magnitude of gradient of Test Surface 1 is considerably larger than that of Hanford.

TEST SURFACE 2

Some of the results using Test Surface 1 indicate that greater accuracy could be obtained by lowering the gradient magnitude to more closely represent that of the Hanford Reservation. The uniform gradient was therefore decreased from 0.002 ft/ft to 0.0005 ft/ft in Test Surface 2 shown in Figure 5. Figure 17 shows the gradient magnitude of the analytical surface about halfway into the studied time period, while Figure 18 shows the gradient magnitude of the pathline surface for the same time period. Comparing Figures 17 and 18 with Figure 16 shows that the gradient magnitudes of Test Surface 2 more closely resemble those of Hanford than do Test Surface 1.

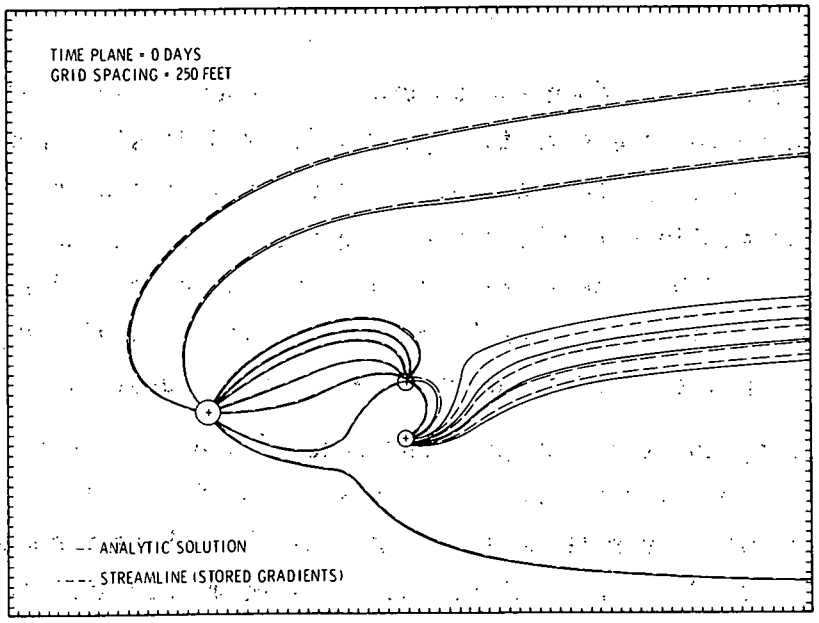

FIGURE 14

TEST SURFACE 1, DOWN GRADIENT STREAMLINES ON A SMALL GRID

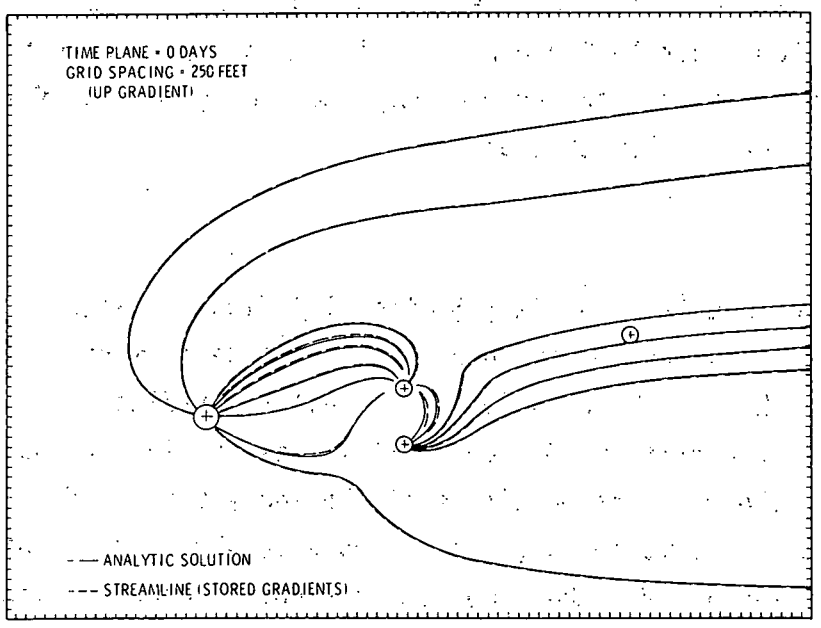

FIGURE 15

TEST SURFACE 1, UP GRADIENT STREAMLINES ON A SMALL GRID

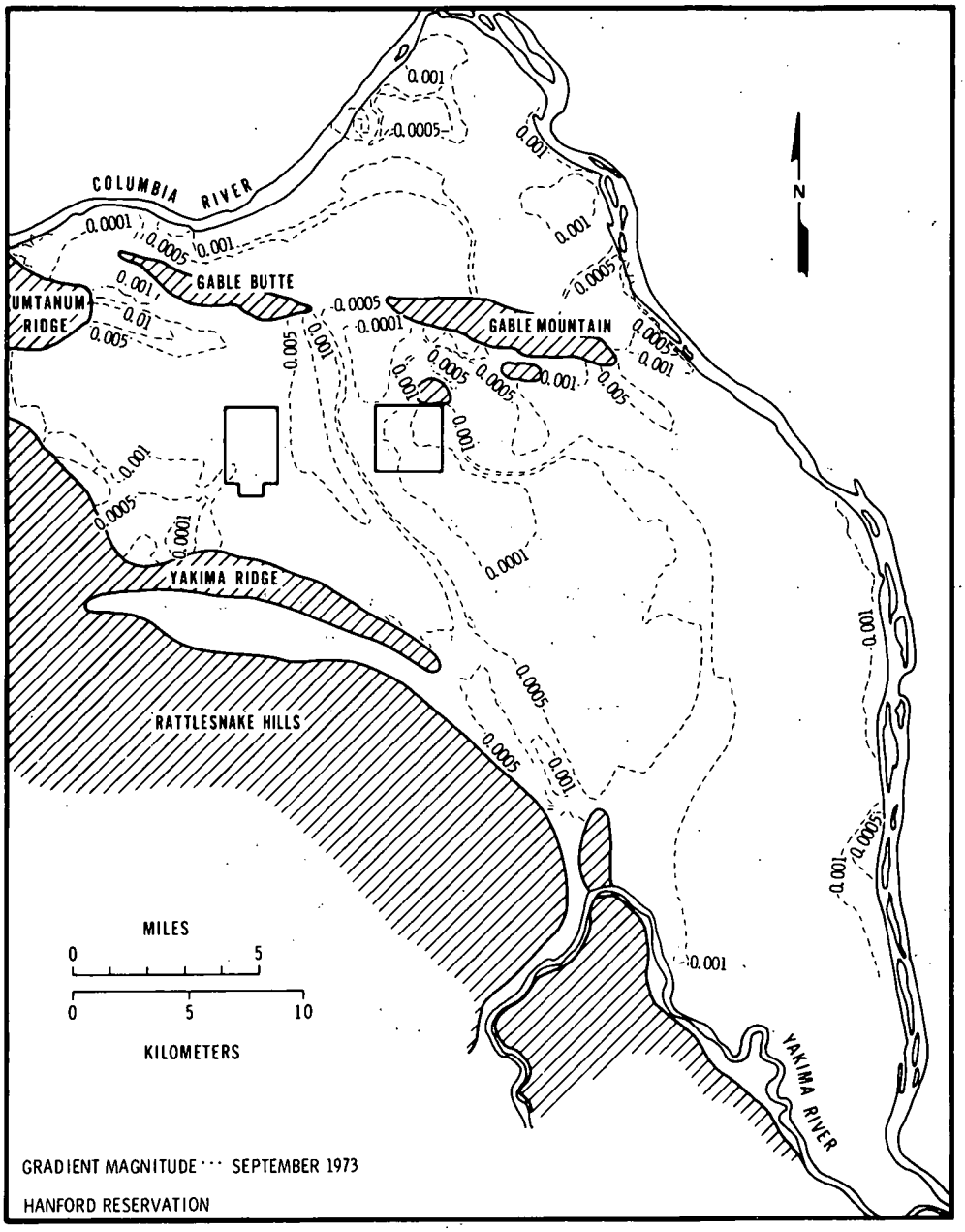

FIGURE 16

HANFORD SITE GROUNDWATER GRADIENT MAGNITUDE FOR SEPTEMBER 1973

Nine pathlines or streamlines were used to study Test Surface 2. The line numbers assigned and referred to in the following text for this test surface are given in Figure 19.

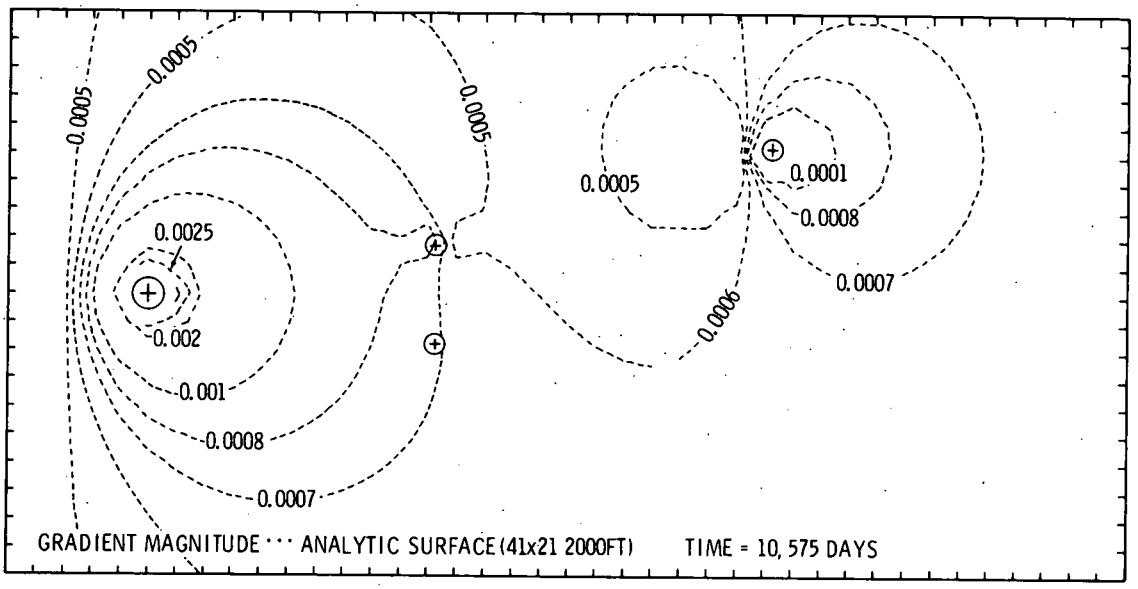

FIGURE 17

TEST SURFACE 2 GRADIENT MAGNITUDE OF THE ANALYTICAL SURFACE AT TIME T_o = 10,575 DAYS

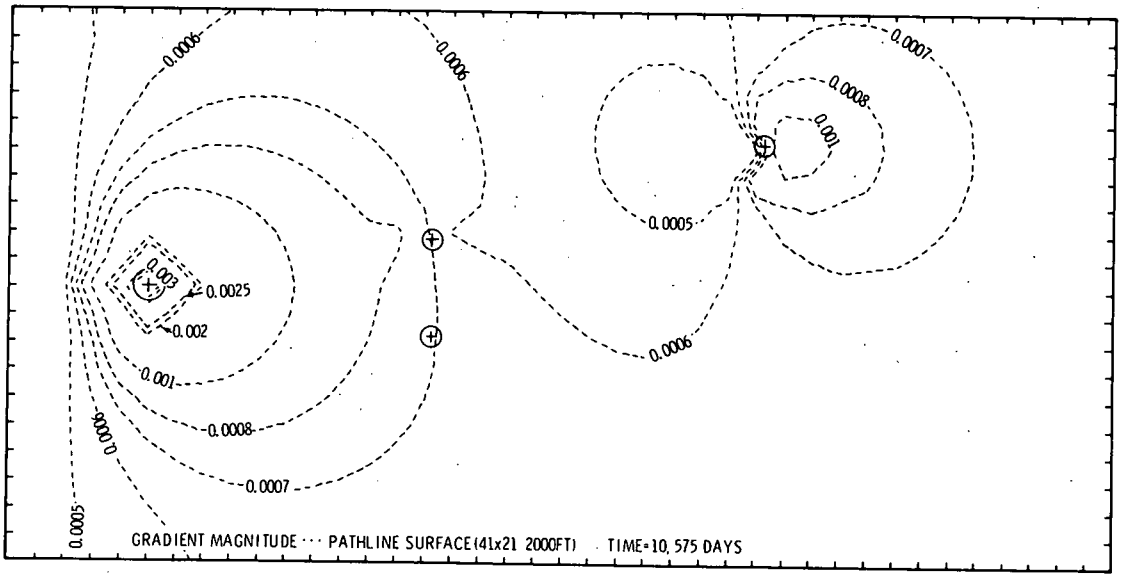

FIGURE 18

TEST SURFACE 2 GRADIENT MAGNITUDES OF THE STORED POTENTIALS USED BY THE HPCP AT TIME T_o = 10,575 DAYS

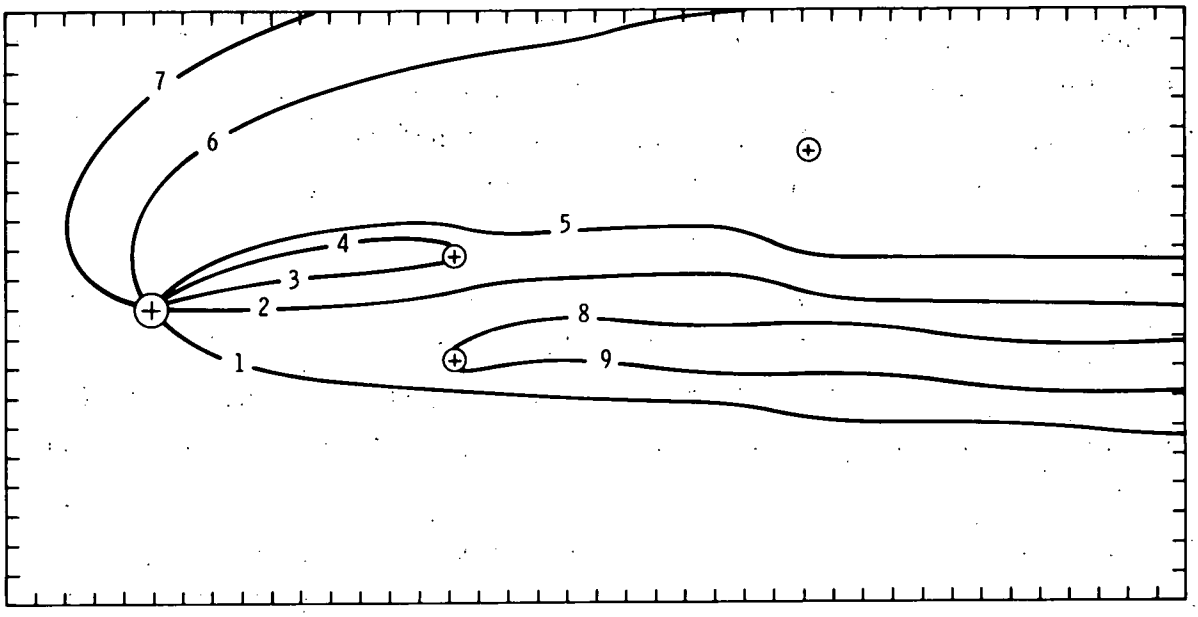

FIGURE 19

LINE NUMBERS FOR TEST SURFACE 2

As with Test Surface 1, several cases were studied using Test Surface 2. Pathlines and streamlines were run starting at different times and traveling both up and down gradient. The up gradient cases starting away from the sources showed the same improvement in accuracy over the corresponding down gradient as those run on Test Surface 1; these figures have been excluded to permit presentation of a more detailed examination on the less accurate and more meaningful down gradient cases.

Two different data algorithms were used on Test Surface 2 by the HPCP:

(1) stored gradients in the master data file and

(2) stored potentials in the master data file. It was believed that more accurate gradient components could be obtained by calculating the actual gradient at each step from the four surrounding potential values in the matrix rather than by interpolating the gradient components from the stored gradients. This belief was verified as will be shown. In addition, data storage was reduced by half; initial data setup time was reduced by one third; and pathline calculational time was reduced by about 10%.

The potential surfaces for the HPCP Model were generated at 30-day time periods for a total period of 53 years, 9 months (644 time planes). In addition to using either stored gradients or stored potentials, the HPCP also used two different calculational techniques: one interpolated between time planes and the other did not.

The cases shown in Figures 20 and 21 used stored gradients for the pathline analysis with 10-day pathline time steps. These and all of the following cases have tick marks plotted every 300 days along the pathlines. For Figure 20, interpolation between time planes was not used, whereas time plane interpolation was used for Figure 21.

For Figures 22 and 23 stored potentials were used and from these the gradient components for the pathline analysis were calculated. Ten-day time steps were also used by the Pathlines with these cases. Figure 22 did not interpolate between time planes, while time plane interpolation was used in Figure 23. Comparing the interpolated cases with the corresponding non-interpolated cases shows no appreciable difference. This is probably due to the rather small potential surface time plane spacing (30 days). It would be expected that interpolation between time planes would prove to be an advantage in cases where the time planes were further apart. However, because normal Hanford groundwater modeling procedures for predicting changing potential distributions usually involves 30-day time planes, the value of using periods between time planes longer than 30 days was not investigated as part of this study.

When comparing the two cases using stored gradients (Figures 20 and 21) with the two cases using stored potentials (Figures 22 and 23) improvements can be seen in almost all of the pathlines using the stored potential procedure.

Since the previous studies showed that the stored potential method was more accurate than the stored gradient method, additional test cases were run to show the effects of changing the pathline time step. The cases illustrated in Figures 24 and 25 use stored potentials with the pathline step

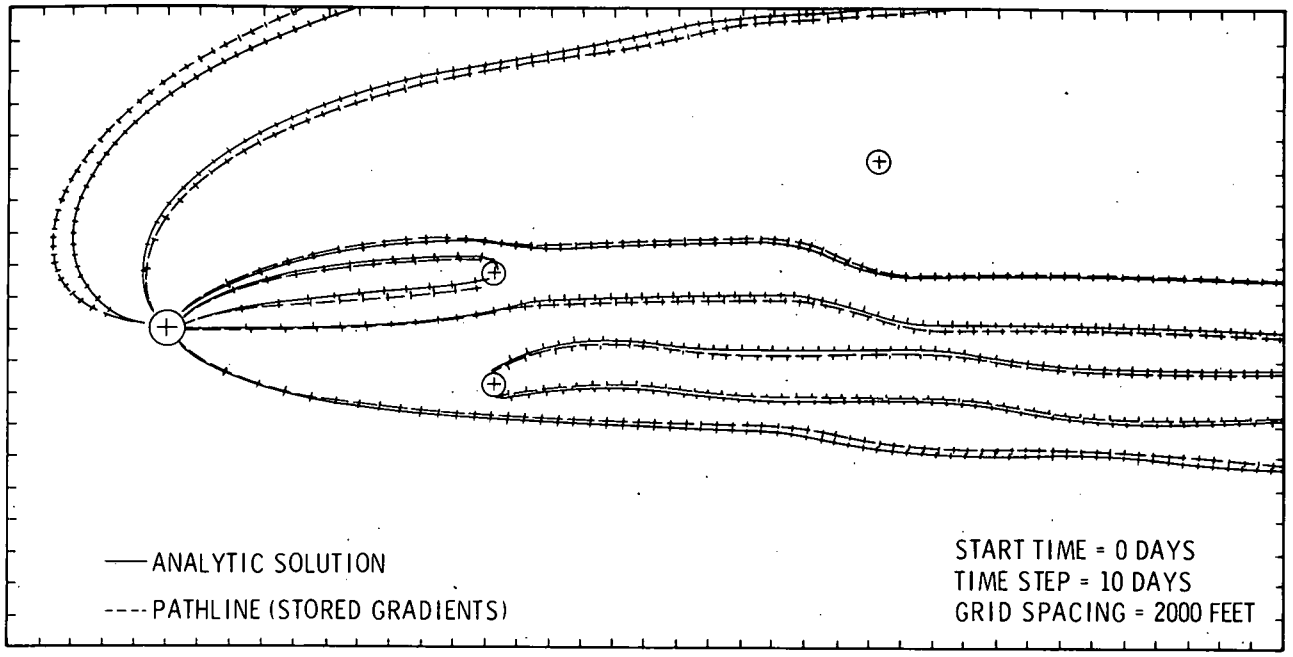

FIGURE 20

TEST SURFACE 2, DOWN GRADIENT PATHLINES USING STORED GRADIENTS AND NOT INTERPOLATING BETWEEN TIME PLANES

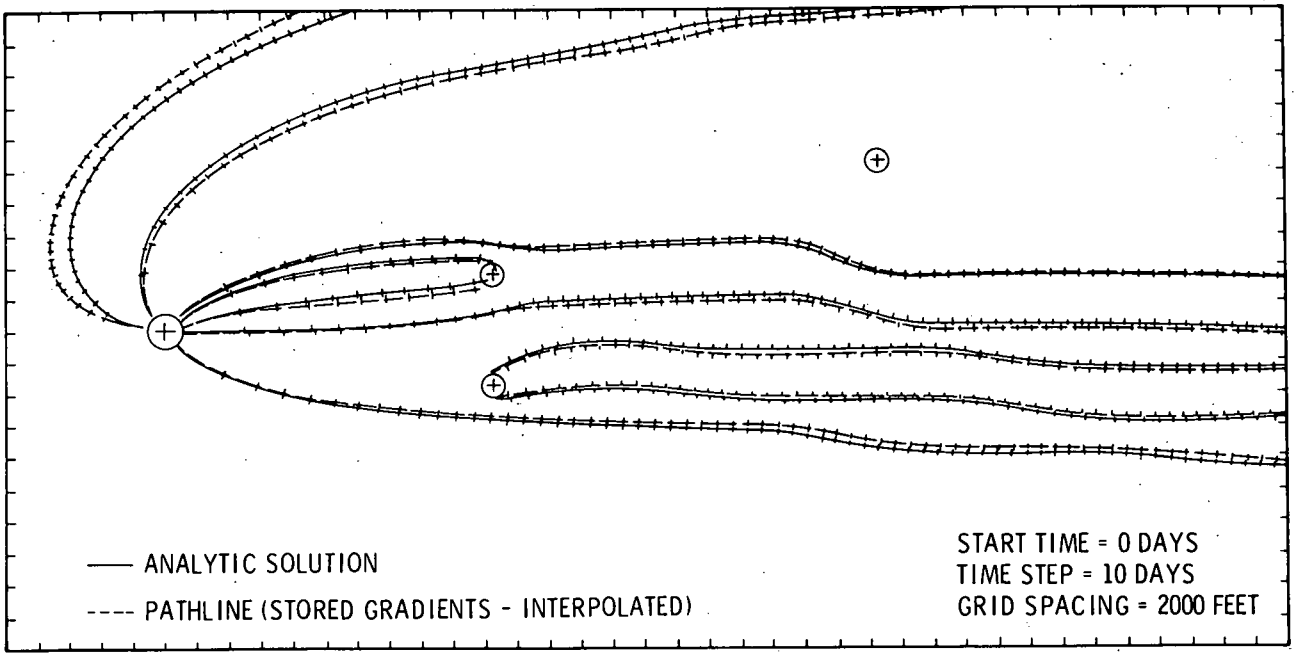

FIGURE 21

TEST SURFACE 2, DOWN GRADIENT PATHLINES USING STORED GRADIENTS AND INTERPOLATING BETWEEN TIME PLANES

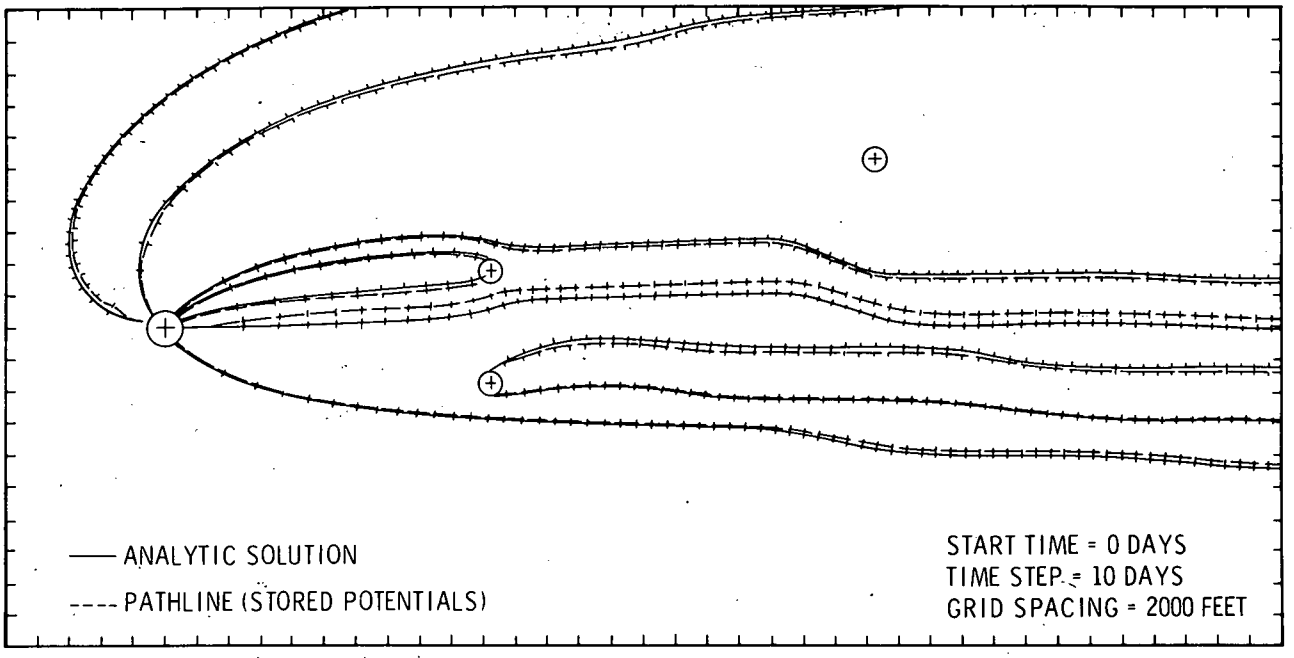

FIGURE 22

TEST SURFACE 2, DOWN GRADIENT PATHLINES USING STORED POTENTIALS AND NOT INTERPOLATING BETWEEN TIME PLANES

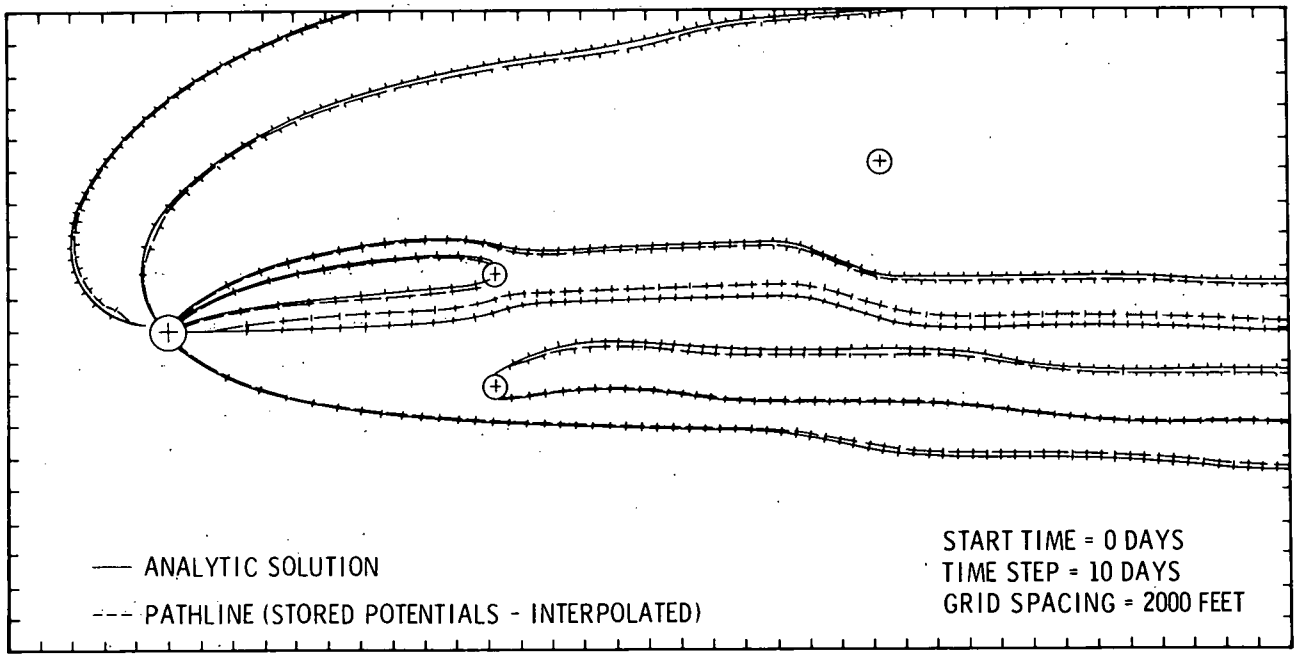

FIGURE 23

TEST SURFACE 2, DOWN GRADIENT PATHLINES USING STORED POTENTIAL AND INTERPOLATING BETWEEN TIME PLANES

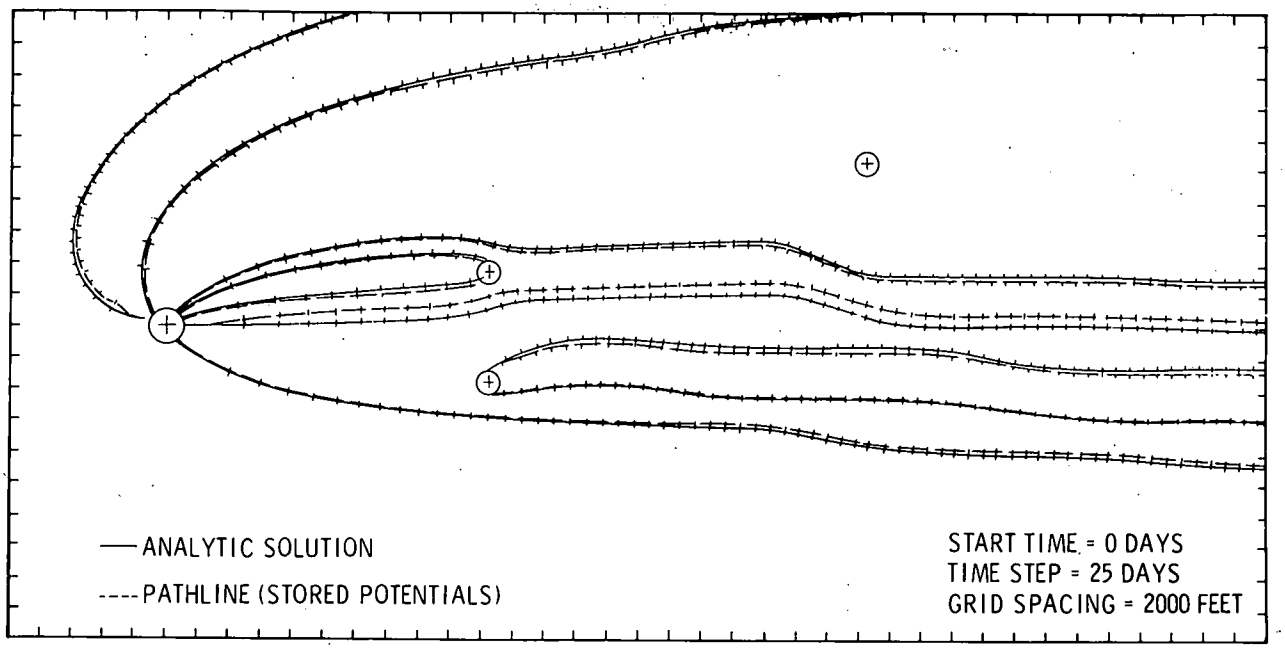

FIGURE 24

TEST SURFACE 2, DOWN GRADIENT PATHLINES USING 25 DAY TIME STEPS.
TIME PLANE INTERPOLATION IS NOT USED

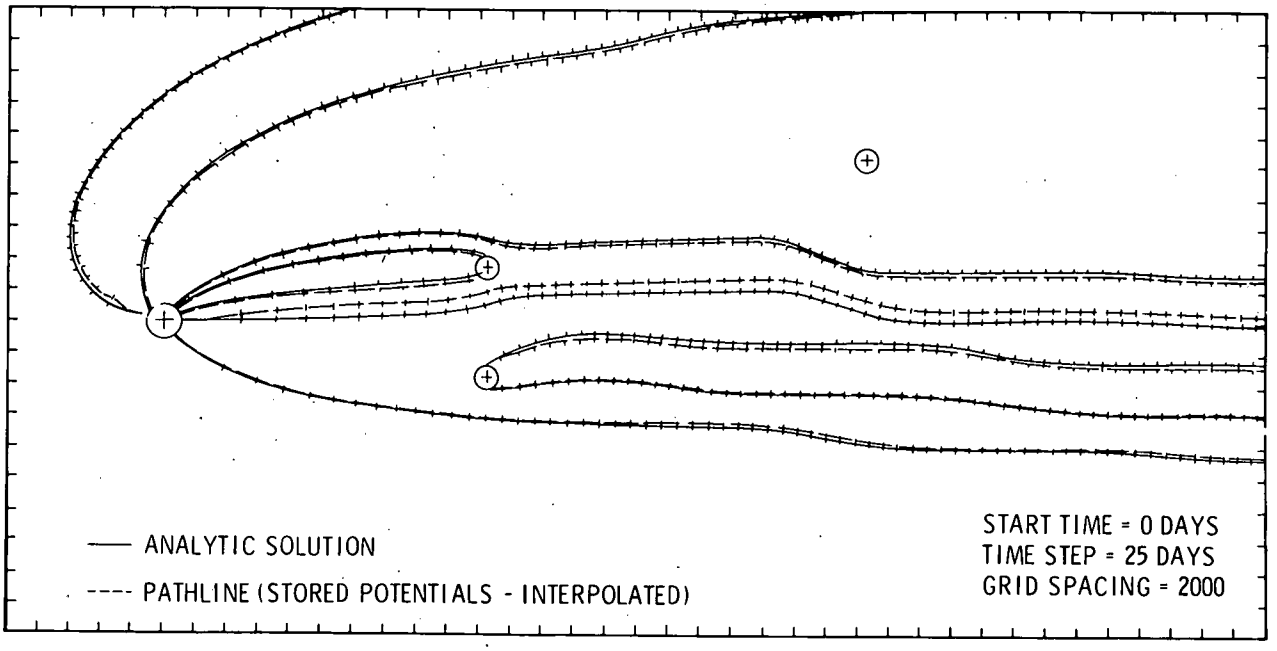

FIGURE 25

TEST SURFACE 2, DOWN GRADIENT PATHLINES USING 25 DAY TIME STEPS.
TIME PLANE INTERPOLATION IS USED.

size increased from 10 days to 25 days. Figure 24 used no interpolation between time planes and can be compared with Figure 22. Figure 25 used time interpolation and can be compared with Figure 23. No appreciable difference in accuracy could be found by increasing the pathline step size, but the cases using the 25-day steps took less calculational time than those using 10-day pathline steps.

Several cases were also run for Test Surface 2 using streamlines to show the effects of grid spacing. The time plane selected for the cases in Figures 26 and 27 was at 10,560 days because the cyclic source was almost at maximum strength and showed the most dramatic effects of reduced grid spacing.

Since the previous studies showed that stored potentials produced more accurate results than stored gradients, the stored potential method was used on both of the cases in Figures 26 and 27. A 2000-ft grid spacing was used for Figure 26, with a much smaller grid spacing (500 ft) used for Figure 27. These tests again demonstrated more accurate results with reduced grid spacing. By examining Figure 26 it can be seen that the major streamline inaccuracies again occur near the areas where sources or sinks are located. By reducing the grid spacing, Figure 27 shows that the streamlines calculated by the HPCP agree much better with the reference streamlines than those of Figure 26.

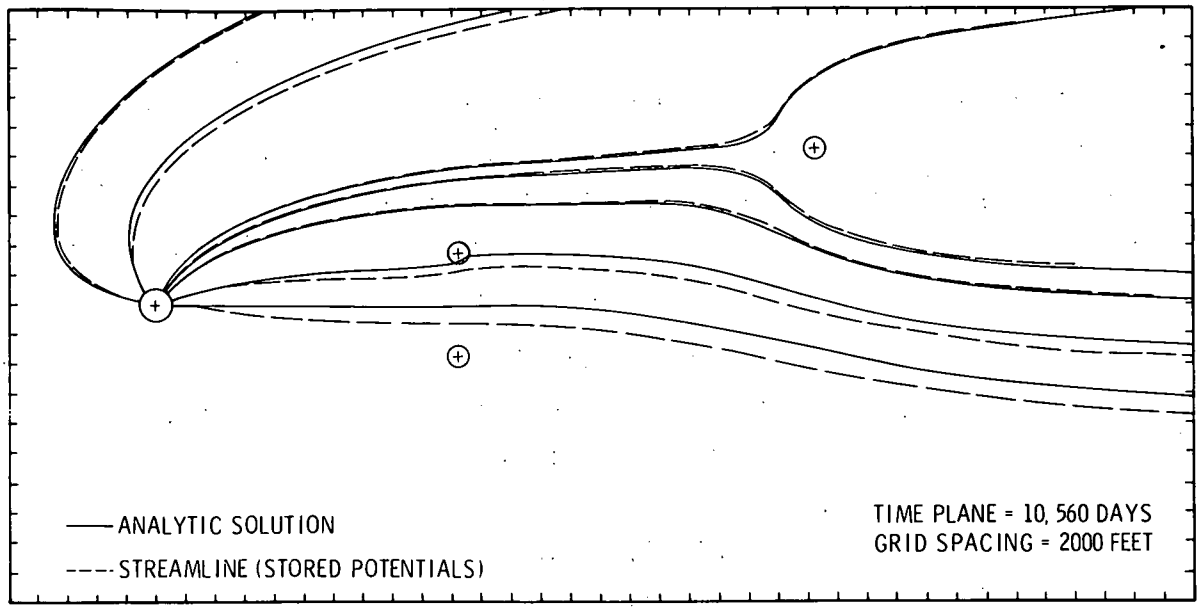

FIGURE 26

TEST SURFACE 2, DOWN GRADIENT STREAMLINES USING STORED POTENTIALS ON A LARGE GRID

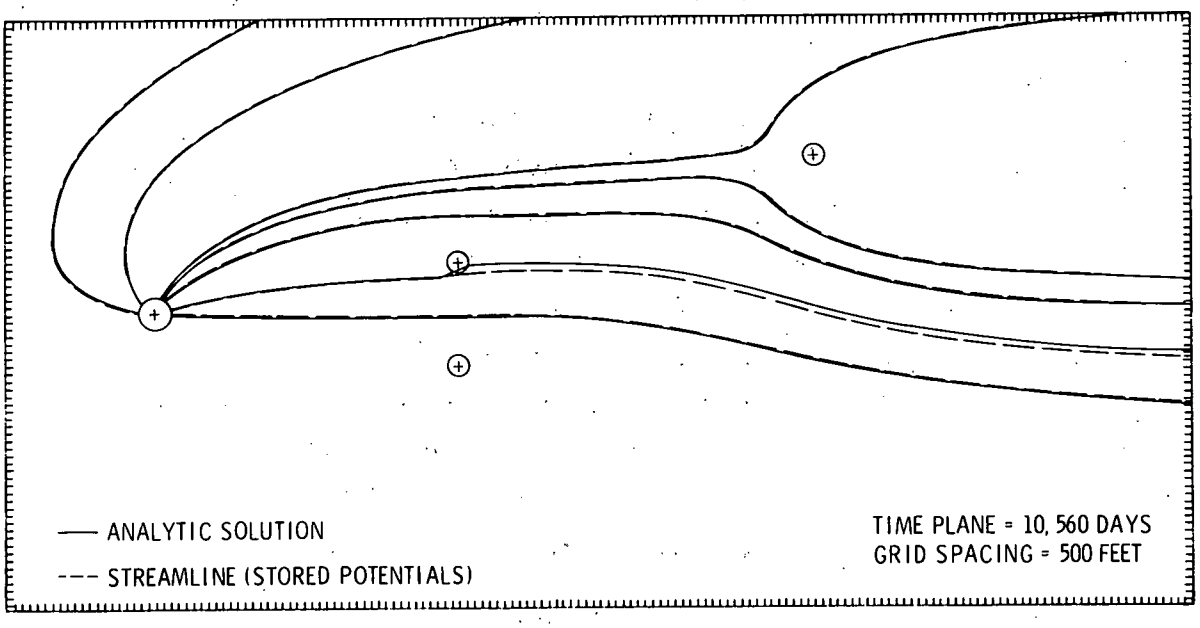

FIGURE 27

TEST SURFACE 2, DOWN GRADIENT STREAMLINES USING STORED POTENTIALS ON A SMALL GRID

ERROR ANALYSIS

An error analysis was performed on Test Surface 2 using the four down gradient pathline cases with 10-day time steps (Figures 20, 21, 22, and 23). These cases were chosen because the down gradient cases had shown greater errors than the up gradient cases. In addition, down gradient will be used in most modeling studies.

Time versus distance plots were made for each of the nine pathlines for each of the down gradient cases. These showed the variance in time along the entire length of a HPCP pathline with respect to its reference pathline. In all four cases the variance between the HPCP solution and the analytical solution is very small for eight of the nine pathlines, the exception is Pathline 7. Figure 28 is a typical example of one of the eight pathlines where the variance is small.

A somewhat larger variance was produced for Pathline 7 when the HPCP used stored gradients (Figures 29 and 30). When Pathline 7 was generated using stored potentials, the agreement with its reference pathline was very good (Figures 31 and 32).

Tables 1 through 4 give the errors in time and in distance at the end of each pathline where the pathlines using the analytical solution and the pathlines using the HPCP were terminated at the same total length. In the cases using stored gradient components, the maximum error in distance at the end of the pathlines is 8.4%; the minimum error is 0.09%. The maximum error in time at the end of the pathlines is -12.8% and the minimum error is 0.1%. In contrast, the cases using stored potentials have a maximum error in distance at the end of the pathlines of 1.5% and a minimum error of 0.1%, while the maximum error in time at the end of the pathlines is -1.2% and the minimum error is 0.03%.

The final investigation involved a study of the data storage requirements, data storage timing and program calculational times utilized by the various HPCP methods. This information can be found in Appendix A.

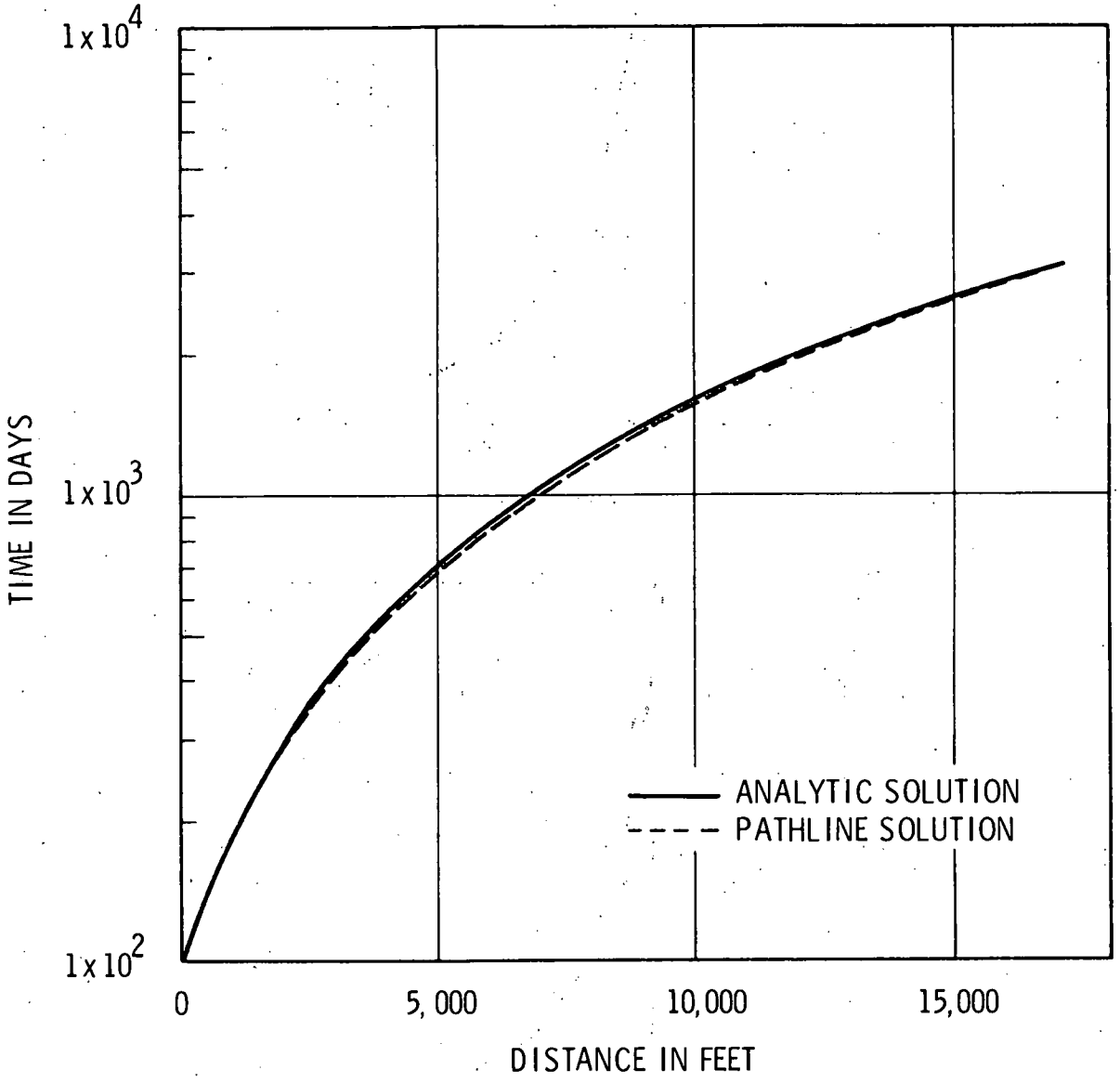

FIGURE 28

TIME VERSUS DISTANCE CURVE FOR PATHLINE NUMBER 3
(STORED GRADIENT COMPONENTS--NON-INTERPOLATED)

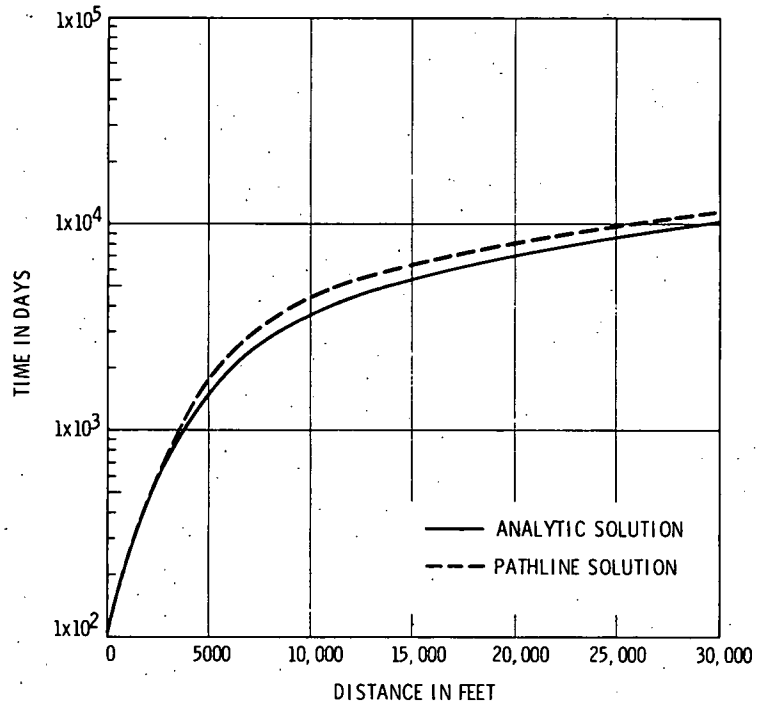

FIGURE 29

TIME VERSUS DISTANCE CURVE FOR PATHLINE NUMBER 7 (STORED GRADIENT COMPONENTS--NON-INTERPOLATED)

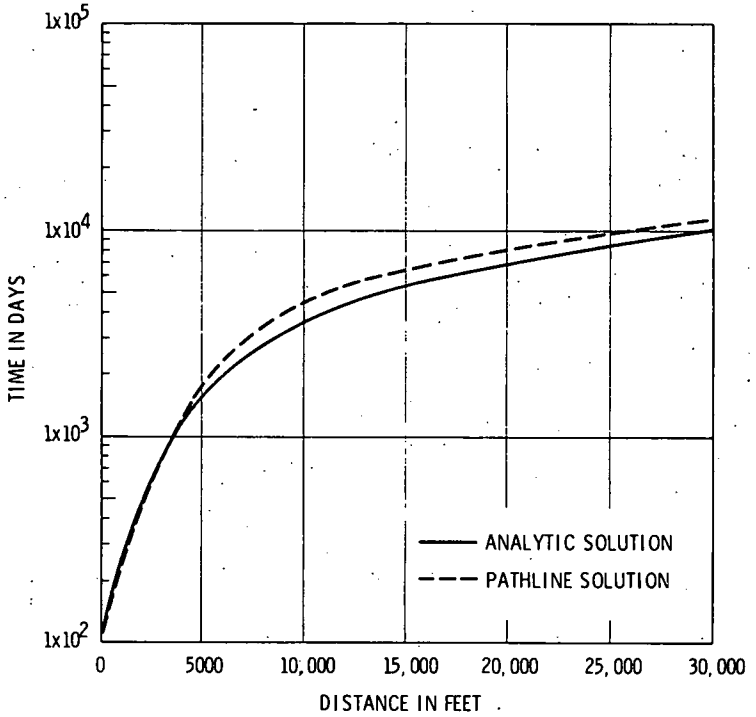

FIGURE 30

TIME VERSUS DISTANCE CURVE FOR PATHLINE NUMBER 7 (STORED GRADIENT COMPONENTS--INTERPOLATED)

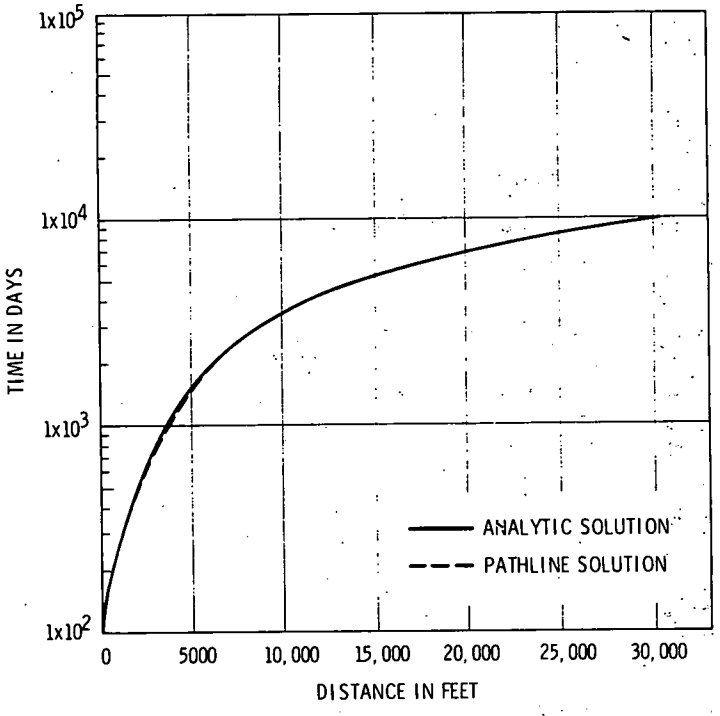

FIGURE 31

TIME VERSUS DISTANCE CURVE FOR PATHLINE NUMBER 7
(STORED POTENTIALS--NON-INTERPOLATED)

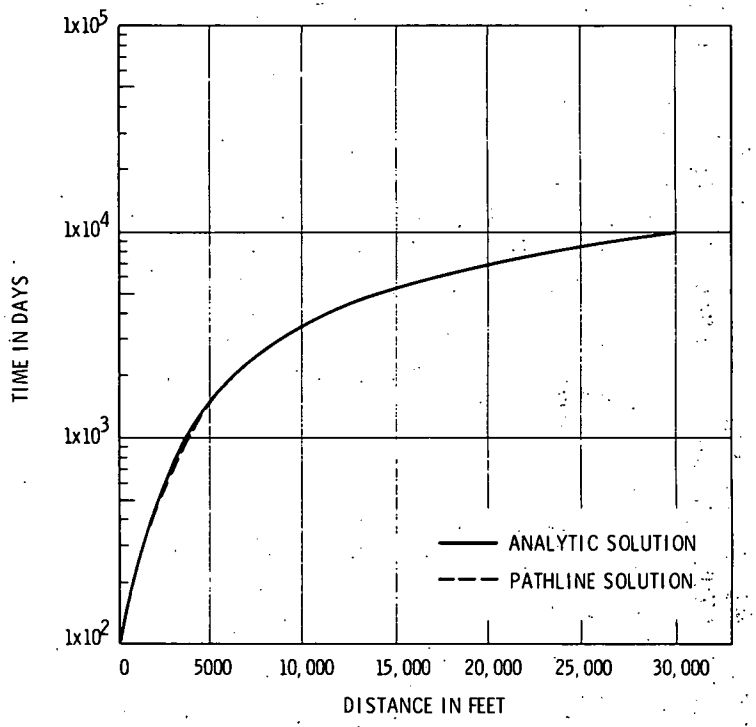

FIGURE 32

TIME VERSUS DISTANCE CURVE FOR PATHLINE NUMBER 7
(STORED POTENTIALS--INTERPOLATED)

TABLE 1

ERRORS IN TIME AND DISTANCE BETWEEN ANALYTIC SOLUTION AND HPCP USING STORED GRADIENT COMPONENTS (NON-INTERPOLATED)

Pathline Number	Total Distance Along Pathlines (FT)	Maximum Distance Between Pathlines (FT)	Error In Distance (Percent)	Total Time For Analytic Solution (Days)	Total Time For Numerical Solution (Days)	Error In Time (Percent)
1	68591.	317.	0.46	19742.	19720.	0.11
2	67471.	366.	0.54	19350.	19253.	0.50
3	17110.	351.	2.05	3063.	3100.	-1.21
4	18465.	183.	0.99	3450.	3500.	-1.44
5	58934.	61.	0.09	20022.	19940.	0.41
6	51798.	758.	1.46	15000.	14918.	0.55
7	29818.	2508.	8.41	10050.	11340.	-12.83
8	49600.	311.	0.63	16097.	16160.	-0.39
9	49384.	200.	0.41	15975.	16036.	-0.38

TABLE 2

ERRORS IN TIME AND DISTANCE BETWEEN ANALYTIC SOLUTION AND HPCP USING STORED GRADIENT COMPONENTS (INTERPOLATED)

Pathline Number	Total Distance Along Pathlines (FT)	Maximum Distance Between Pathlines (FT)	Error In Distance (Percent)	Total Time For Analytic Solution (Days)	Total Time For Numerical Solution (Days)	Error In Time (Percent)
1	68590.	301.	0.44	19741.	19720.	0.11
2	67417.	378.	0.56	19350.	19254.	0.50
3	17097.	352.	2.06	3061.	3100.	-1.28
4	18453.	179.	0.97	3448.	3500.	-1.51
5	68921.	67.	0.10	20017.	19940.	0.39
6	51798	749.	1.45	15000.	14919.	0.54
7	29802.	2518.	8.45	10045.	11340.	-12.89
8	49641.	336.	0.68	16098.	16160.	-0.39
9	49384.	184.	0.37	15975.	16036.	-0.38

TABLE 3

ERRORS IN TIME AND DISTANCE BETWEEN ANALYTIC SOLUTION AND HPCP USING STORED POTENTIALS (NON-INTERPOLATED)

Pathline Number	Total Distance Along Pathlines (FT)	Maximum Distance Between Pathlines (FT)	Error In Distance (Percent)	Total Time For Analytic Solution (Days)	Total Time For Numerical Solution (Days)	Error In Time (Percent)
1	68615.	194.	0.28	19750.	19737.	0.07
2	67417.	631.	0.94	19350.	19346.	0.02
3	17125.	258.	1.51	3065.	3100.	-1.13
4	18547.	103.	0.56	3467.	3500.	-0.94
5	69215.	298.	0.43	20050.	20012.	0.19
6	61794.	406.	0.78	15000.	14996.	0.03
7	30126.	322.	1.07	10150.	10043.	1.05
8	49588.	296	0.60	16093.	16160.	-0.41
9	49380.	50.	0.10	15975.	16038.	-0.40

TABLE 4

ERRORS IN TIME AND DISTANCE BETWEEN ANALYTIC SOLUTION AND HPCP USING STORED POTENTIALS (INTERPOLATED)

Pathline Number	Total Distance Along Pathlines (FT)	Maximum Distance Between Pathlines (FT)	Error In Distance (Percent)	Total Time For Analytic Solution (Days)	Total Time For Numerical Solution (Days)	Error In Time (Percent)
1	66615.	183.	0.27	10750.	19737.	0.07
2	67417.	623.	0.92	19350.	19345.	0.03
3	17114.	260.	1.52	3064.	3100.	-1.19
4	18525.	105.	0.57	3463.	3500.	-1.07
5	59015.	281.	0.41	20050.	20017.	0.16
6	51798.	401.	0.77	15000.	14996.	0.03
7	32126.	310.	1.03	10150.	10048.	1.00
8	49590.	322.	0.65	16094.	16160.	-0.41
9	49384.	67.	0.14	15975.	16038.	-0.40

HANFORD APPLICATIONS

Once it was shown that the HPCP could accurately calculate pathlines for a calculated transient surface, it was applied to the Hanford site. The purpose of this application was to determine the 21-year prediction for the two-dimensional contaminant pathlines from high-level radioactive waste storage areas to the Columbia River, and to make comparisons between the 21-year pathline prediction and instantaneous streamlines.

The HPCP used with the previously discussed test surface study would only allow calculation within one region with a fixed spatial resolution. However, the result of this study showed that closer nodal spacing was required near sources in order to more accurately determine the pathlines. To provide these more accurate calculations for use with the Hanford study, the HPCP was modified to work in conjunction with the Variable Thickness Groundwater Flow Model[7] which can supply potential surfaces divided into multiple regions with different nodal spacing. To facilitate higher resolution areas, these modifications were made to allow use of one large region and up to nine individual or overlapping subregions with up to three spatial resolutions.

As the HPCP calculates the steps along a pathline it determines the highest resolution area that exists for the current location and uses that set of data to calculate the next pathline location. Figure 33 shows the three regions selected for use with the Hanford study. The pathline program uses the highest resolution potential data in doing its calculations and switches from one region to another as it follows a flow path.

DESCRIPTION OF THE VTT FLOW MODEL

The Variable Thickness Transient (VTT) Flow Model[7] was used to provide input to the HPCP. The VTT model calculates the changes in the water table and produces time variant data matrices by simulating the flow of an incompressible fluid that saturates a rigid, porous soil matrix. In this model the hydraulic conductivity (K) is assumed to be isotropic but heterogeneous (K dependent upon location) and the flow is presumed to obey Darcy's law.

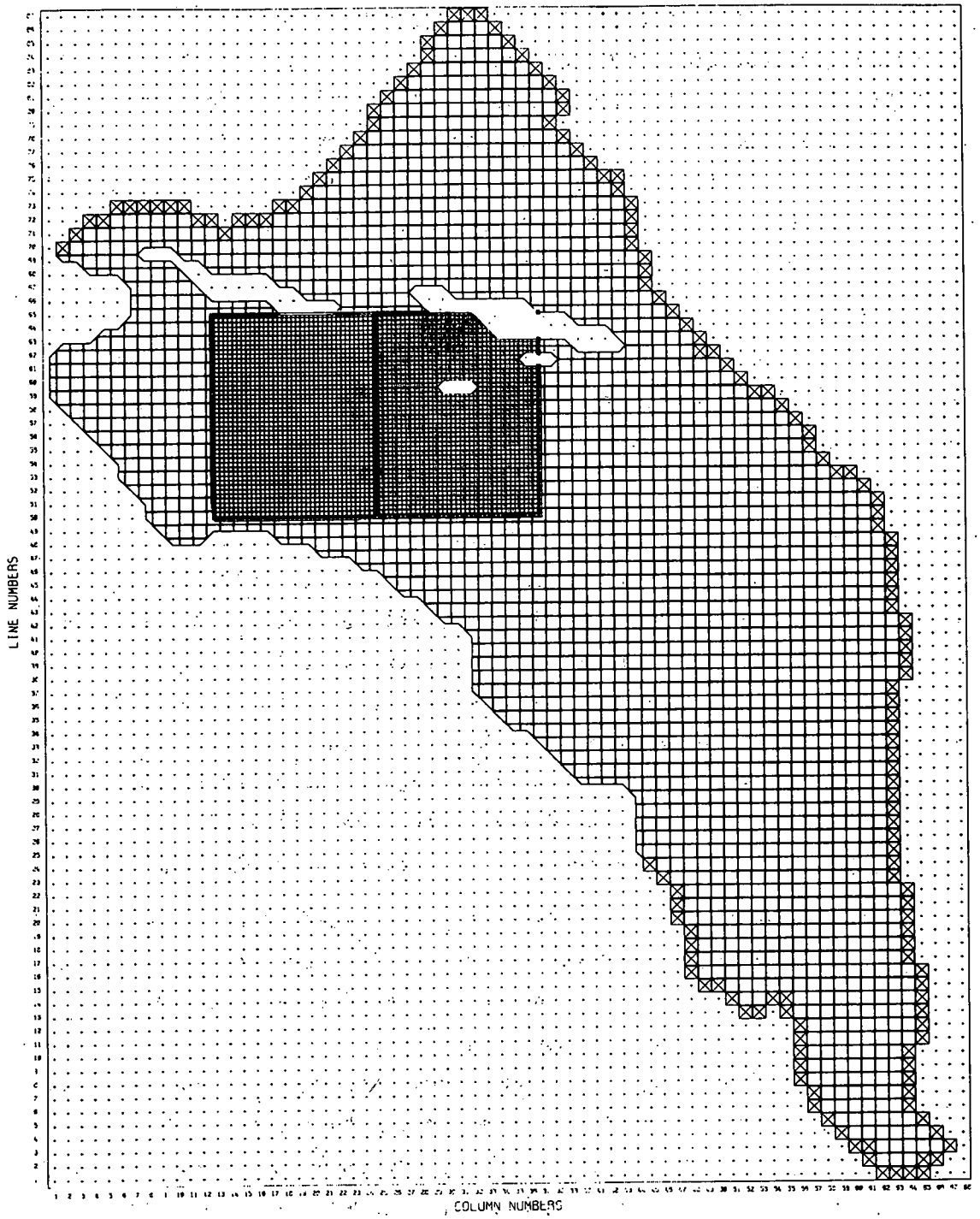

FIGURE 33

DIAGRAM OF THE LARGE REGION NODE MAP WITH THE TWO SMALL REGION (200 WEST AND 200 EAST) NODE MAPS SUPERIMPOSED

Basically, the model is constructed on the Boussinesq equation of unsteady flow. This formulation assumes that a two-dimensional (areal) formulation is adequate and, consequently, all of the aquifer properties are represented by their average over the saturated thickness of the aquifer. The variations of the aquifer thickness with space are considered, however, and the free-surface boundary condition with accretion is incorporated into the differential equation. Seepage surfaces are neglected in this model in order to carry out the averaging in the vertical direction.

The basic computer model based on the above assumptions and equation is described in detail by Kipp et al.,[7] with the exception of some recent improvements. The model provides a means of applying a specific set of boundary conditions to the above equations in order to produce a transient simulation.

The VTT model uses data on a square grid pattern (Figure 33). For the Hanford study the Columbia River bounds the region on the north and east. The western and southern sides are bounded irregularly by the Umtanum, Yakima, and Rattlesnake ridges and are broken by two alluvial valleys and the Yakima River in the southernmost part. The east-west trending void areas in the northern portion of the Reservation, as shown in Figure 33, are basaltic outcrops and as such are assumed to be no-flow areas. Water entering the region from the valley alluvium is accounted for in the model as a flux across the boundary such that the proper water table elevation is maintained.

The VTT Model can operate in a regional (far-field mode) as well as a subregional (near-field mode). Data utilized in the model have been developed over an extensive period of time as part of the Hanford Waste Management Program. Modeling consists of one or more computer runs for each case examined. A regional simulation over the large region reflects the effective aquifer stresses and yields a potentiometric surface from which boundaries may be interpolated for a subregional model. The subregional model may be used to resolve the detail of a local area such as that immediately surrounding the vicinity of a recharge/discharge site.

The hydraulic conductivity is assumed to be heterogeneous over the Hanford Reservation. Its spatial distribution was determined from pump test data and numerous measurements of aquifer water levels. These data were used in a computer routine which makes it possible to estimate the distribution of hydraulic conductivity throughout large areas of the Hanford Reservation.[8] Due to limited field data the storage coefficient is assumed to be constant at 0.1.[8] The aquifer bottom, necessary input to the model, is generally considered to be the top of the basalt or the top of an overlying clay unit.

The VTT model stores all of the potential data for each time step. These data can then be used to calculate the boundaries and potential distribution for as many small regions as desired. For the Hanford study, the 21 years from 1975-1995 were run with the latest projections for waste discharges for this time period. The large region (68 x 87 grid - 2000-ft node spacing) simulation and two small regions, one around 200 East area and one around 200 West area, were run to obtain the necessary resolution for the pathline study. Figure 33 indicates the large region and the positions of the two small regions. The 200 West region node spacing is 666.67 ft and the lower left coordinates in the large region nodal system are 13x, 50y. The upper right coordinates in the large region are 25x, 65y making the 200 West region a 37x46 node system as pictured in Figure 33. The 200-East region is also a 37x46 node system with a 666.67 ft node spacing where the lower left and upper right large region coordinates are 25x, 50y and 37x, 65y, respectively.

SELECTION OF PATHLINE STARTING LOCATIONS

The primary applications of the HPCP model at Hanford result in predictions of travel time and Columbia River arrival locations of contaminated ground water originating beneath the high-level waste areas (200-East and 200-West Areas). Thus, the starting locations of a series of pathlines or streamlines are often grouped around a particular radioactive waste discharge site. In order to make the application of multiple pathlines more meaningful, a method was devised to calculate the starting coordinates in a uniform manner.

The method chosen spaces the pathline starting coordinates equally in the flow field so that between any two adjacent pathline starting coordinates there will be equal flow (i.e., the pathline or streamline starting points will bound flow tubes having equal flow). Most often this procedure involves defining a circle or circular arc which intersects all groundwater flow lines leaving the vicinity of a given site. A groundwater flow rate increment between adjacent pathlines is specified and the program determines the number of pathlines and their starting locations along the circular arc. The starting locations as determined by the above procedure for the Hanford unconfined aquifer applications are given in Figure 34. The details of the starting location procedure and values of the input parameters for the Hanford application can be found in Appendix B.

METHODS AND INPUT DATA

Once the VTT model has been run, the resulting potential time plane data stored and the pathline starting locations determined for the modeled region, one additional step is required prior to operating the HPCP. This step involves setting up blocked data for rapid access by the HPCP.

The data required by the HPCP include: 1) VTT generated-time dependent potential surface(s), 2) hydraulic conductivity distribution and 3) storage coefficient distribution. To conserve computer core requirements these data are restructured into blocks[9] and stored in random access form for use by the HPCP. Figure 35 shows an example of this blocking method.

The only differences in the procedure described in Reference 10 and the data storage technique utilized by the HPCP are: 1) the addition of separate blocked data files to allow use of multiple regions, 2) automatic adjustment of the individual data files according to the size of the region or subregion, 3) use of input command files to describe the region to be stored and 4) addition of a random access header file containing information describing each region and subregion that has been stored.

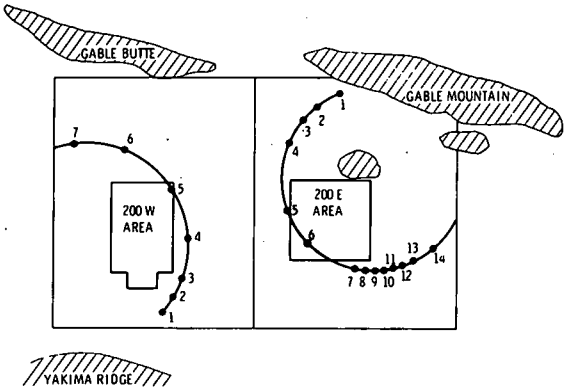

FIGURE 34

SELECTED PATH-STREAMLINE STARTING LOCATIONS FOR HANFORD STUDY

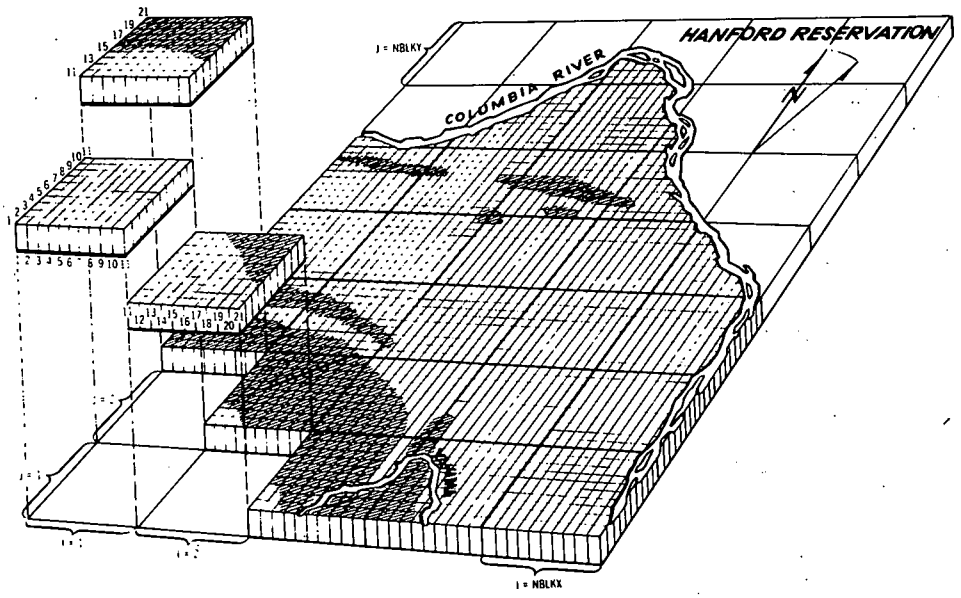

FIGURE 35

EXAMPLE OF DATA MATRIX BLOCKING METHOD

When all of the preceding procedures have been completed, the Program may be utilized. As mentioned previously, the HPCP can use several different regions of different resolution to produce more accurate pathlines. As the program follows along a pathline it must determine the highest resolution area that exists for the current pathline location and use that set of data in its calculations. The earlier studies using the test surfaces were made on rectangular regions, and bilinear interpolation was sufficient; however, the odd-shaped region of the Hanford groundwater system required that linear interpolation on triangles be added in order for the HPCP to properly interpolate data needed in the pathline calculations. Appendix C illustrates the procedure that was added to the HPCP to allow for triangular interpolation where required.

Potential surfaces were generated for the Hanford study for the 21 years from 1975 to 1995 with 30 day time planes for a total of 252 time planes and the pathlines were calculated at 10 day time steps.

Appendix D contains plots of the Large Region, 200 West Region and 200 East Region potential contours for the years 1975, 1980, 1985, 1990 and 1995. These plots show the effects on the groundwater system by the reduction of crib discharge flow rates over this 21 year period of time.

The Hanford 21 year study entailed the evaluation of both the 200 East and 200 West Areas and shows the results of both streamlines and pathlines originating in these areas. All of the streamlines and pathlines originate at the starting locations shown in Figure 34, these line numbers are referred to in the following text.

RESULTS

Figures 36 and 37 show the predicted path-streamlines (with tick marks at 5 year intervals) from each of the associated areas in 200-West and 200-East Areas to termination at a model boundary. When the year 1995 is reached the pathlines revert to streamlines using the predicted 1995 potential surface for the period beyond 1995. The apparent "crossing" of the pathlines in Figure 37 is possible because of the changing potential surface. Liquid particles traveling along different pathlines of a two-dimensional surface may pass through the same point but not at the same time. The discharges to the Hanford unconfined aquifer from man-related activities are estimated to be over 80% of the total

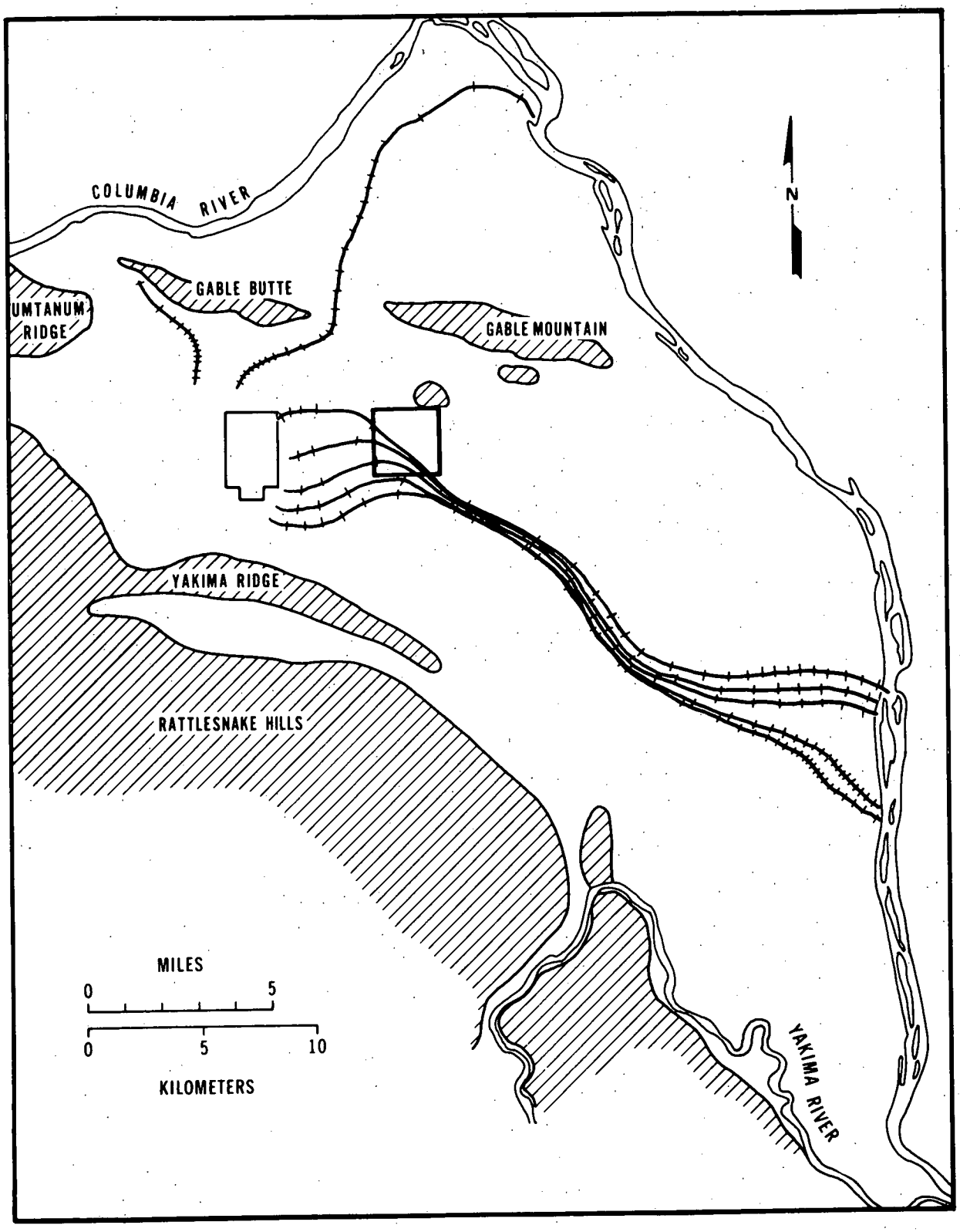

FIGURE 36

200 WEST AREA PATH-STREAMLINES

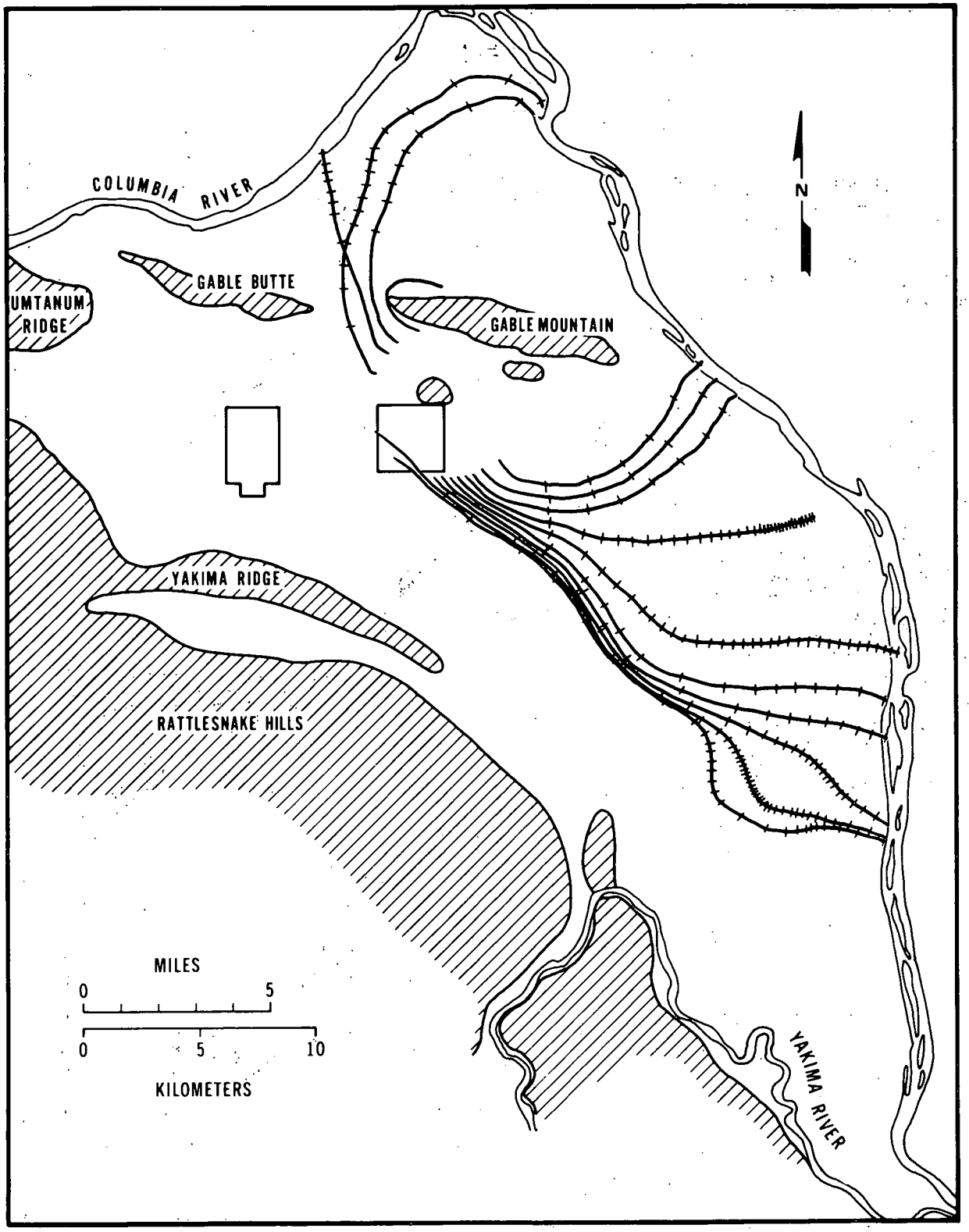

FIGURE 37

200 EAST AREA PATH-STREAMLINES

TABLE 5

TIME VERSUS DISTANCE SUMMARY FOR THE SEVEN 200 WEST AREA
PATH-STREAMLINES SHOWN IN FIGURE 36

Path-Streamline Number	Total Distance in Ft	Total Time in Days
1	105,600	58,790
2	104,261	52,400
3	98,572	30,530
4	98,745	31,880
5	103,200	47,090
6	70,244	50,590
7	17,221	27,460

Average Distance = 85,406 ft
Average Time = 42,677 days

TABLE 6

TIME VERSUS DISTANCE SUMMARY FOR THE FOURTEEN 200 EAST AREA
PATH-STREAMLINES SHOWN IN FIGURE 37

Path-Streamline Number	Total Distance in Ft	Total Time in Days
1	16,217	1,450
2	51,048	15,580
3	31,082	15,670
4	63,487	29,630
5	96,357	76,240
6	95,263	45,820
7	82,691	45,550
8	76,104	25,840
9	74,129	26,020
10	70,556	59,230
11	52,106	89,920
12	45,594	14,230
13	41,573	10,000
14	38,443	11,170

Average Distance = 59,604 ft
Average Time = 33,310 days

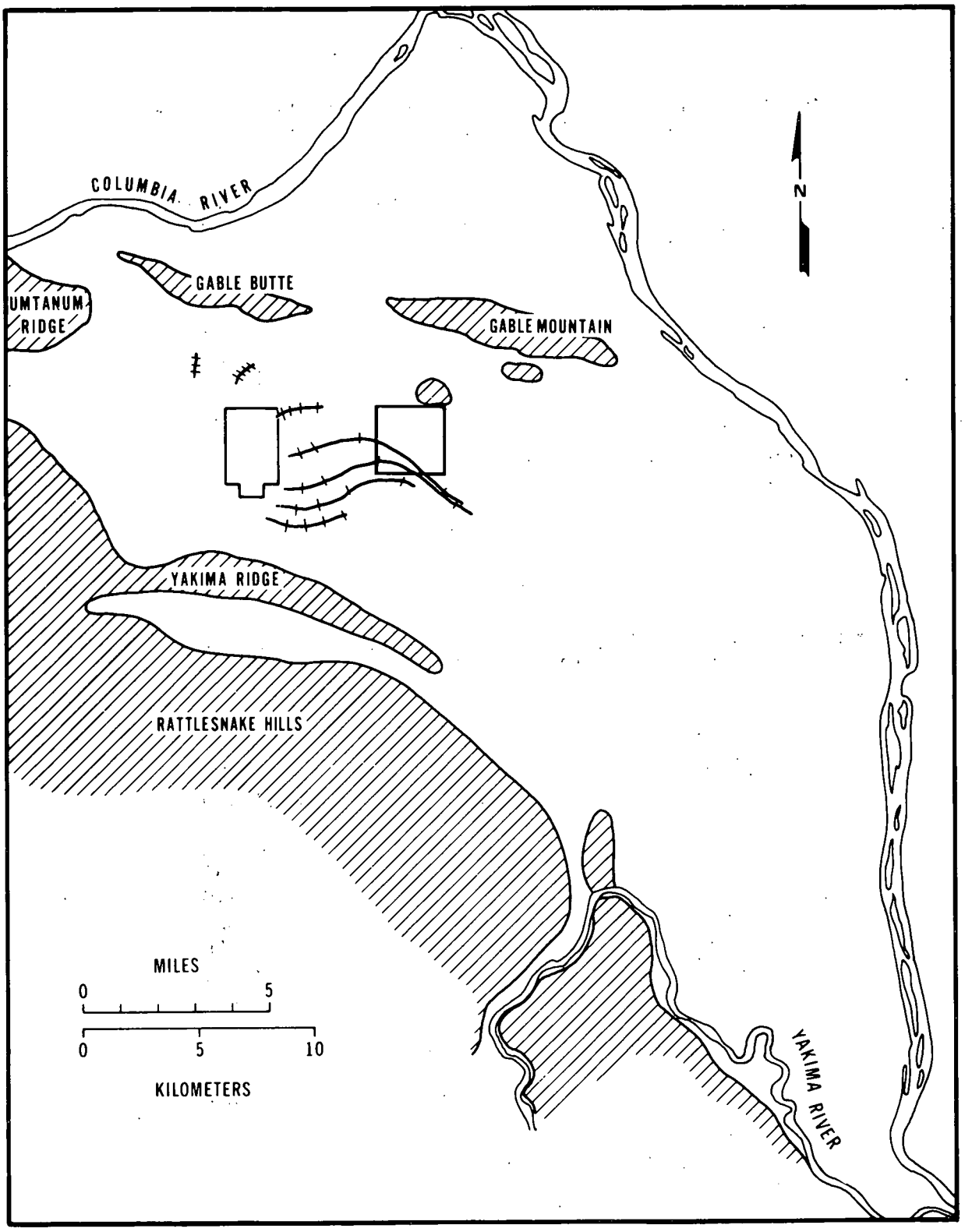

FIGURE 38

PLOT OF THE 21 YEAR PATHLINES FOR THE 200 WEST AREA

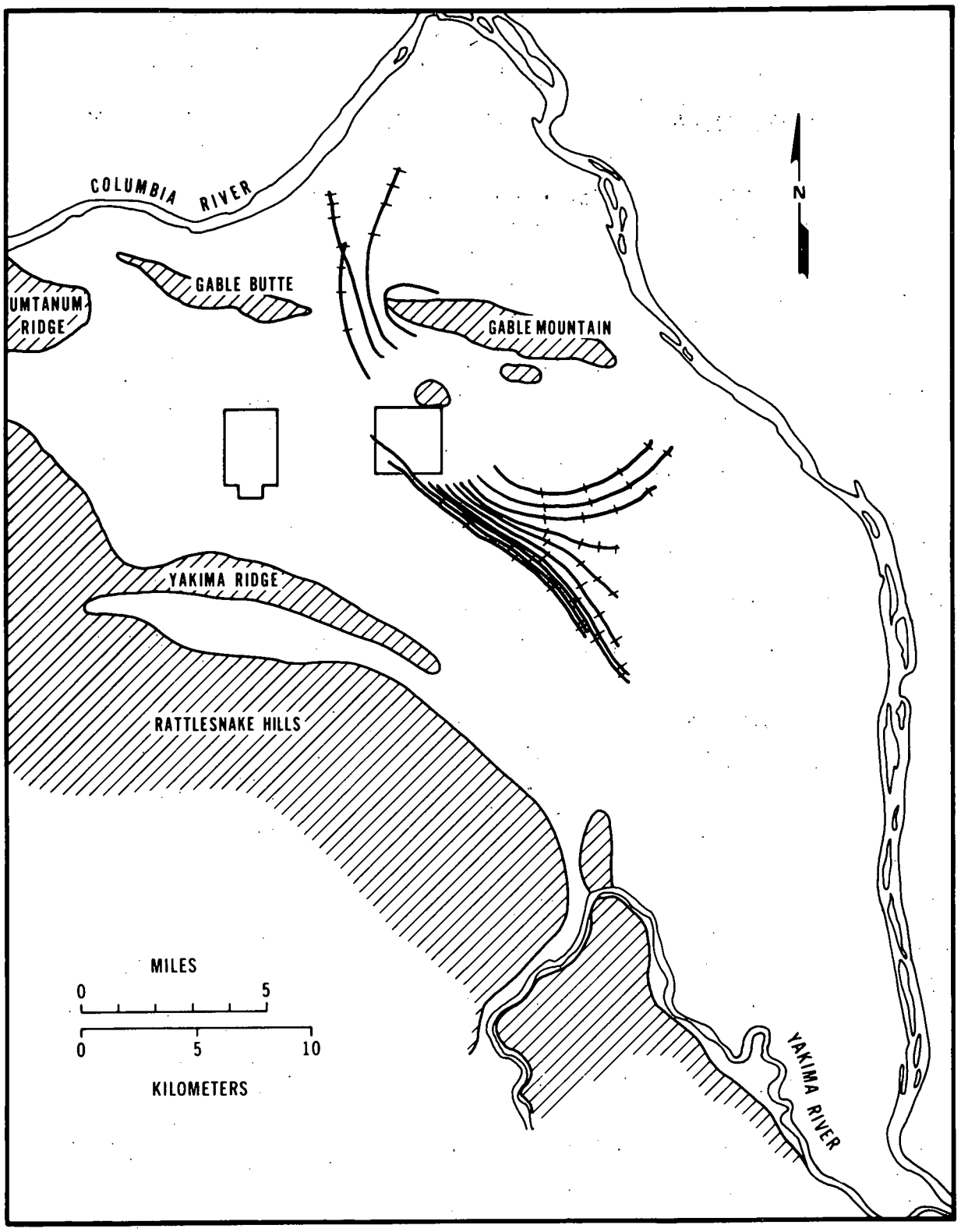

FIGURE 39

PLOT OF THE 21 YEAR PATHLINES FOR THE 200 EAST AREA

TABLE 7

SUMMARY OF THE 200-WEST AREA 21-YEAR PATHLINES AS SHOWN IN FIGURE 38

Pathline Number	Total Distance in Ft	Total Time in Days
1	11,371	7,660
2	20,159	7,660
3	28,871	7,660
4	27,037	7,660
5	6,684	7,650
6	3,329	7,650
7	3,110	7,650

Average Distance = 14,366 ft
Average Time = 7,655 days

TABLE 8

SUMMARY OF THE 200-EAST AREA 21-YEAR PATHLINES AS SHOWN IN FIGURE 39

Pathline Number	Total Distance in Ft	Total Time in Days
1	16,217	1,450
2	27,229	7,660
3	24,952	7,660
4	20,214	7,670
5	41,135	7,660
6	37,356	7,660
7	40,101	7,660
8	38,121	7,660
9	33,676	7,660
10	28,022	7,660
11	24,529	7,660
12	28,476	7,660
13	31,092	7,660
14	25,751	7,660

Average Distance = 29,777 ft
Average Time = 7,217 days

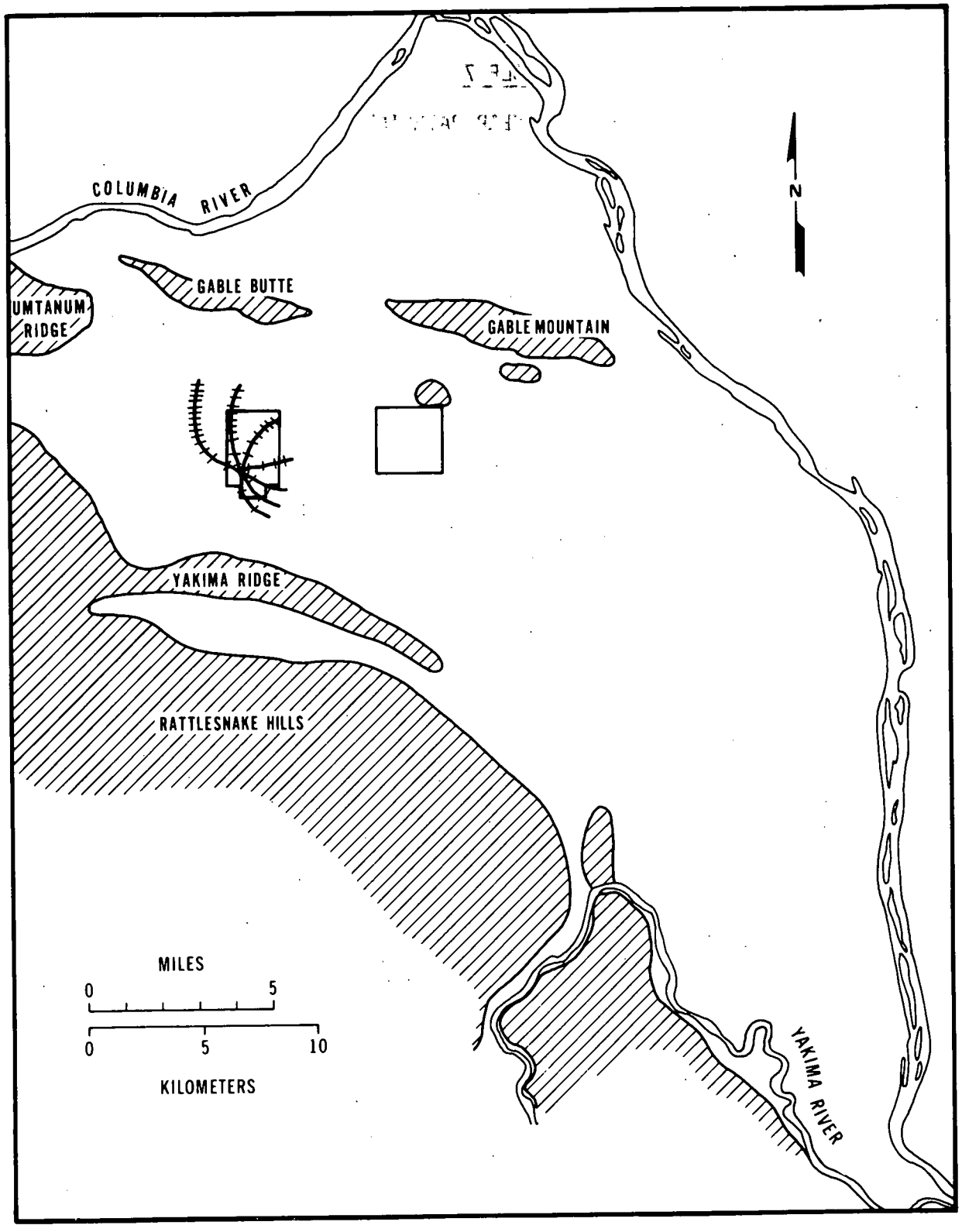

FIGURE 40

PLOT OF THE UP GRADIENT STREAMLINES FROM THE 200 WEST AREA PATHLINE STARTING LOCATIONS

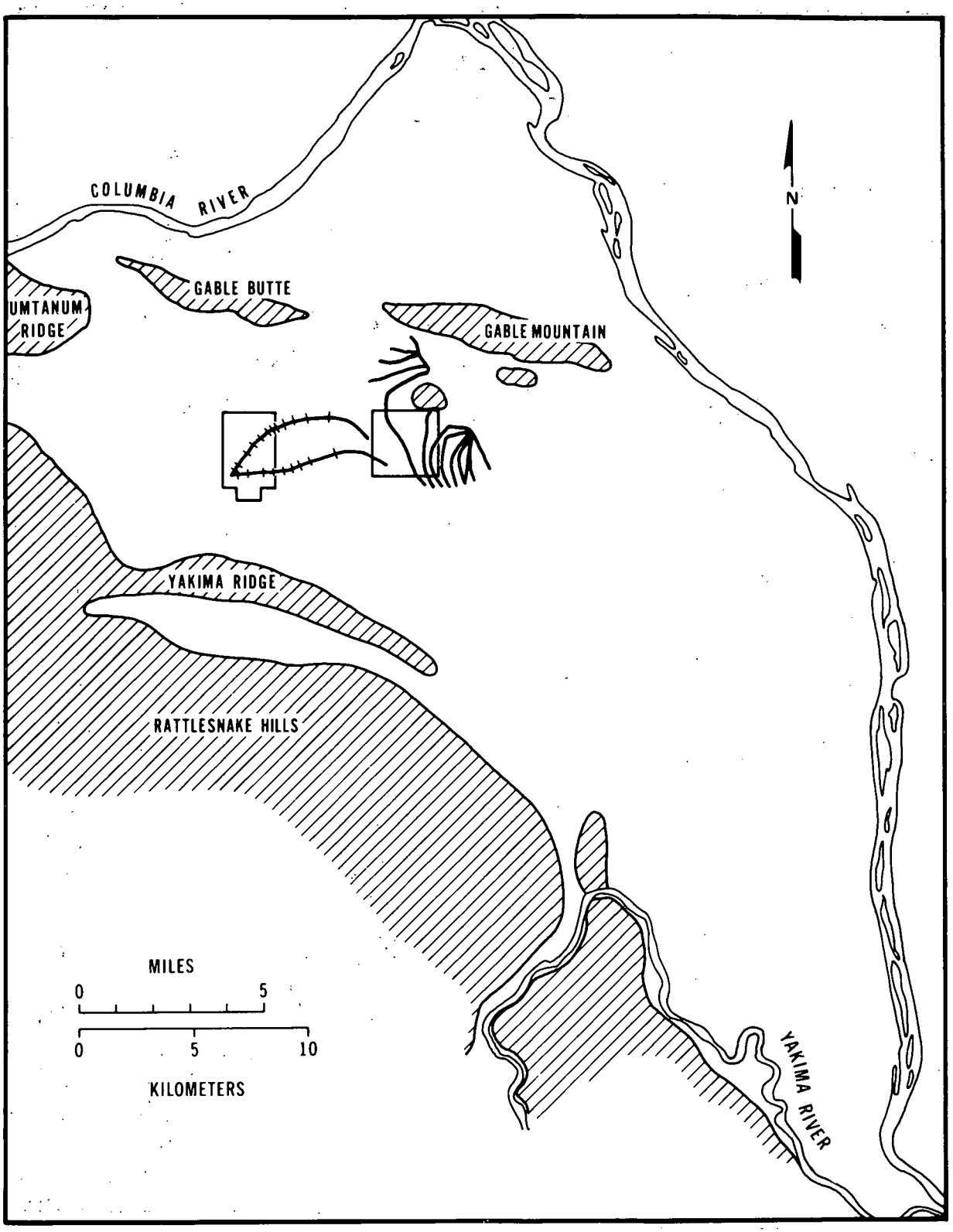

FIGURE 41

PLOT OF THE UP GRADIENT STREAMLINES FROM THE 200 EAST AREA PATHLINE STARTING LOCATIONS

TABLE 9

SUMMARY OF THE 200 WEST AREA UP GRADIENT STREAMLINES AS SHOWN IN FIGURE 40

Streamline Number	Total Distance in Ft	Total Time in Days
1	8,511	6,210
2	7,715	5,310
3	7,296	5,760
4	7,873	10,260
5	9,936	15,210
6	12,844	20,250
7	16,160	27,270

Average Distance = 10,048 ft
Average Time = 12,895 days
1975 Surface

TABLE 10

SUMMARY OF THE 200 EAST AREA UP GRADIENT STREAMLINES AS SHOWN IN FIGURE 41

Streamline Number	Total Distance in Ft	Total Time in Days
1	4,428	360
2	5,530	360
3	6,219	450
4	5,405	450
5	23,714	23,410
6	22,641	17,290
7	18,681	1,530
8	11,451	1,800
9	11,555	1,170
10	11,089	900
11	8,760	540
12	5,078	450
13	6,008	540
14	4,166	630

Average Distance = 10,337 ft
Average Time = 3,562 days
1975 Surface

flow in the aquifer; thus, changes in the operation of the Hanford facilities, and consequently the discharge flow rate to the ponds and cribs, are likely to have an important effect upon the groundwater potential. Worthwhile estimates of discharge to groundwater for periods greater than about 20 years into the future are not available. For this reason, the VTT model predictions were not extended beyond 1995, and the pathlines become streamlines after that date. Tables 5 and 6 contain the total time and distance traversed by these path-streamlines.

Figures 38 and 39 show the paths that would be traversed in the 21 years from January 1975 to December 1995. Summaries for the pathlines shown in Figures 38 and 39 are contained in Tables 7 and 8, respectively. Figures 40 and 41 illustrate the up gradient streamlines from the 200-West and 200-East Area starting points, while Tables 9 and 10 contain the respective streamline summaries. The tick marks along the pathlines or streamlines are at 5 year intervals.

Comparisons between pathlines and streamlines were also made. Appendix E contains the plots and summaries of the streamlines which were run for both the 200-West and 200-East Areas for 1975, 1980, 1985, 1990, and 1995. Table 11 contains a comparison of the average times and distances, and

TABLE 11

THE AVERAGE TRAVEL TIME (DAYS) AND TRAVEL DISTANCES (FT), TO THE COLUMBIA RIVER. COMPARISON BETWEEN THE 200 EAST AND 200 WEST PATH-STREAMLINES AND THE STREAMLINES FOR 1975, 1980, 1985, 1990 AND 1995

Comparison	Path-Streamlines	1975 Streamlines	1980 Streamlines	1985 Streamlines	1990 Streamlines	1995 Streamlines
Average Time 200 West	42677	36583 (-14%)	33589 (-21%)	40106 (-6%)	48939 (+15%)	46123 (+8%)
Average Distance 200 West	85407	84585 (-1%)	71908 (-16%)	72626 (-15%)	82237 (-4%)	85901 (+1%)
Average Time 200 East	33311	23655 (-29%)	21404 (-36%)	25493 (-23%)	24606 (-26%)	24599 (-26%)
Average Distance 200 East	59604	59902 (+.5%)	57224 (-4%)	55369 (-7%)	54903 (-8%)	55187 (-7%)

Table 12 shows a streamline by streamline comparison. From a look at the streamline and path-streamline plots it becomes apparent that 200 East line 1 should not be used for comparison because of its premature termination. In addition, 200-West lines 6 and 7 comparisons are not useful because they both sometimes terminate prematurely.

The averages shown in Table 12 then become from top to bottom: 200-West Area travel time +7% greater for streamlines and -2.6% shorter distances; 200-East Area travel times 13% shorter for streamlines and 2.8% shorter distances. 200-West travel times for streamlines vary between 34.9% longer and 15.6% shorter than the 200-West path-streamline travel times. Distances traveled for the 200-West streamlines vary from 4.3% greater to 24.5% lesser than the path-streamline distances. 200-East Area travel times for streamlines vary between 77.5% longer to 69.3% shorter than the 200-East Area path-streamline travel times. Distances traveled by the 200-East streamlines vary from 53.5% more to 38.7% less than the 200-East Area path-streamline distances.

In general, there is a significant variation between pathlines and streamlines. As the only fundamental difference between the two approaches is the elimination of the steady-state assumption used in calculating streamlines, the variations described above represent the improvement obtained in predictions using pathlines.

EVALUATION

The predictions of fluid "particle" movement can be significantly improved by using dynamic pathlines over those obtained from static streamlines. However adequate pathline calculations are limited to the quality of the basic data, i.e., hydraulic potentials, hydraulic conductivity and storage coefficients. Also in areas of steep or rapidly changing gradients the pathline predictive capabilities tend to deteriorate. The results of the HPCP can be no better than the input data, however; this study does show that given adequate input data the HPCP can produce very accurate results. The HPCP can be used in conducting management studies such as evaluating the impact of aquifer pumping or recharge to divert waste from a path with a relatively short travel time into one with a longer travel time.

TABLE 12

A COMPARISON BETWEEN PATH-STREAMLINE AND STREAMLINES FOR 1975, 1980 1980, 1985, 1990 AND 1995 ON A LINE BY LINE BASIS FOR THE 200 WEST AND 200 EAST AREAS (PLOTS AND DATA SUMMARIES FOR THE STREAMLINES ARE ARE IN APPENDIX V)

TRAVEL TIME (days)	PATH STREAM	1975 STREAMLINES	1980 STREAMLINES	1985 STREAMLINES	1990 STREAMLINES	1995 STREAMLINES	AVERAGE DIFFERENCE
200 WEST LINE 1	56798.	33410. (-43.2%)	36838. (-37.4%)	57980. (-1.0%)	59240. (0.8%)	60500. (2.9%)	(-15.6%)
2	52404.	29610. (-43.1%)	58163. (11.0%)	49610. (-5.3%)	38000. (-27.5%)	55550. (6.0%)	(-11.8%)
3	36534.	34222. (12.1%)	42680. (39.8%)	293AA. (-3.8%)	32150. (5.3%)	43490. (42.5%)	(19.2%)
4	31844.	44300. (39.0%)	31520. (-1.1%)	61130. (91.8%)	45740. (43.5%)	32330. (1.4%)	(34.9%)
5	47898.	66780. (40.1%)	24690. (-47.6%)	22970. (-51.7%)	89930. (91.0%)	48642. (2.9%)	(0.2%)
6	50598.	19998. (-60.7%)	17740. (-64.9%)	35920. (-29.0%)	51310. (1.4%)	54010. (6.8%)	(-29.3%)
7	27466.	25660. (-6.6%)	23500. (-14.4%)	23770. (-13.4%)	26280. (-4.6%)	28450. (3.6%)	(-7.1%)
DISTANCE TRAVELED (ft)							AVG -0.2%
200 WEST LINE 1	105600.	112630. (6.7%)	111959. (6.0%)	106285. (0.6%)	105692. (0.1%)	105713. (0.1%)	(2.7%)
2	106262.	111039. (7.3%)	109975. (5.5%)	106750. (0.5%)	108359. (-3.7%)	106370. (0.1%)	(1.9%)
3	98572.	111303. (13.0%)	104575. (6.1%)	99244. (0.7%)	98120. (-0.5%)	100554. (2.0%)	(4.3%)
4	98746.	110936. (12.3%)	101583. (2.9%)	97121. (-1.6%)	99325. (0.6%)	98380. (-0.4%)	(2.7%)
5	103241.	113240. (9.5%)	42991. (-58.3%)	89551. (-54.9%)	84020. (-18.6%)	102970. (-0.2%)	(-24.5%)
6	74245.	15243. (-79.6%)	15286. (-79.2%)	36710. (-47.7%)	70673. (0.6%)	71795. (2.2%)	(-40.3%)
7	17222.	17239. (0.1%)	16987. (-1.4%)	17715. (2.9%)	17463. (1.4%)	17591. (2.1%)	(1.6%)
TRAVEL TIME (days)							AVG -7.5%
200 EAST LINE 1	1454.	0110. (-59.3%)	1630. (12.4%)	1720. (18.6%)	2440. (68.3%)	3790. (161.4%)	(144.0%)
2	15584.	13620. (-13.9%)	12430. (-20.2%)	20980. (34.7%)	10890. (-35.2%)	11890. (-23.7%)	(-11.7%)
3	15678.	6130. (-60.9%)	15310. (-2.3%)	15760. (0.6%)	16120. (2.9%)	17650. (12.6%)	(-9.0%)
4	29634.	10220. (-39.2%)	9190. (-69.0%)	12880. (-56.5%)	22330. (-24.6%)	25120. (-15.2%)	(-40.9%)
5	76248.	41230. (-45.9%)	28620. (-73.0%)	56170. (-26.3%)	46180. (-39.4%)	25380. (-66.8%)	(-50.3%)
6	45428.	33240. (-27.9%)	39340. (-14.1%)	22780. (-50.3%)	25030. (-45.4%)	26280. (-42.8%)	(-36.1%)
7	45556.	38800. (-14.8%)	31960. (-29.8%)	23680. (-48.0%)	24490. (-46.2%)	23680. (-48.0%)	(-37.4%)
8	25843.	23610. (-9.4%)	10550. (-26.2%)	22608. (-12.5%)	36012. (39.4%)	45108. (74.5%)	(12.7%)
9	26826.	21270. (-19.4%)	33760. (29.7%)	37080. (42.2%)	69760. (160.1%)	69492. (159.1%)	(77.6%)
10	59234.	47528. (-19.6%)	59688. (0.8%)	82980. (40.0%)	38400. (-35.1%)	40330. (-31.9%)	(-9.2%)
11	84928.	52648. (-61.2%)	28980. (-67.9%)	26833. (-70.2%)	14233. (-84.2%)	15488. (-82.9%)	(-69.3%)
12	14234.	9910. (-30.4%)	10360. (-27.2%)	11350. (-20.2%)	11620. (-18.3%)	11260. (-20.9%)	(-23.4%)
13	14888.	7570. (-24.1%)	8110. (-18.9%)	10180. (1.6%)	11530. (15.3%)	11260. (12.6%)	(-2.7%)
14	11174.	14090. (-14.5%)	9820. (-12.1%)	12870. (8.1%)	16210. (65.1%)	17922. (69.4%)	(14.2%)
DISTANCE TRAVELED (ft)							AVG -2.7%
200 EAST LINE 1	16216.	46984. (189.7%)	15982. (-1.5%)	13472. (-16.9%)	12212. (-24.7%)	16411. (1.2%)	(29.6%)
2	51489.	51970. (5.7%)	53664. (5.1%)	45295. (-11.3%)	47766. (-6.4%)	48211. (-5.6%)	(-2.5%)
3	31882.	28656. (-7.6%)	55035. (77.1%)	52350. (68.5%)	50998. (64.1%)	51347. (65.0%)	(53.5%)
4	63886.	32217. (-49.6%)	29851. (-53.0%)	31879. (-49.8%)	38644. (-20.2%)	50326. (-20.7%)	(-38.7%)
5	96357.	99225. (3.0%)	87364. (-9.3%)	84660. (-12.1%)	86781. (-10.0%)	86736. (-10.0%)	(-7.7%)
6	95264.	95256. (0.0%)	84883. (-6.6%)	83138. (-12.7%)	82609. (-13.3%)	83267. (-12.6%)	(-9.0%)
7	82691.	82195. (-0.6%)	80115. (-3.1%)	77941. (-6.6%)	76238. (-7.8%)	75951. (-8.2%)	(-5.3%)
8	76194.	77077. (1.3%)	75232. (-1.1%)	74982. (-1.5%)	75839. (-0.5%)	74953. (-1.5%)	(-0.6%)
9	74138.	75072. (1.3%)	74154. (0.0%)	74461. (0.4%)	80118. (8.0%)	66563. (-10.2%)	(-3.9%)
10	74956.	66847. (-2.4%)	64699. (-8.9%)	63869. (-9.5%)	52507. (-25.6%)	52170. (-26.1%)	(-14.3%)
11	52186.	54044. (3.7%)	51412. (-1.5%)	50333. (-3.6%)	45759. (-12.2%)	45895. (-11.9%)	(-5.0%)
12	45395.	45380. (0.0%)	44387. (-2.2%)	44335. (-2.3%)	42987. (-5.5%)	42034. (-5.6%)	(-3.1%)
13	41573.	41710. (0.3%)	41681. (0.2%)	41161. (-1.0%)	40751. (-2.0%)	40623. (-2.3%)	(-1.1%)
14	38444.	38180. (-0.7%)	38439. (0.0%)	38207. (-0.6%)	37507. (-2.2%)	37333. (-2.9%)	(-1.3%)
							AVG -0.7%

This study shows that the use of stored potentials by the HPCP produces more accurate results than stored gradient components and also that predictive capabilities can be improved in areas of steep or rapidly changing gradients by reducing the grid spacing in these areas.

The use of potential surfaces generated at 30 day time planes and pathlines calculated at 10 day time steps appears to be adequate for the Hanford groundwater analysis.

CONCLUSIONS

The extensive testing of the HPCP has shown that this method can be used to accurately calculate times of travel and direction of flow of fluid "particles" for a two-dimensional transient groundwater potential surface. These results lead us to conclude that given accurate input data, an improved estimate of the paths (ignoring dispersion) and travel times (ignoring sorption, chemical reaction, and radioactive decay) from a contaminant source to a groundwater discharge area can be obtained for the Hanford or similar groundwater system.

The Hanford Pathline Calculational Program can be used as a rapid, economical, and convenient means of obtaining a preliminary comparison of the contaminant travel direction, travel distance, and travel times under different water table (or potential) conditions and as such can be a valuable tool for management of groundwater resources.

REFERENCES

1. R. A. Deju, R. E. Gephart, "Hydrologic Management at the Hanford Nuclear Waste Facility," ARH-SA-235, Atlantic Richfield Hanford Company, Richland, Washington, 1975.

2. D. A. Myers, et al., "Environmental Monitoring Report on the Status of Ground Water Beneath the Hanford Site, January-December 1975," BNWL-2034, Battelle, Pacific Northwest Laboratories, Richland, Washington, 1976.

3. R. C. Arnett et al., "Conceptual and Mathematical Modeling of the Hanford Groundwater Flow Regime," ARH-ST-140, Atlantic Richfield Hanford Company, October 1976.

4. R. C. Arnett, R. E. Gephart, and R. A. Deju, "Hanford Groundwater Scenario Studies", ARH-SA-292, Atlantic Richfield Hanford Company, April, 1977.

5. "Final Environmental Statement, Waste Management Operations, Hanford Reservation, Richland, Washington", ERDA-1538, United States Energy Research and Development Administration, December 1975.

6. R. W. Nelson, "Evaluating the Environmental Consequences of Groundwater Contamination," BCSR-6/UC-11, Boeing Computer Services, Richland, Inc., December 1976.

7. K. L. Kipp, A. E. Reisenauer, C. R. Cole, and C. A. Bryan, "Variable Thickness Transient Groundwater Flow Model Theory and Numerical Implementation," BNWL-1703, Battelle, Pacific Northwest Laboratories, 1972 (Updated 1976).

8. D. B. Cearlock, K. L. Kipp, and D. R. Friedrichs, "The Transmissivity Iterative Calculation Routine - Theory and Numerical Implementation," BNWL-1706, Battelle, Pacific Northwest Laboratories, 1972, (revised 1976).

9. D. R. Friedrichs, "Comprehensive Information Retrieval and Model Input Sequence (CIRMIS)," BNWL-2235, Battelle, Pacific Northwest Laboratory, 1977.

APPENDIX A

HPCP Data Storage Timing, Data Storage Requirements and Program Calculational Timing

APPENDIX A

During the evaluation of the Hanford Pathline Calculational Program, two methods of data storage were used: 1) stored gradients and 2) stored potentials. The results of interpolating between time planes were also compared with those obtained by not interpolating between time planes. This appendix describes these techniques and the timing and storage requirements used by each method.

STORED GRADIENTS

This method calculates the gradient components $\frac{\partial \Phi}{\partial x}$ and $\frac{\partial \Phi}{\partial y}$ and stores these in two separate files for each time plane. The gradient at a given node is calculted by a simple interpolation formula which uses the two potential values on either side of the node. In mathematical terms this formula can be expressed by:

$$\left.\frac{\partial \Phi}{\partial x}\right|_i = \frac{(\Phi_{i+1} - \Phi_{i-1})}{2\Delta x} \qquad \text{(A-1)}$$

$$\left.\frac{\partial \Phi}{\partial y}\right|_j = \frac{(\Phi_{j+1} - \Phi_{j-1})}{2\Delta y} \qquad \text{(where } j = i\text{)} \qquad \text{(A-2)}$$

where:

$\left.\frac{\partial \Phi}{\partial x}\right|_i$ = x gradient component at i^{th} node

$\left.\frac{\partial \Phi}{\partial y}\right|_i$ = y gradient component at i^{th} node

Φ = hydraulic potential

Δx = node spacing in x direction

Δy = node spacing in y direction.

The x,y coordinate position is then used to calculate the pathline position in the matrix and from this all data for the four surrounding nodes are retrieved from data storage (i.e., $\frac{\partial \Phi}{\partial x}$, $\frac{\partial \Phi}{\partial y}$, σ, K).

Once the program has this information available a simple interpolation is performed on each set of data to get the values at the x,y coordinate position.

STORED POTENTIALS

This method stores the actual potential values (Φ) for each calculated time plane. These Φ values along with σ and K are retrieved the same way as described above.

The actual gradient components are now calculated at the x,y coordinate position as a function of Φ.

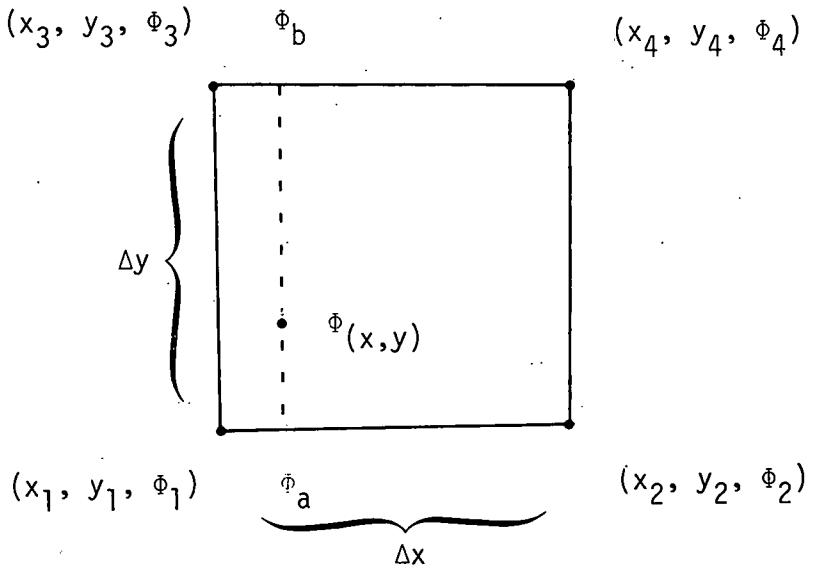

$$\Phi_{(x,y)} = \Phi_a + \frac{(y - y_1)}{\Delta y} (\Phi_b - \Phi_a) \qquad \text{(A-3)}$$

where

$$\Phi_a = \Phi_1 + \left(\frac{x - x_1}{\Delta x}\right) (\Phi_2 - \Phi_1) \qquad \text{(A-4)}$$

and

$$\Phi_b = \Phi_3 + \left(\frac{x - x_1}{\Delta x}\right) (\Phi_4 - \Phi_3) \qquad \text{(A-5)}$$

Substituting Equations (A-4) and (A-5) into Equation A-3 results in an equation in terms of x and y:

$$\Phi_{(x,y)} = \Phi_1 + \left(\frac{x - x_1}{\Delta x}\right)(\Phi_2 - \Phi_1) + \left(\frac{y - y_1}{\Delta y}\right)$$

$$\left[\Phi_3 + \left(\frac{x - x_1}{\Delta x}\right)(\Phi_4 - \Phi_3) - \Phi_1 - \left(\frac{x - x_1}{\Delta x}\right)(\Phi_2 - \Phi_1)\right] \qquad \text{(A-6)}$$

and differentiating Equation (A-6) results in:

$$\frac{\partial \Phi}{\partial x} = \frac{\Phi_2 - \Phi_1}{\Delta x} + \left(\frac{y - y_1}{\Delta y}\right)\left[\left(\frac{\Phi_4 - \Phi_3}{\Delta x}\right) - \left(\frac{\Phi_2 - \Phi_1}{\Delta x}\right)\right] \qquad \text{(A-7)}$$

and

$$\frac{\partial \Phi}{\partial y} = \frac{\Phi_3 - \Phi_1}{\Delta y} + \left(\frac{x - x_1}{\Delta x}\right)\left[\left(\frac{\Phi_4 - \Phi_3}{\Delta y}\right) - \left(\frac{\Phi_2 - \Phi_1}{\Delta y}\right)\right] \qquad \text{(A-8)}$$

which are the x and y gradient components at location (x,y).

TIMING

From the various tests, the results obtained by the HPCP using stored potentials are better than the results using stored gradients. However, other factors to consider include: 1) time involved in storing the potential or gradient surfaces in the data base used by the program, 2) the amount of space required to store these data and 3) the calculational time required by the program to operate on these different data.

DATA STORAGE TIMING AND DISC ALLOCATION

The second test surface was used for timing both the data storage and calculational times. The surface was generated using a 41 x 21 node matrix with 644 time planes. The time required to calculate and store the gradient components ($\partial\Phi/\partial x$ and $\partial\Phi/\partial y$) into the data base was 1 hr, 30 min, while the time required to store potentials into the data base was 26 min.

The amount of space required to store both gradient components was approximately ten thousand 256-word blocks, while the amount of space required to store the potentials was just five thousand 256-word blocks. The method using stored potentials requires only half the storage required by the stored gradient method.

PROGRAM CALCULATIONAL TIMING

Internal clock timing was used by the program to monitor the times required to retrieve data and calculate pathlines. These tests involved a set of nine pathlines for eight separate cases. Table A-1 lists the results.

These results indicated that use of stored potentials is approximately 10% faster than use of stored gradient components in all cases. Where time plane interpolation was examined as a timing parameter interpolation between time planes was approximately 65% slower than not interpolating for similar cases (Table A-1).

TABLE A-1

PATHLINE PROGRAM CALCULATIONAL TIMING

Test	Data Type: Gradient Components	Data Type: Potentials	Time Plane Interpolation	Direction: Down	Direction: Up	Time (Seconds)
1	X			X		165
2	X				X	189
3	X		X	X		242
4	X		X		X	283
5		X		X		148
6		X			X	173
7		X	X	X		230
8		X	X		X	266

APPENDIX B

Procedure Used to Calculate Starting Coordinates of Pathlines Bounding Equal Flow

APPENDIX B

The procedure described here was designed to calculate pathline starting coordinates in a uniform manner by spacing the coordinates in a flow field so that equal flow exists between any two adjacent pathlines. To accomplish this it is necessary to: 1) calculate the signed flows in the x and y direction and build a binary data file for each, 2) use these data files to calculate the starting coordinates and 3) plot the resulting coordinates along with the associated circular arc.

To produce the binary data files, the desired potential matrix is generated using the source term in the selected region and calculations are performed to produce the signed flows in the x and y direction at each VTT node which does not have a 01 calculational type.[a] A y direction flow from low to high y node numbers has a positive sign as does an x direction flow from low to high x node numbers. The transmissivity, gradients and flow channel widths are the same as used by the VTT calculational codes. Figure B-1 illustrates the method used to calculate the signed x flow (Fx) and signed y flow (Fy) at a VTT node.

The pathline starting locations are calculated by beginning at the specified location on the circumference of the circle which has its center at (Xc, Yc) and a radius, R. The starting location on the circle is specified in the local Cartesian coordinate system with the (0,0) at (Xc, Yc). A delta angle increment is also specified. The initial starting point is taken as the first pathline starting point, a delta angle increment of arc is added, and the flow through that portion of arc is calculated and added to a running sum. Delta arc increments and their flow contributions are added until the running sum has equalled or just surpassed the desired flow spacing between pathlines specified in the input file. The current location on the circumference is then taken as the next starting point; the running sum is set to zero; and the process is repeated until all the desired pathline starting points have been defined.

---

[a] W. V. DeMier, A. E. Reisenauer and K. L. Kipp, "Variable Thickness Transient Groundwater Flow Model User's Manual," BNWL-1704, Battelle, Pacific Northwest Laboratories, 1974.

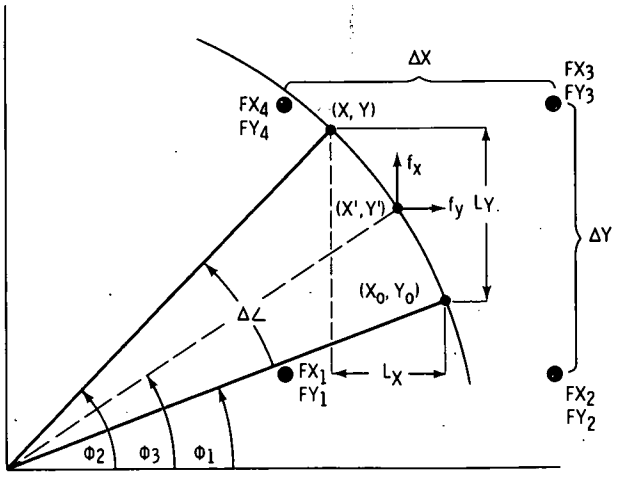

where:

L_x = width of y flow channel = abs(x_ϕ-x_1)

L_y = width of x flow channel = abs(y_ϕ-y_1)

FRC_x = fraction of interpolated x flow for point (x', y') passing through the arc = $\frac{L_x}{\Delta y}$

FRC_y = same as FRC_x but for y flow = $\frac{L_y}{\Delta y}$

FY' = bilinear interpolated Y flow at (x', y') from $FY_1 \rightarrow FY_4$ values

FX' = bilinear interpolated X flow at (x',y') from $FX_1 \rightarrow FX_4$ values

then:

fx = FY' * FRC_y * SIGNY (quadrant)

fy = FX' * FRC_x * SIGNX (quadrant)

where:

SIGNX (quadrant) = +1 (quadrant 1 and 4)
-1 (quadrant 2 and 3)

SIGNY (quadrant) = +1 (quadrant 1 and 2)
-1 (quadrant 3 and 4)

TOTAL ARC FLOW = fy + fx

FIGURE B-1

DIAGRAM ILLUSTRATING HOW THE SIGNED FLOW AT A NODE IS CALCULATED FOR BOTH THE X AND Y DIRECTIONS

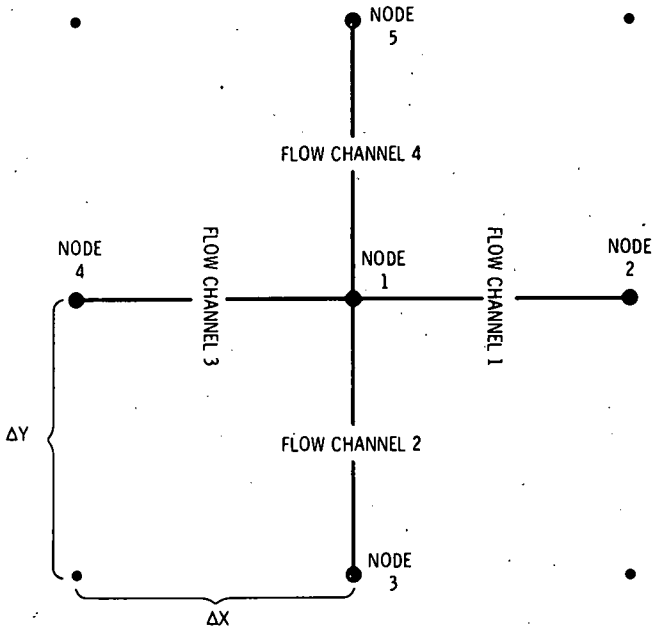

$$T_i = (h_i - h_i^o)\, K_i \quad (i = 1,5)$$

where:

T = transmissivity
h = hydraulic potential
h^o = aquifer bottom elevation
K = vertically averaged hydraulic conductivity
i = node number

$$F_1 = \left[\left(\frac{T_1 + T_2}{2}\right)\left(\frac{h_1 - h_2}{\Delta x}\right)\right] A\, \Delta_y$$

$$F_2 = \left[\left(\frac{T_1 + T_3}{2}\right)\left(\frac{h_3 - h_1}{\Delta y}\right)\right] A_2 \Delta x$$

$$F_3 = \left[\left(\frac{T_1 + T_4}{2}\right)\left(\frac{h_4 - h_1}{\Delta x}\right)\right] A_3 \Delta y$$

$$F_4 = \left[\left(\frac{T_1 + T_5}{2}\right)\left(\frac{h_1 - h_5}{\Delta y}\right)\right] A_4 \Delta x$$

$$Fx = \frac{F_1 + F_3}{2}, \quad Fy = \frac{F_2 + F_4}{2}$$

where:

F_i = signed flow
A_i = function of calculational type of node
(= fraction of total width available for flow)
i = flow channel (1-4)
Δx = grid spacing in y direction
Δy = grid spacing in x direction
Fx = total signed flow in x direction
Fy = total signed flow in y direction

FIGURE B-2

DIAGRAM ILLUSTRATING HOW THE FLOW FROM A Δ ARC IS CALCULATED FROM THE ARC PARAMETERS AND THE X AND Y FLOW FILES

Figure B-2 shows the mathematics used to calculate the flow through any delta arc segment. Delta arc steps are taken whenever possible unless the delta step crosses the boundary between nodes. The delta step is then cut back so that the entire arc length lies within one set of four nodes as shown in Figure B-2.

Once the x and y flow files have been calculated these data are used to calculate the pathline starting coordinates along the circumference of an arc with specified center and radius and a specified flow increment in ft^3/day between locations. Three cases were used in this study. The first case used a VTT-generated surface with one source and one sink with three test circles; the second case used a VTT-generated Hanford potential surface to determine if the procedure could reproduce the calculated flow at 200-East and 200-West Areas; and the final case used the same VTT-generated Hanford potential surface to produce the starting locations of the pathlines used in the Hanford study.

The potential plot in Figure B-3 illustrates the steady-state potential contours and calculational types for the first test problem used to analyze this procedure. This test problem is for a 1000-ft 35x35 grid system with a uniform K of 5000 ft/day, held node potentials at 100-ft and bottom elevation at 1 ft. There is one source and one sink. The source is at line 17 column 20 at 300,000 ft^3/day and the sink is at line 17 column 14 at -300,000 ft^3/day. This test problem was set up and run to steady state with the VTT calculational code, and then the x flow data file and y flow data file were created. Three circles were then used to demonstrate the procedure. The first test circle (Figure B-4) was centered at the sink location with a radius 3000 ft so the source would not be included. The total flow calculated was -298,800 ft^3/day (only 0.4% in error). The second test circle (Figure B-4) was centered at the source location with a 3000-ft radius and the calculated flow was 298,300 ft^3/day (only 0.6% in error). The third test circle (Figure B-5) was centered between the source and sink with a radius of 6000 ft so both the source and sink would be included and the calculated flow was 584 ft^3/day (less than 1% error when compared to the magnitude of the source and sink values).

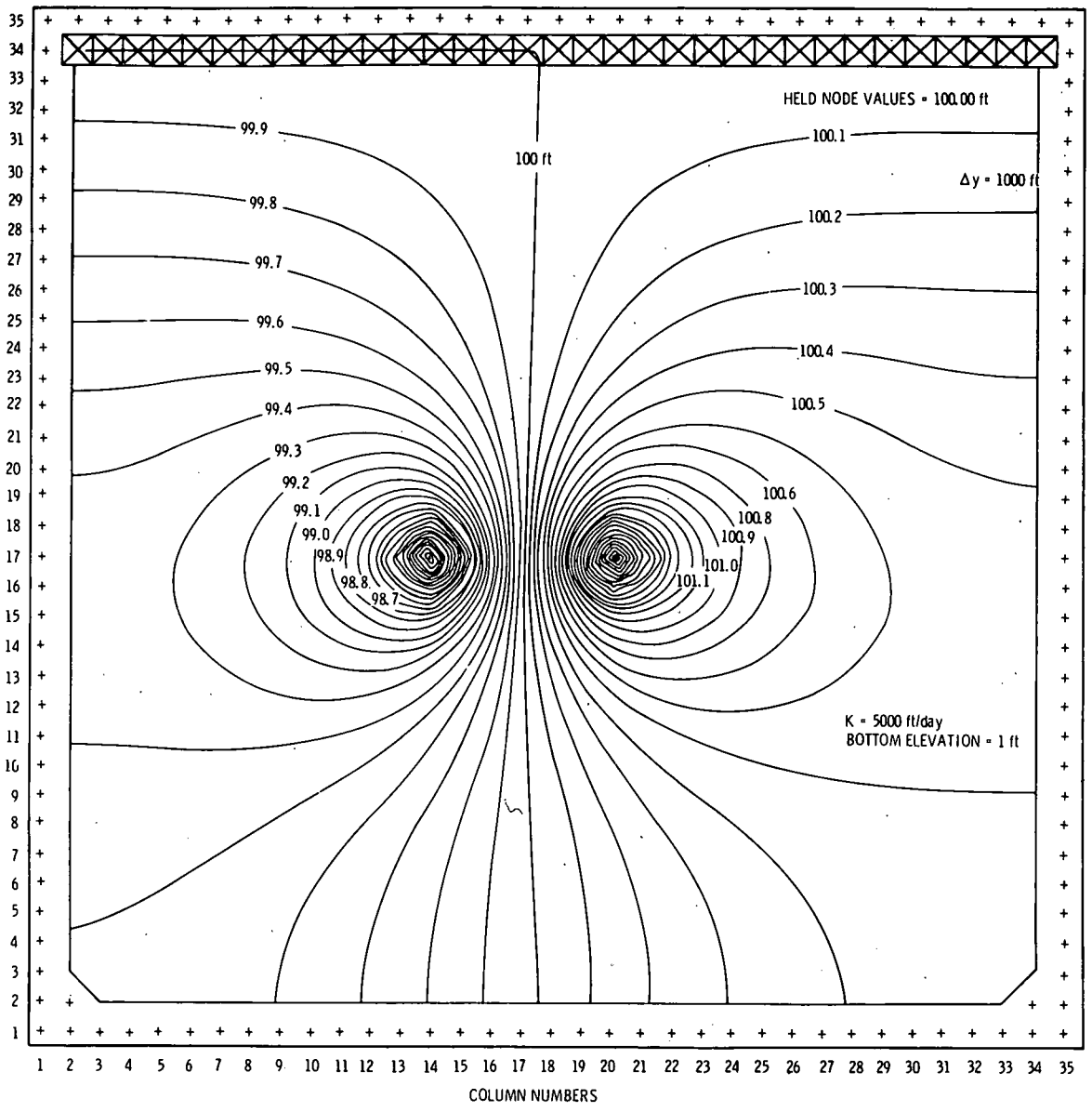

FIGURE B-3

STEADY-STATE POTENTIAL CONTOURS AND CALCULATIONAL TYPES FOR TEST SURFACE USED TO CHECK EQUAL FLOW PROCEDURE

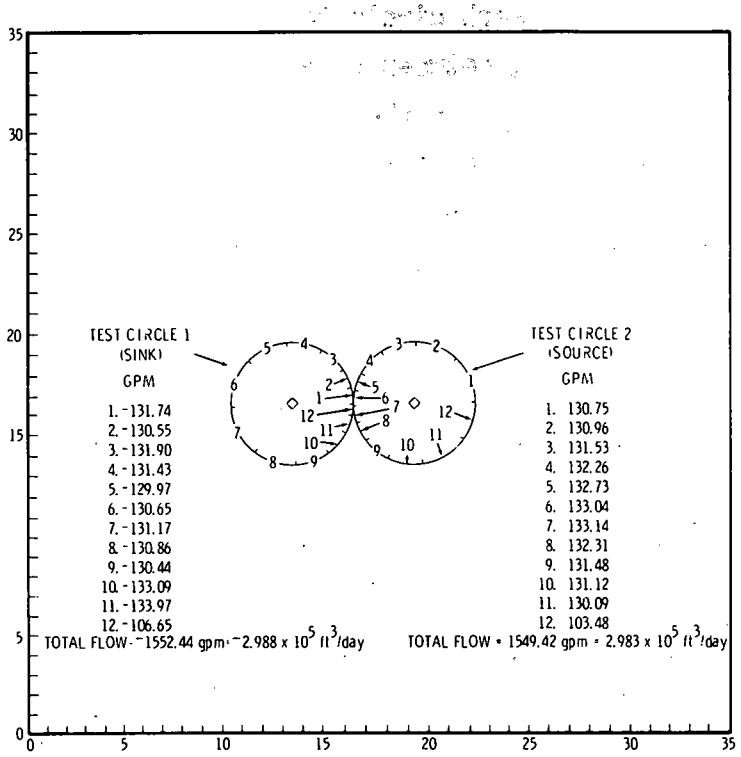

FIGURE B-4

PLOT SHOWING RESULTS OF EQUAL FLOW PROCEDURE FOR TEST CIRCLE 1 (SINK) AND TEST CIRCLE 2 (SOURCE)

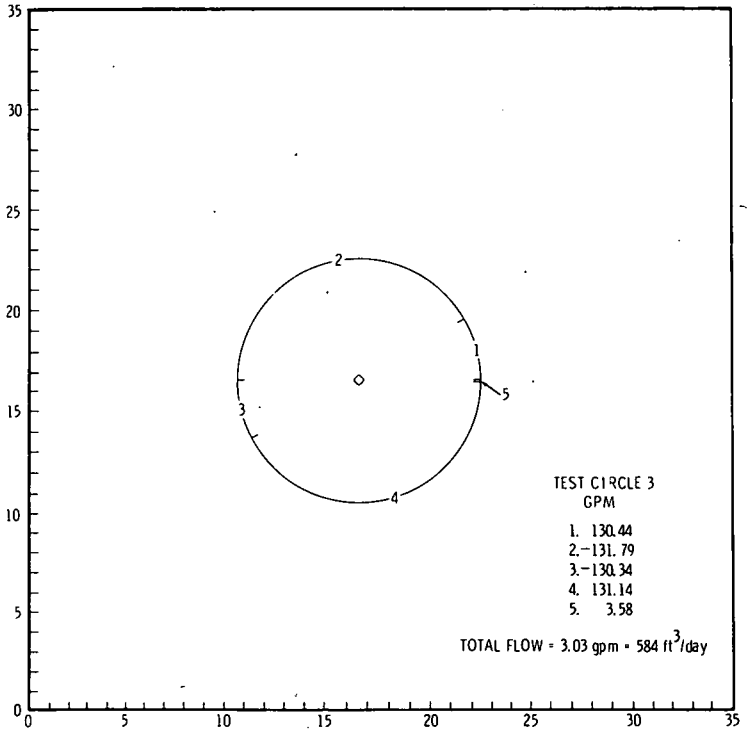

FIGURE B-5

PLOT SHOWING RESULTS OF EQUAL FLOW PROCEDURE FOR TEST CIRCLE 3

These two plots show for each circle the requested arc, pathline starting locations, the flow exiting between pathline starting points, the location of the center of the circle and the total flow exiting the arc requested. The input parameters and resulting equally spaced flow locations for these three test circles are shown in Table B-1.

In the second test case the Hanford 1974 average Q's were used and a steady-state solution was obtained. The results of this test are shown in Figure B-6. The total 200-West and 200-East disposal rates were summed by hand and compared to the results obtained from the computer calculated methods. As with Test Case 1, the Q's agreed to within 1%.

Since the test cases proved this method to be effective it was used to determine the starting pathline location in the 200-East and 200-West Areas for the Hanford study. Figure B-7 shows a plot illustrating the position of the 200-West Area and 200-East Area pathline starting points and associated area boundaries used in the Hanford Pathline Study.

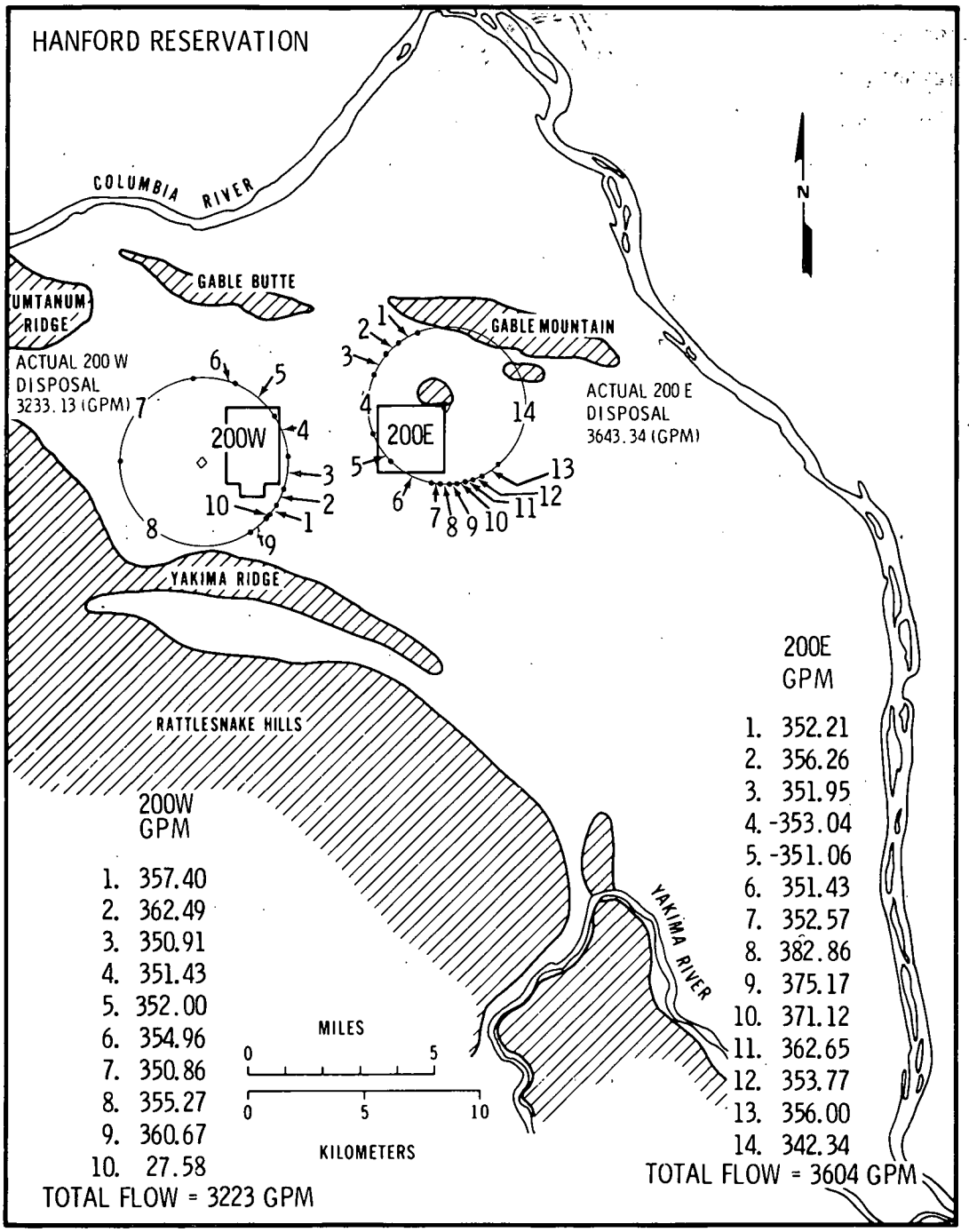

FIGURE B-6

DIAGRAM ILLUSTRATING THAT BY USING A REALISTIC HANFORD SURFACE THE CALCULATED FLOW CLOSELY COMPARES WITH THE ACTUAL DISPOSAL RATES IN THE 200 EAST AND 200 WEST AREAS

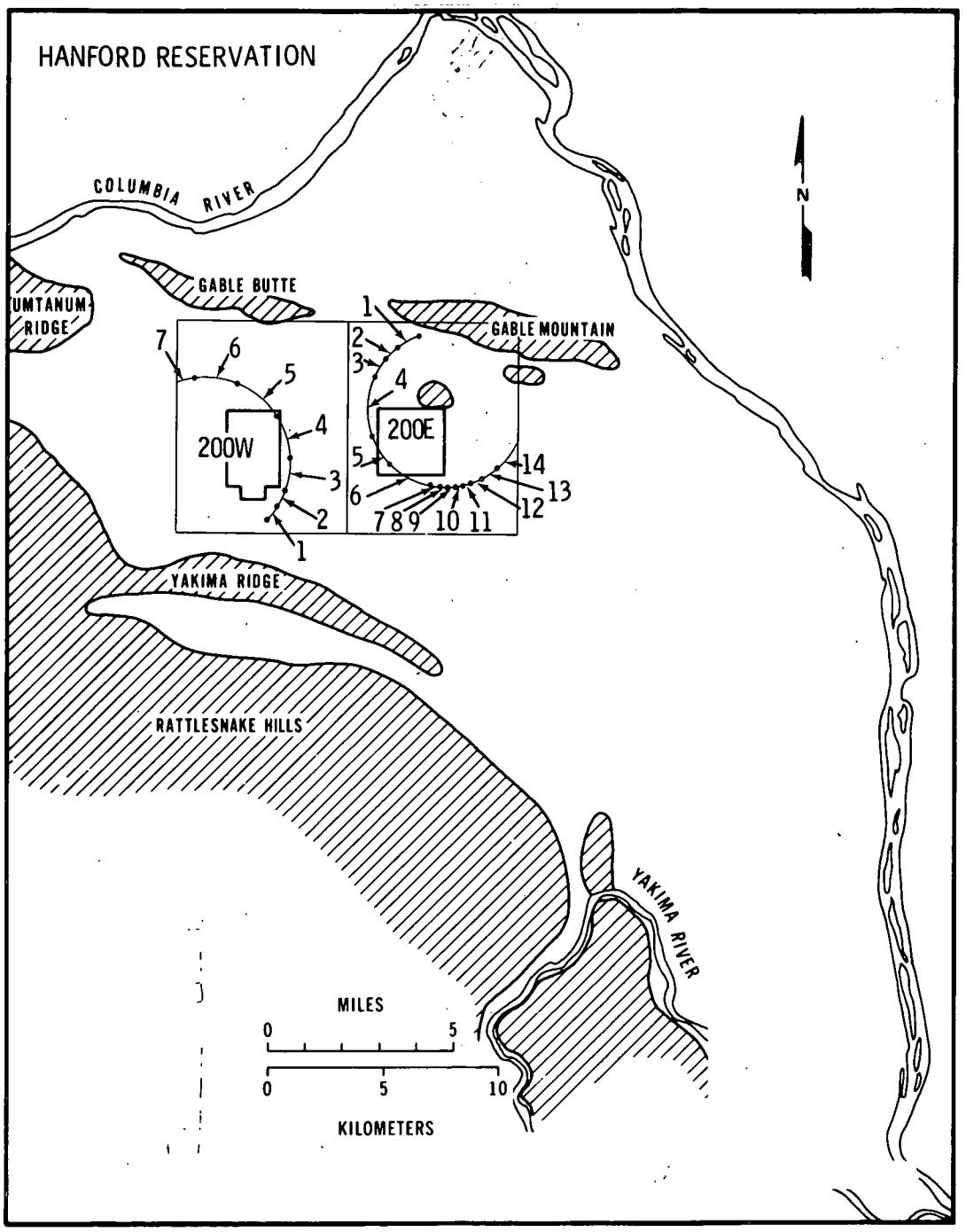

FIGURE B-7

DIAGRAM ILLUSTRATING THE POSITIONS CHOSEN FOR PATHLINE STARTING LOCATIONS IN BOTH THE 200 EAST AND 200 WEST AREAS THE BOXES SHOW THE POSITIONS OF THE HIGH RESOLUTION REGIONS (666.67 FT NODE SPACING)

APPENDIX C

Hanford Pathline Calculational Program Interpolation Scheme

APPENDIX C

Hanford Pathlines Calculational Program Interpolation Scheme

I. When all four nodal values of the parameter to be interpolated are >0 normal bilinear interpolation on rectangles is used.

II. If only 2 nodal values are >0 the pathline or streamline is terminated.

III. If 3 nodal values exist linear interpolation on triangles is used if the point to be interpolated lies within the triangle defined by the nodal values which exist.

IV. The triangular interpolation formula for the parameter and the x and y gradients of the parameter are:

$$VAL = VAL1\ (1 - \xi - \eta) + VAL2\ (\xi) + VAL3\ (\eta)$$

$$\frac{\partial VAL}{\partial x} = -VAL1\ \frac{\partial \xi}{\partial X} + VAL2\ \frac{\partial \xi}{\partial X}$$

$$\frac{\partial VAL}{\partial Y} = -VAL1\ \frac{\partial \eta}{\partial Y} + VAL3\ \frac{\partial \eta}{\partial Y}$$

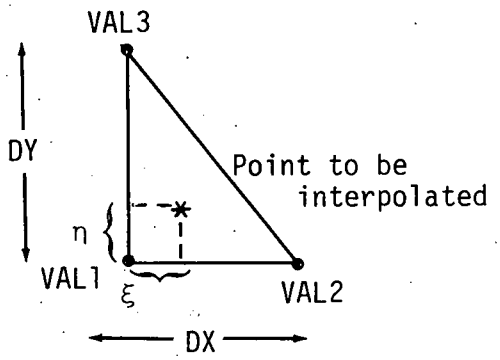

V. For the four possible triangles that might exist Figure C-1 defines the variables for the formula in IV above.

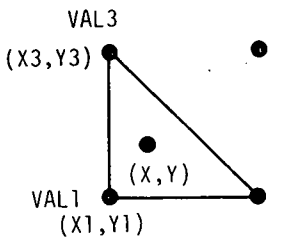

Point (X,Y) within the triangle if $\alpha + \beta \leq 1$

$\alpha = (X-X1)/DX$

$\beta = (Y-Y1)/DY$

$\eta = \frac{Y-Y1}{DY}$, $\xi = \frac{X-X1}{DX}$, $\frac{\partial \xi}{\partial X} = \frac{1}{DX}$, $\frac{\partial \eta}{\partial Y} = \frac{1}{DY}$

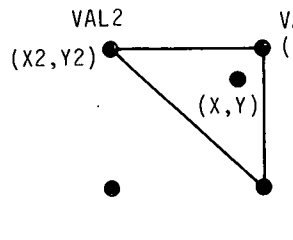

Point (X,Y) within the triangle if $\alpha + \beta \geq 1$

$\alpha = (X-X2)/DX$

$\beta = (Y-Y3)/DY$

$\eta = \frac{Y1-Y}{DY}$, $\xi = \frac{X1-X}{DX}$, $\frac{\partial \xi}{\partial X} = \frac{-1}{DX}$, $\frac{\partial \eta}{\partial Y} = \frac{-1}{DY}$

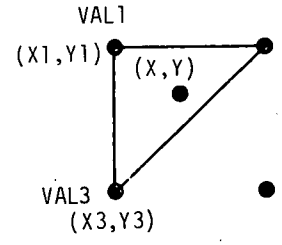

Point (X,Y) within the triangle if $\alpha - \beta \leq 0$

$\alpha = (X-X1)/DX$

$\beta = (Y-Y3)/DY$

$\eta = \frac{Y1-Y}{DY}$, $\xi = \frac{X-X1}{DX}$, $\frac{\partial \xi}{\partial X} = \frac{1}{DX}$, $\frac{\partial \eta}{\partial Y} = \frac{-1}{DY}$

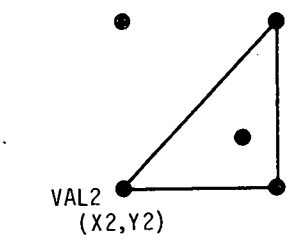

Point (X,Y) within the triangle if $\alpha - \beta \geq 0$

$\alpha = (X-X2)/DX$

$\beta = (Y-Y1)/DY$

$\eta = \frac{Y-Y1}{DY}$, $\xi = \frac{X1-X}{DX}$, $\frac{\partial \xi}{\partial X} = \frac{-1}{DX}$, $\frac{\partial \eta}{\partial Y} = \frac{1}{DY}$

FIGURE C-1

DIAGRAM ILLUSTRATING THE INTERPOLATION FORMULA USED BY HPCP IN CALCULATING VARIABLES AND GRADIENTS OF VARIABLES

APPENDIX D

Predicted Potential Plots for the 21 Year Hanford Pathline Study
for the Large Region as Well as the Two Small Regions
(200 West and 200 East)

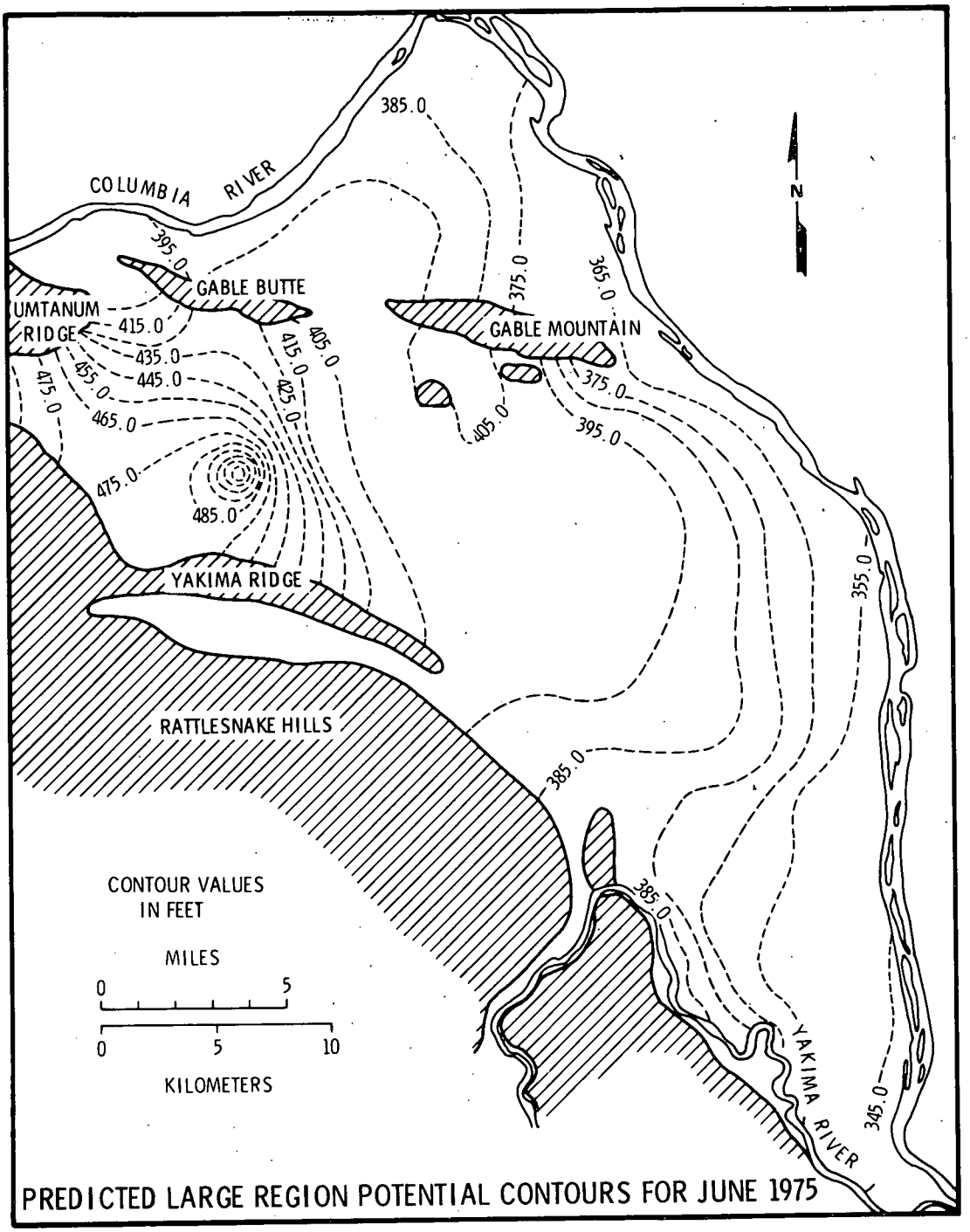

FIGURE D-1

PLOT OF THE VTT PREDICTED POTENTIAL CONTOURS FOR JUNE 1975

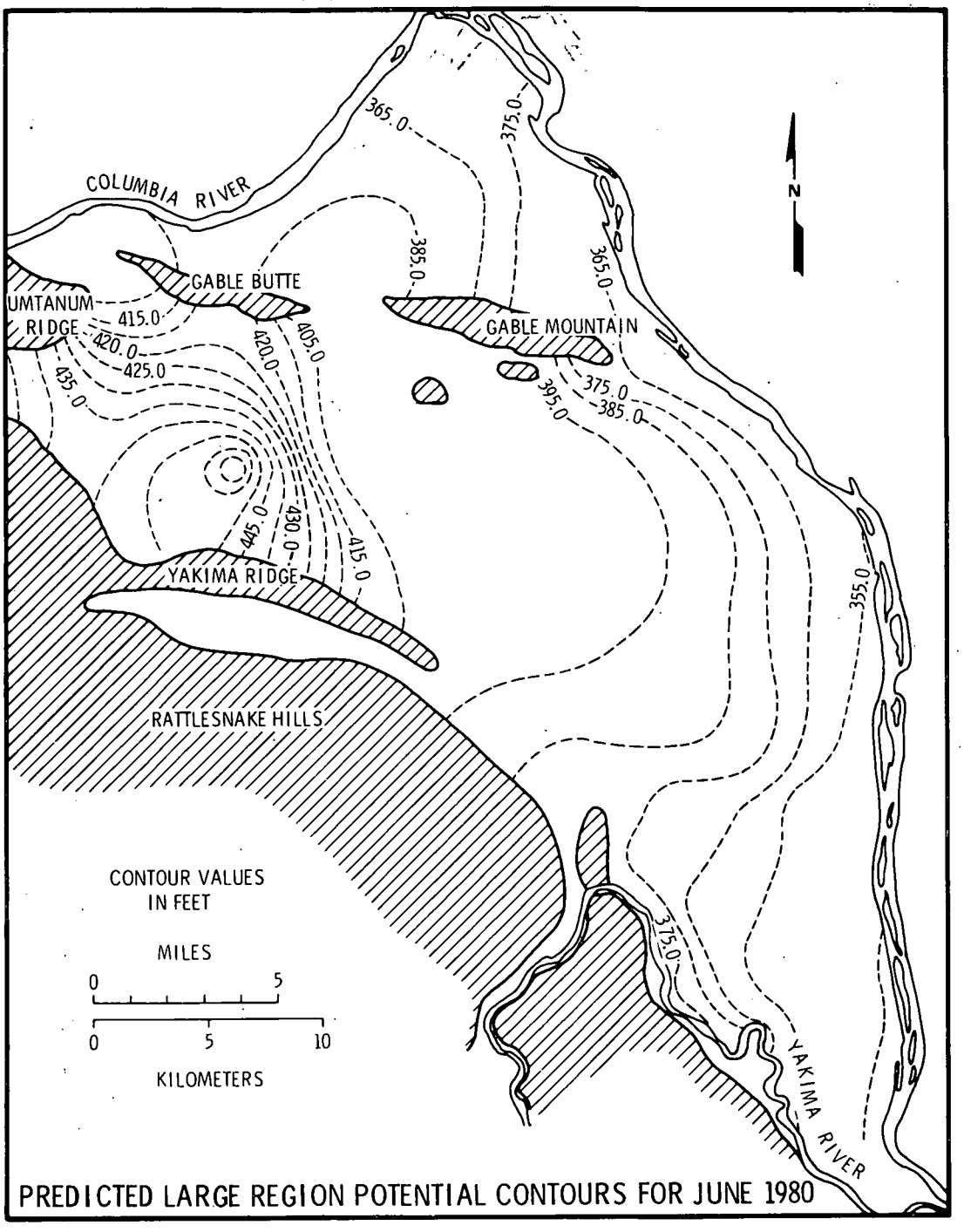

FIGURE D-2

PLOT OF THE VTT PREDICTED POTENTIAL CONTOURS FOR JUNE 1980

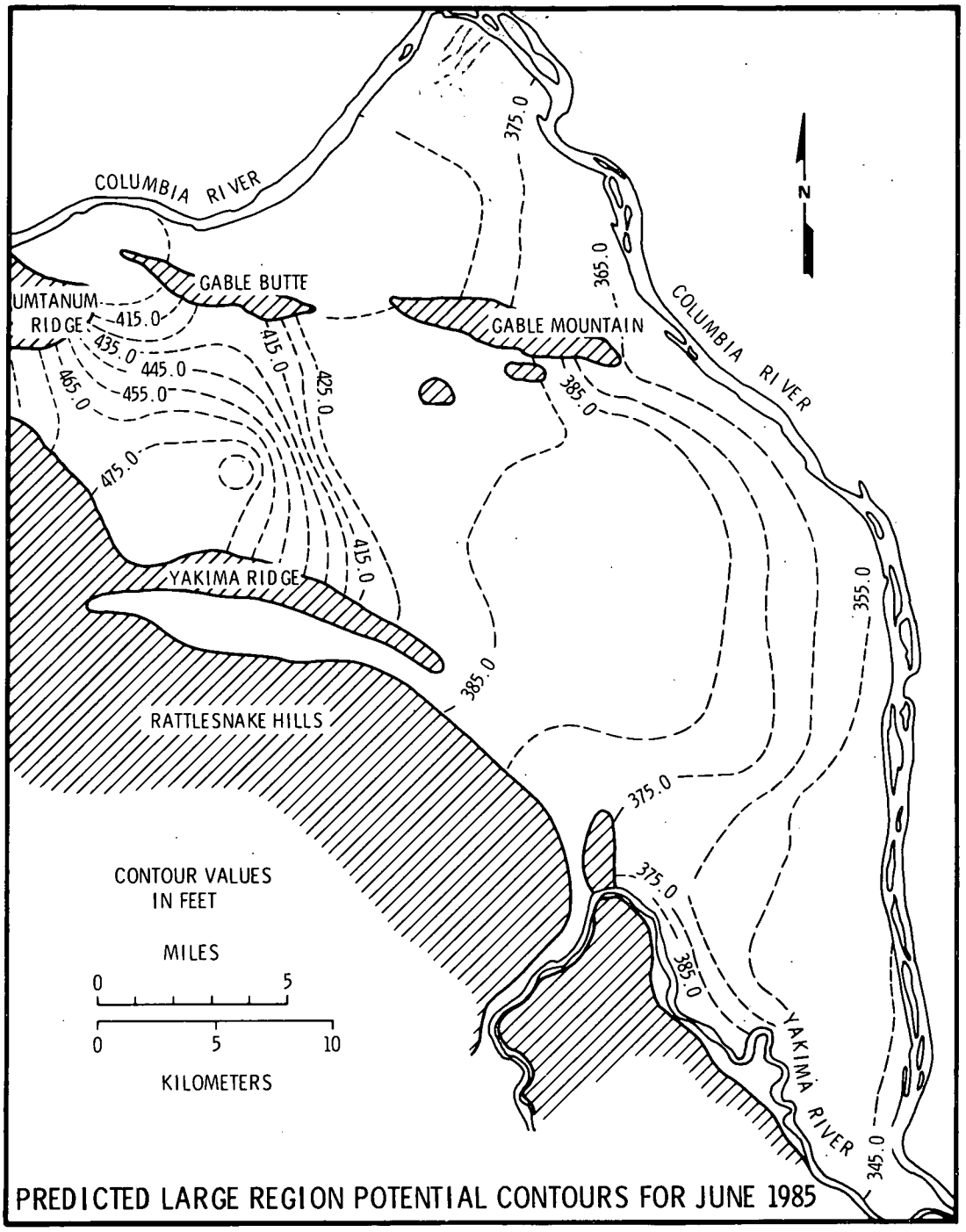

FIGURE D-3

PLOT OF THE VTT PREDICTED POTENTIAL CONTOURS FOR JUNE 1985

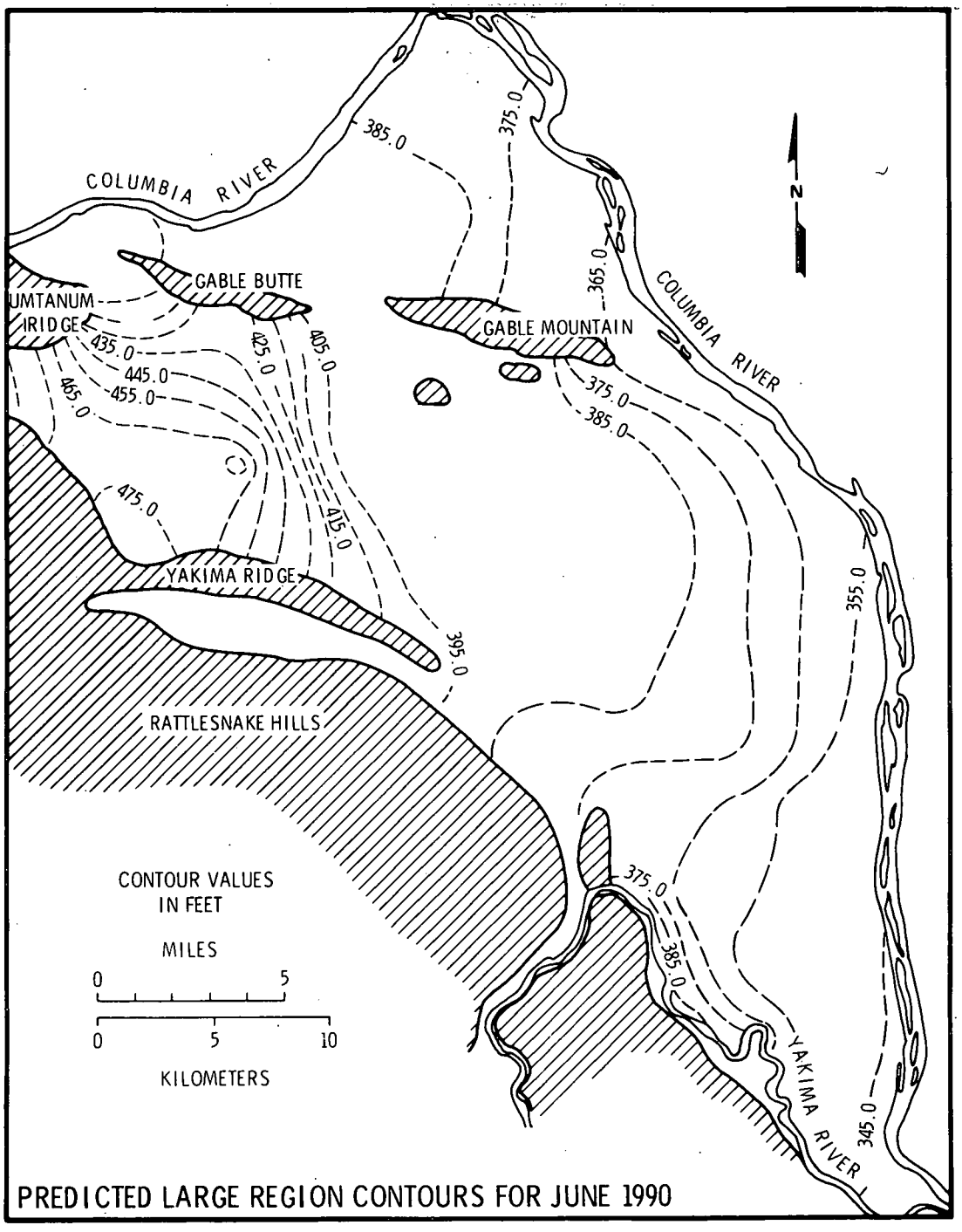

FIGURE D-4

PLOT OF THE VTT PREDICTED POTENTIAL CONTOURS FOR JUNE 1990

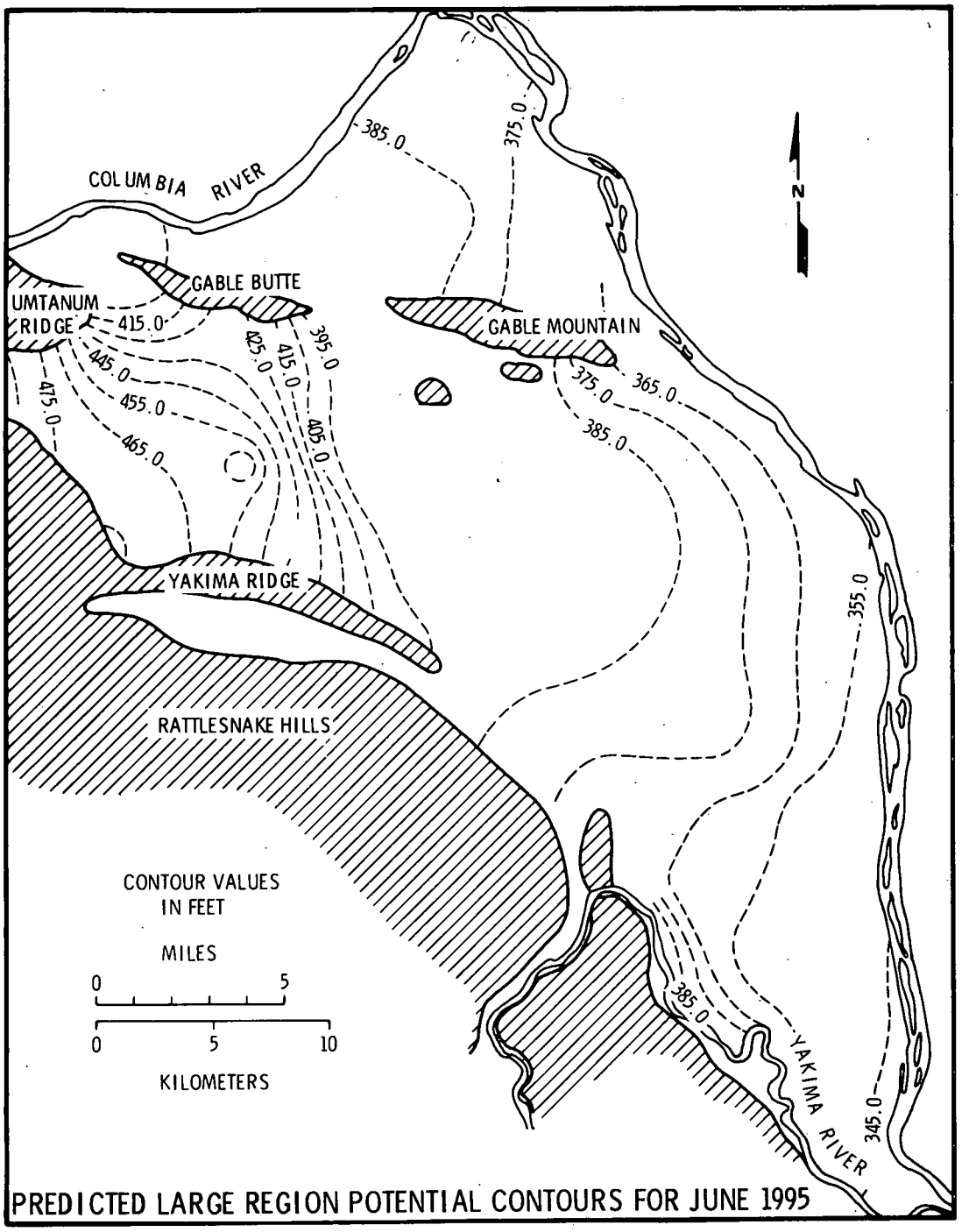

FIGURE D-5

PLOT OF THE VTT PREDICTED POTENTIAL CONTOURS FOR JUNE 1995

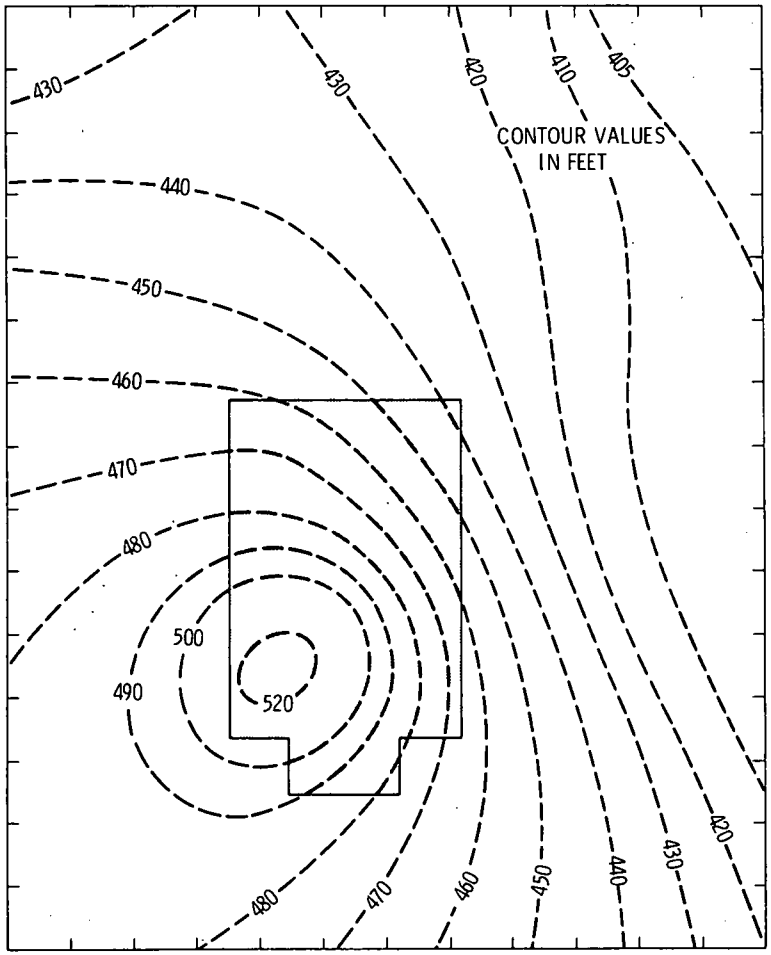

FIGURE D-6

PLOT OF THE VTT PREDICTED POTENTIAL CONTOURS FOR THE SMALL REGION (200 WEST AREA) FOR JUNE 1975

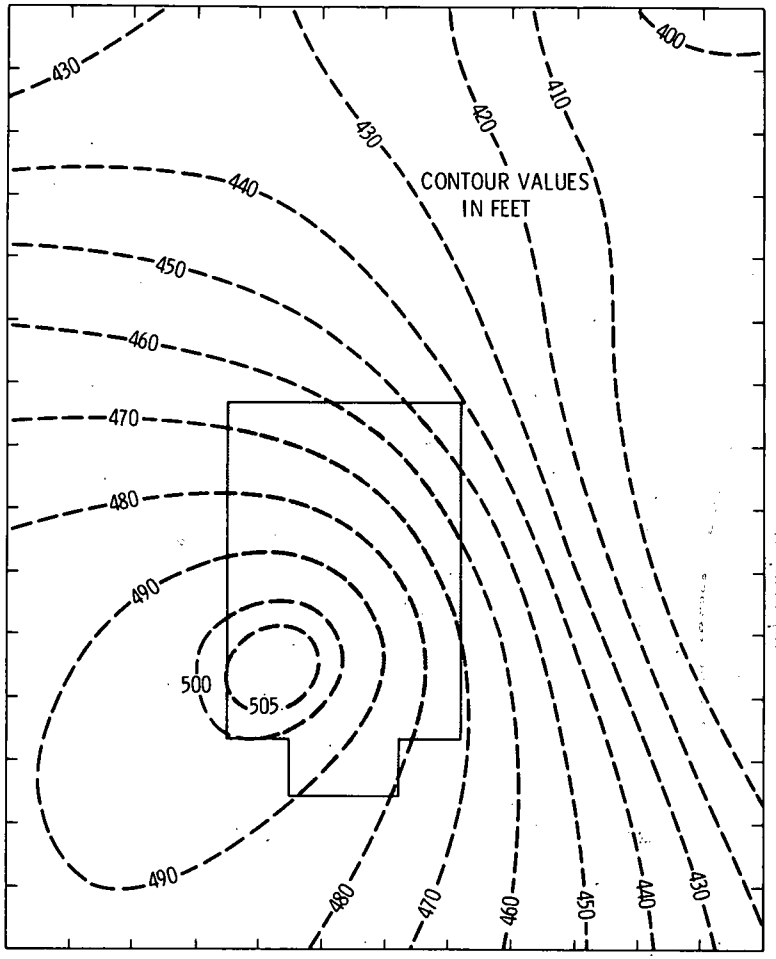

FIGURE D-7

PLOT OF THE VTT PREDICTED POTENTIAL CONTOURS FOR THE SMALL REGION (200 WEST AREA) FOR JUNE 1980

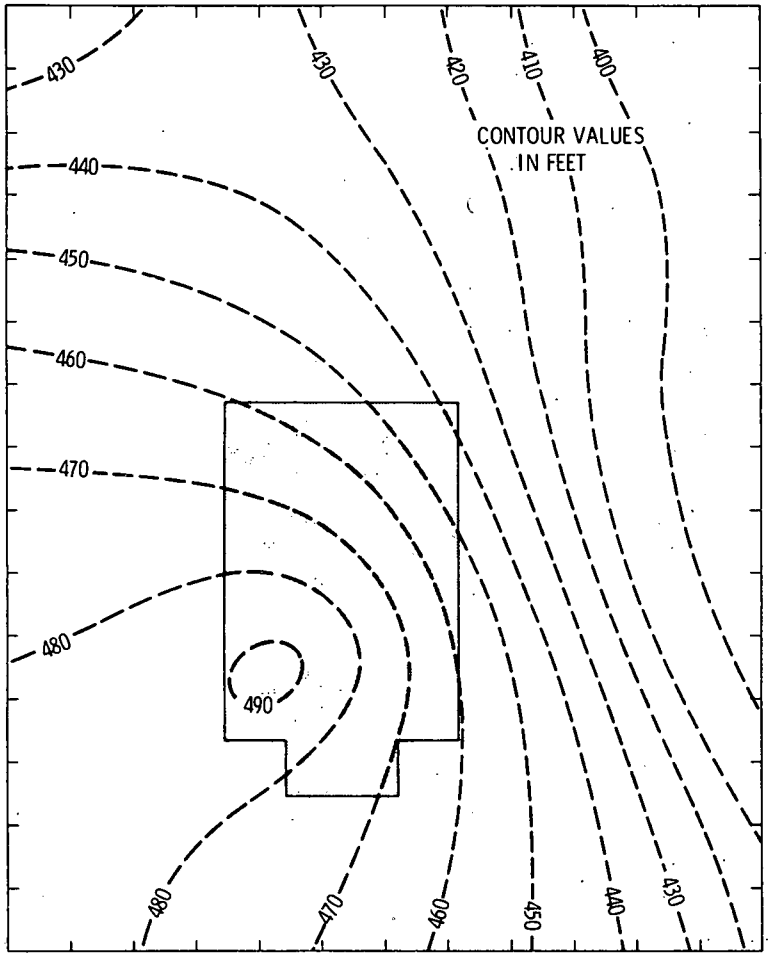

FIGURE D-8

PLOT OF THE VTT PREDICTED POTENTIAL CONTOURS FOR THE SMALL REGION (200 WEST AREA) FOR JUNE 1985

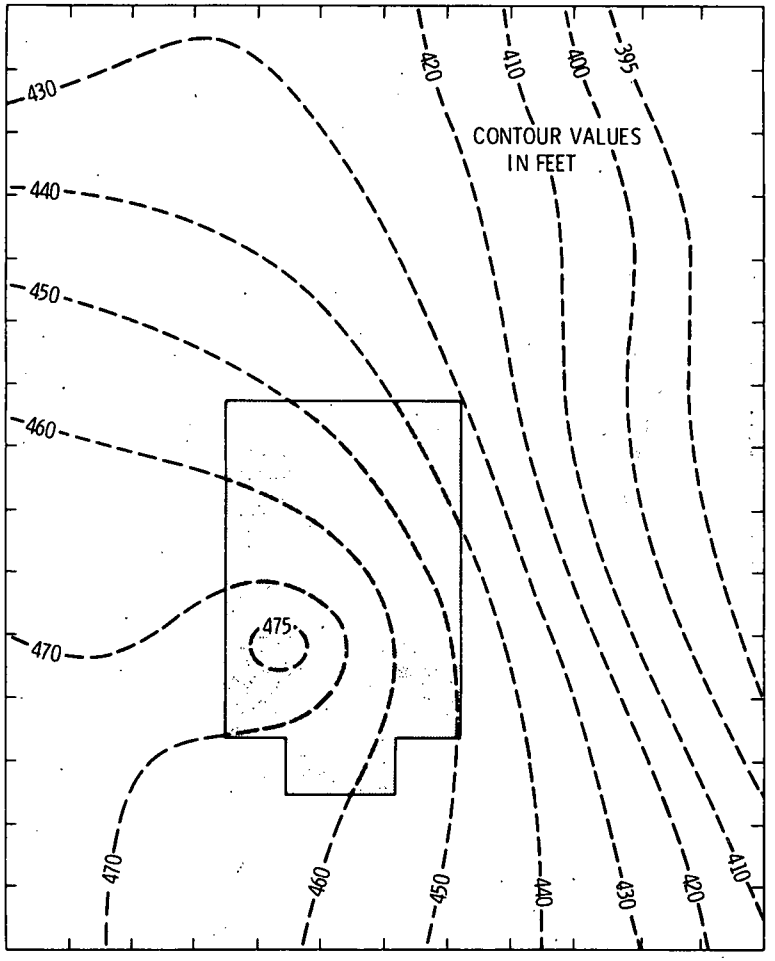

FIGURE D-9

PLOT OF THE VTT PREDICTED POTENTIAL CONTOURS FOR THE SMALL REGION (200 WEST AREA) FOR JUNE 1990

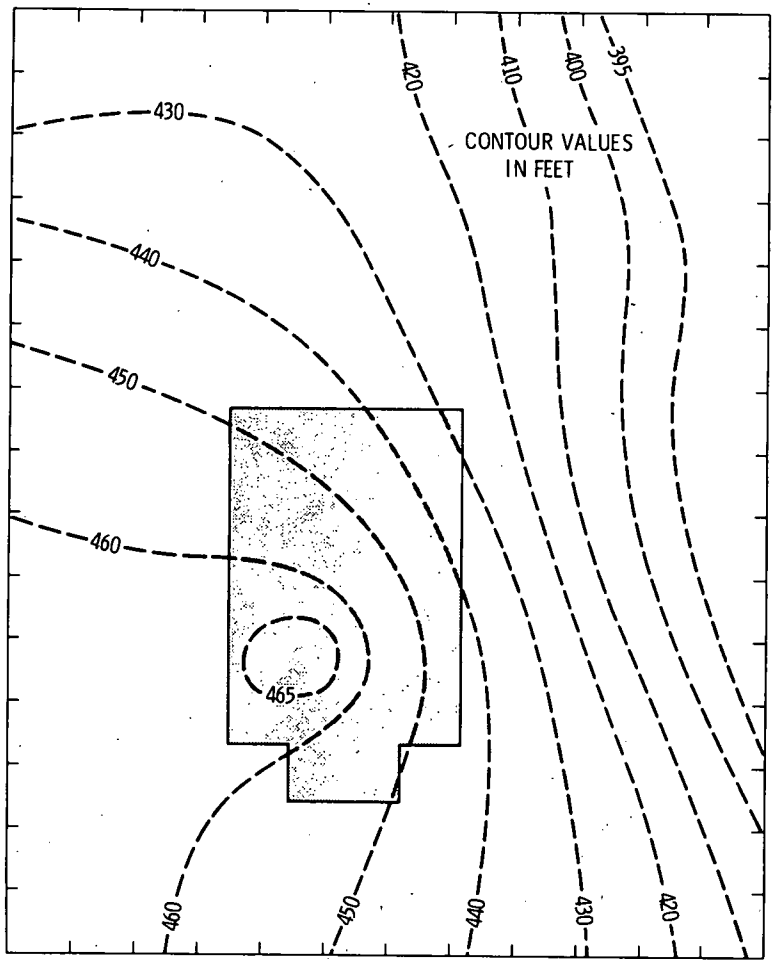

FIGURE D-10

PLOT OF THE VTT PREDICTED POTENTIAL CONTOURS FOR
THE SMALL REGION (200 WEST AREA) FOR JUNE 1995

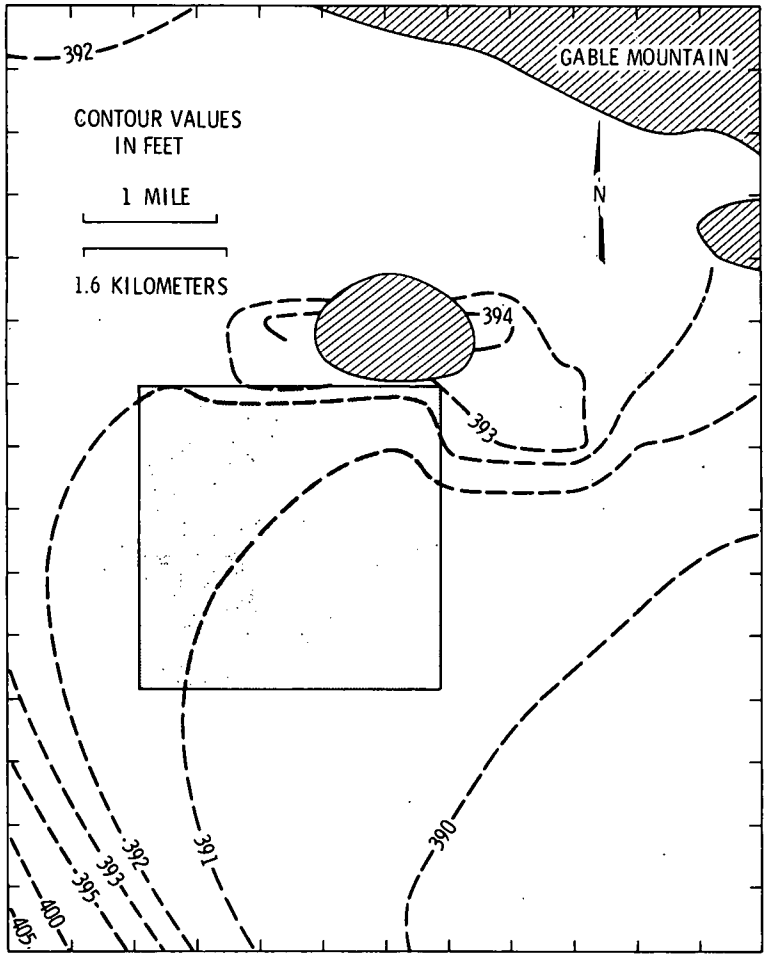

FIGURE D-11

PLOT OF THE VTT PREDICTED POTENTIAL CONTOURS FOR THE SMALL REGION (200 EAST AREA) FOR JUNE 1975

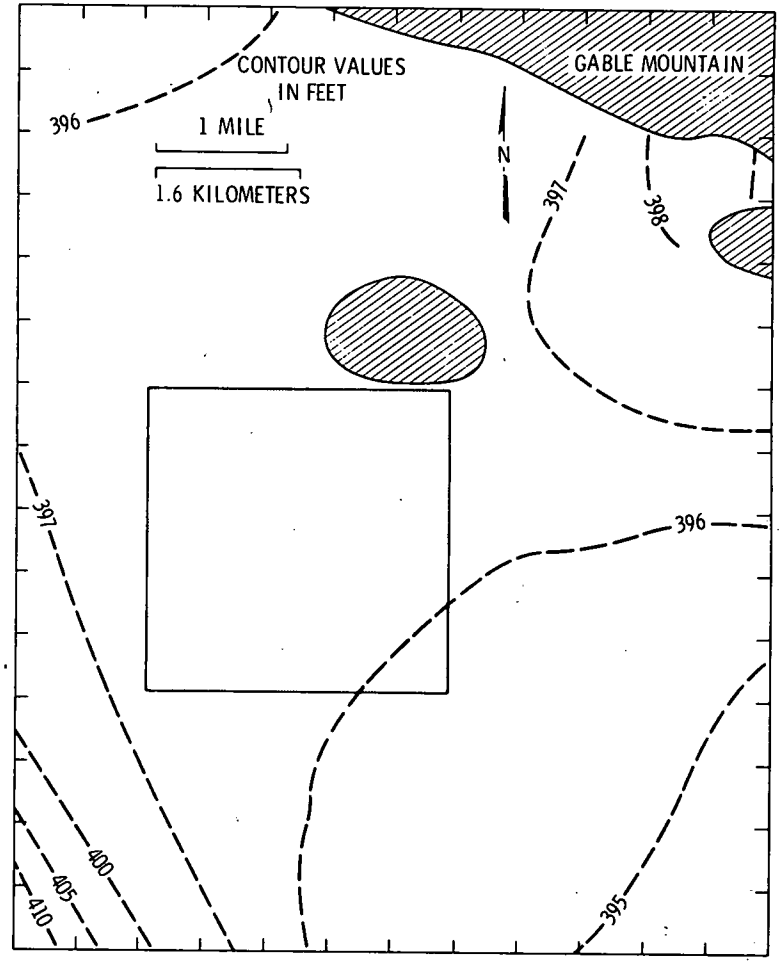

FIGURE D-12

PLOT OF THE VTT PREDICTED POTENTIAL CONTOURS FOR THE SMALL REGION (200 EAST AREA) FOR JUNE 1980

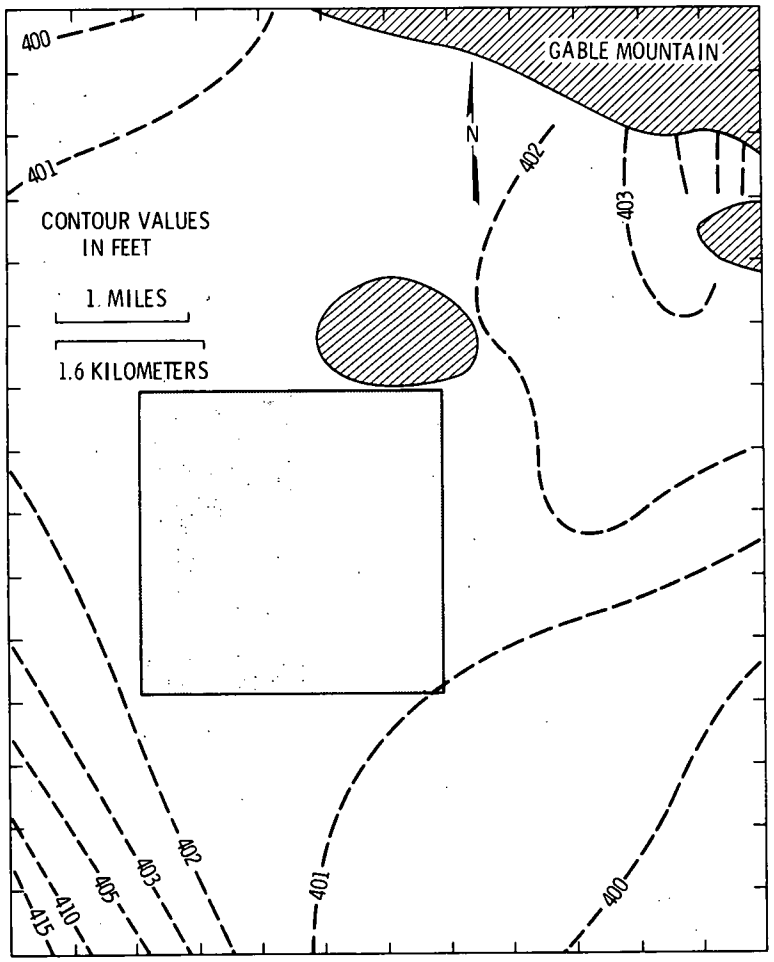

FIGURE D-13

PLOT OF THE VTT PREDICTED POTENTIAL CONTOURS FOR THE SMALL REGION (200 EAST AREA) FOR JUNE 1985

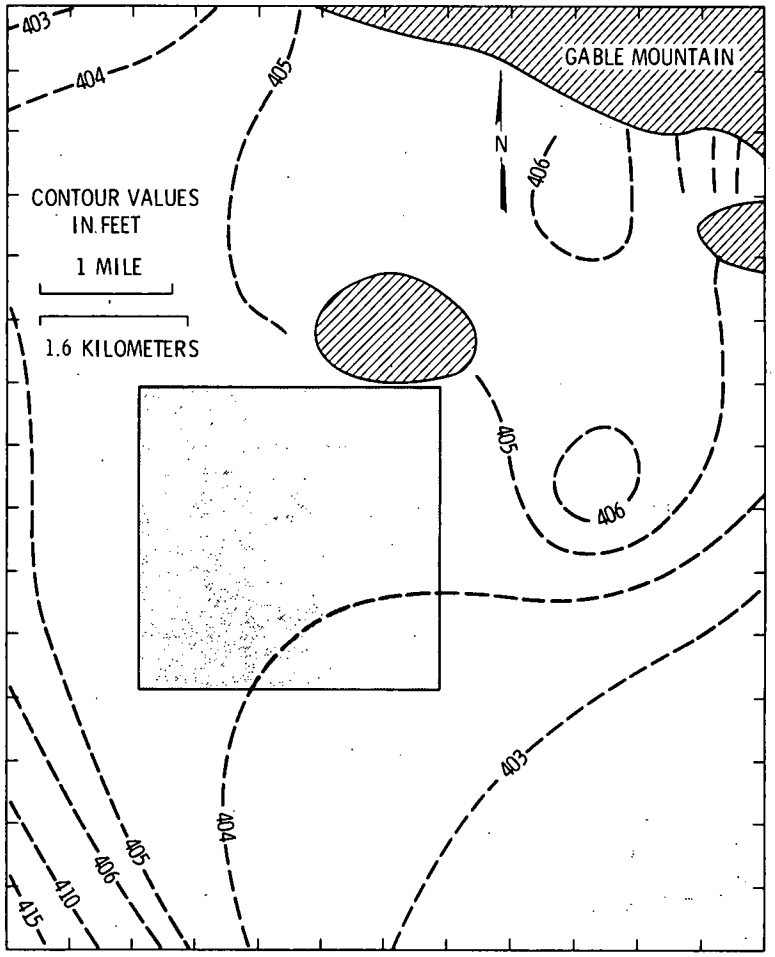

FIGURE D-14

PLOT OF THE VTT PREDICTED POTENTIAL CONTOURS FOR THE SMALL REGION (200 EAST AREA) FOR JUNE 1990

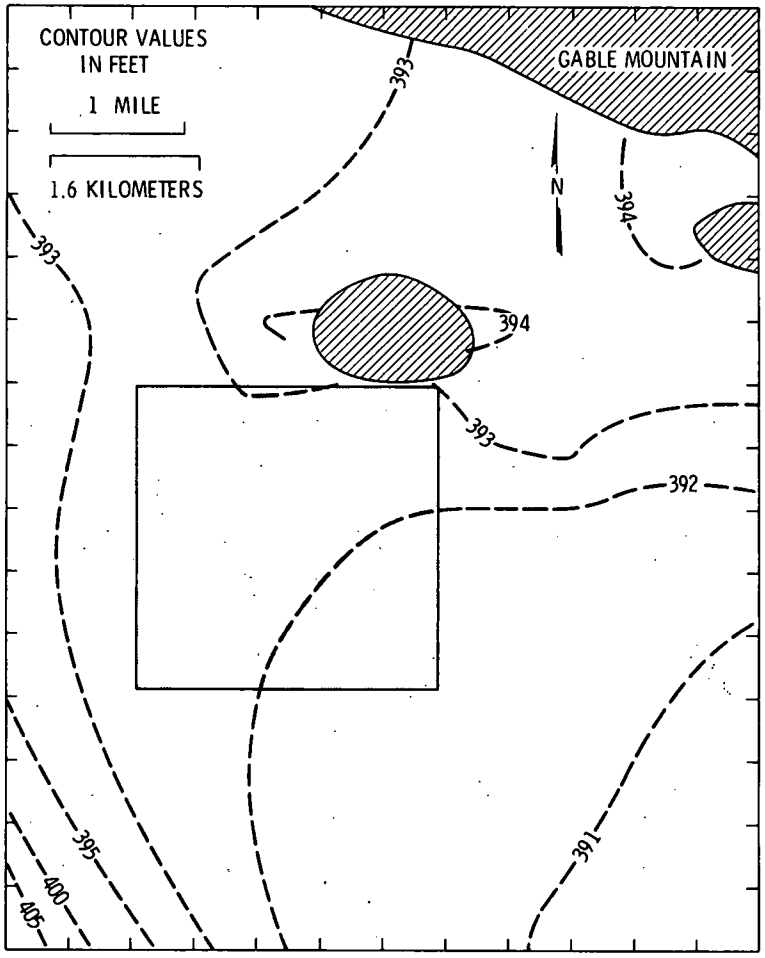

FIGURE D-15

PLOT OF THE VTT PREDICTED POTENTIAL CONTOURS FOR THE SMALL REGION (200 EAST AREA) FOR JUNE 1995

APPENDIX E

Plots of the Streamlines for the 200 West and 200 East Areas
Using the 1975, 1980, 1985, 1990 and 1995 Potential Surfaces
This Appendix Also Contains the Summary Data for These Streamlines

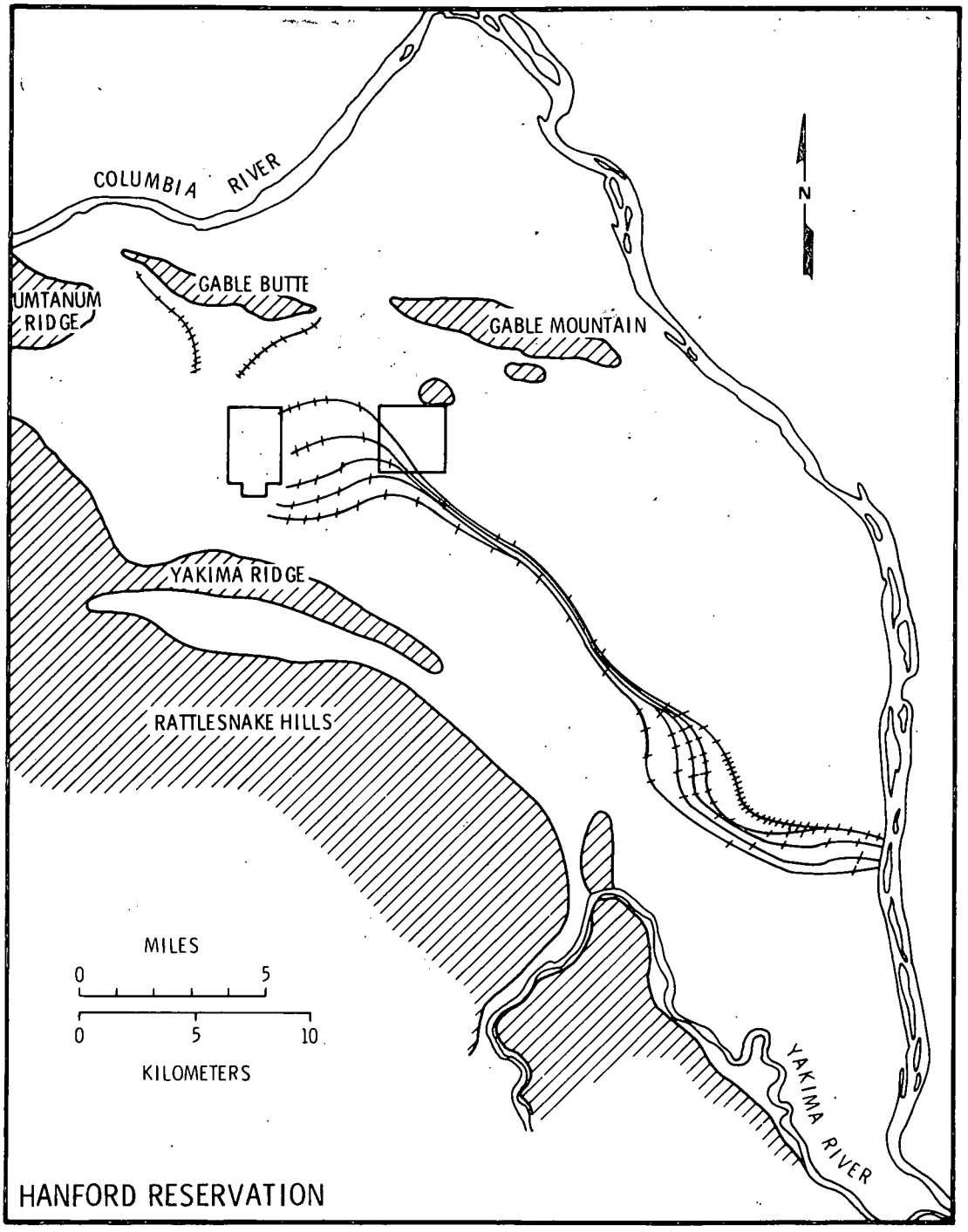

FIGURE E-1

PLOT OF THE STREAMLINES FOR 200 WEST AREA
ON THE 1975 POTENTIAL SURFACE

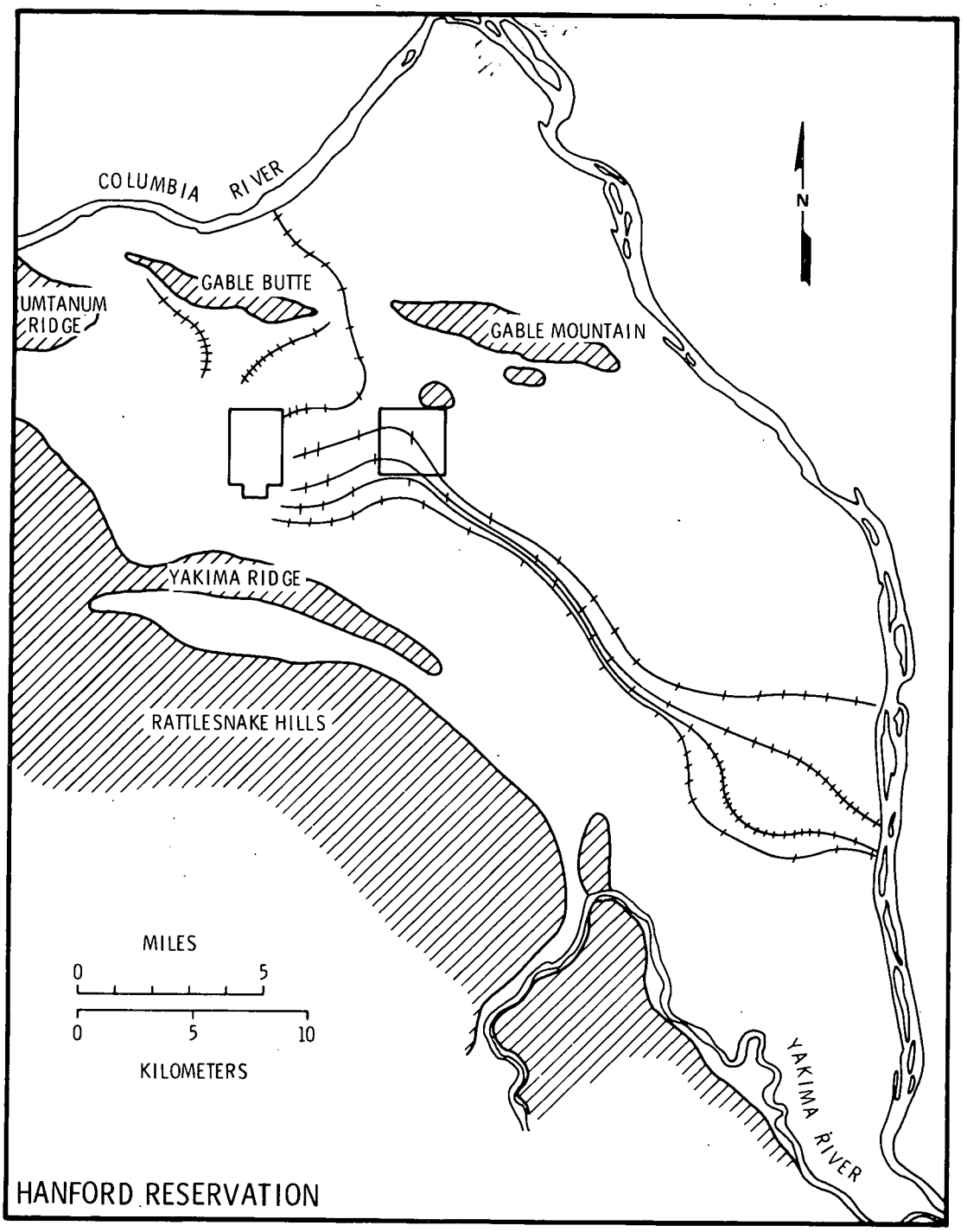

FIGURE E-2

PLOT OF THE STREAMLINES FOR 200 WEST AREA
ON THE 1980 POTENTIAL SURFACE

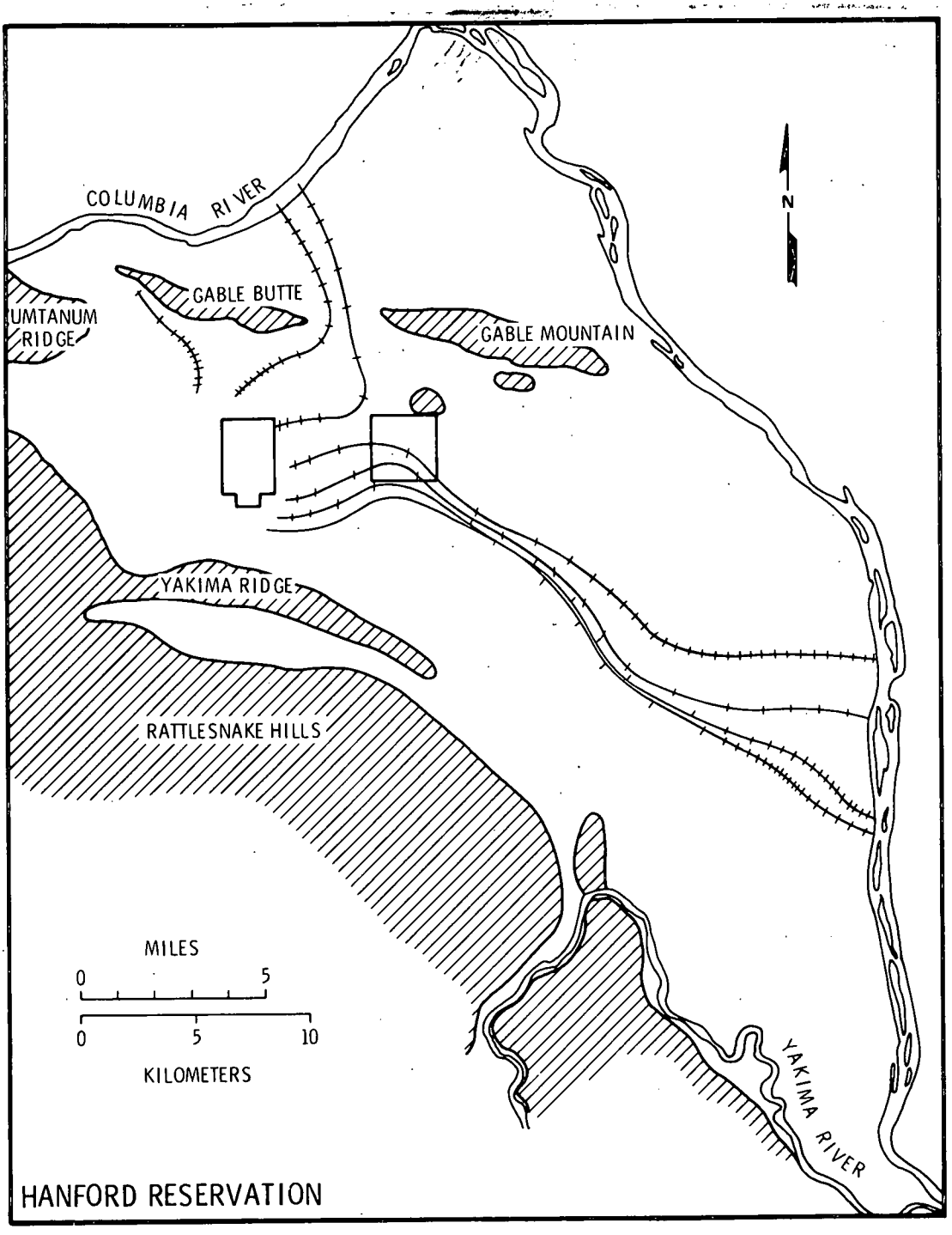

FIGURE E-3

PLOT OF THE STREAMLINES FOR 200 WEST AREA
ON THE 1985 POTENTIAL SURFACE

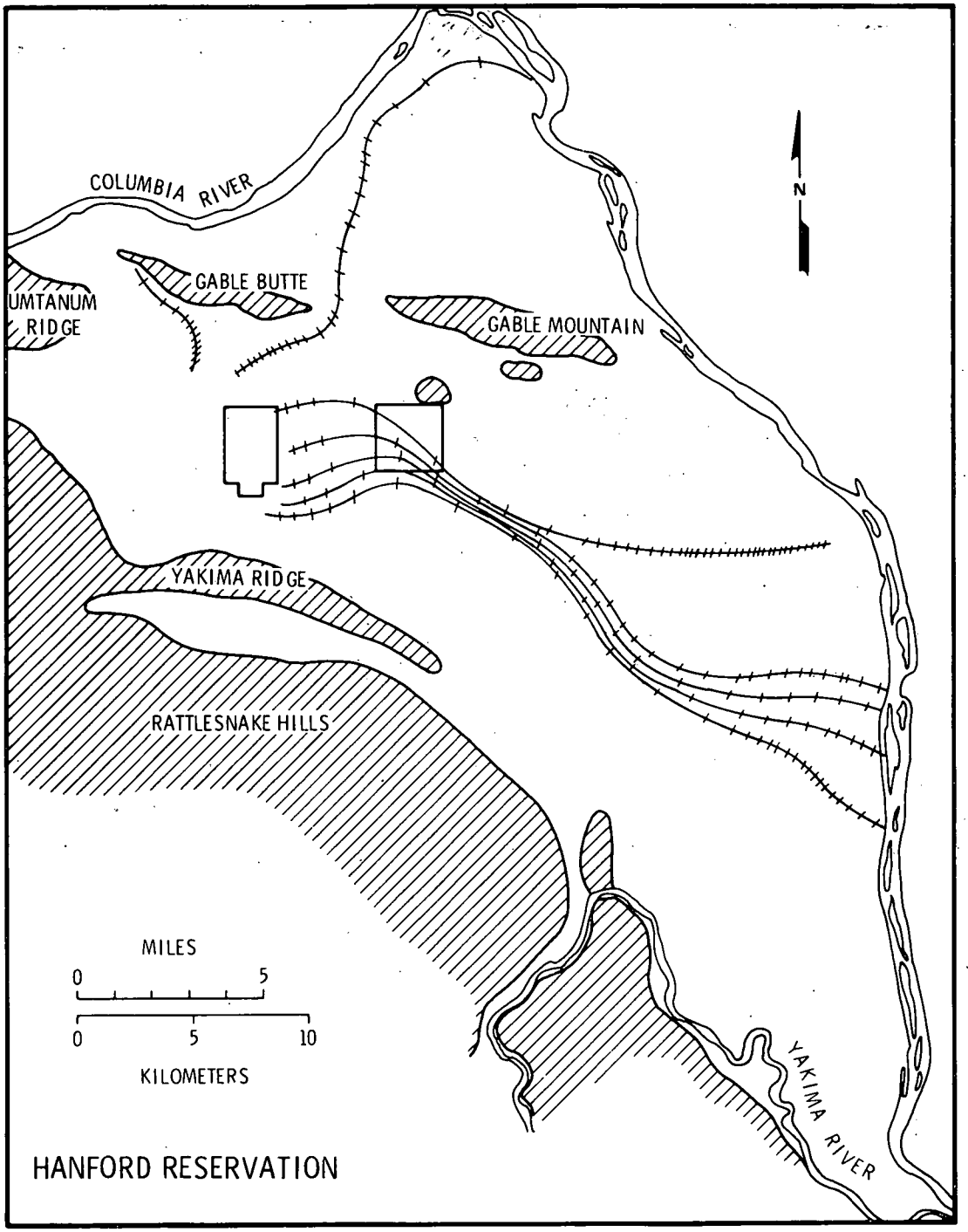

FIGURE E-4

PLOT OF THE STREAMLINES FOR 200 WEST AREA
ON THE 1990 POTENTIAL SURFACE

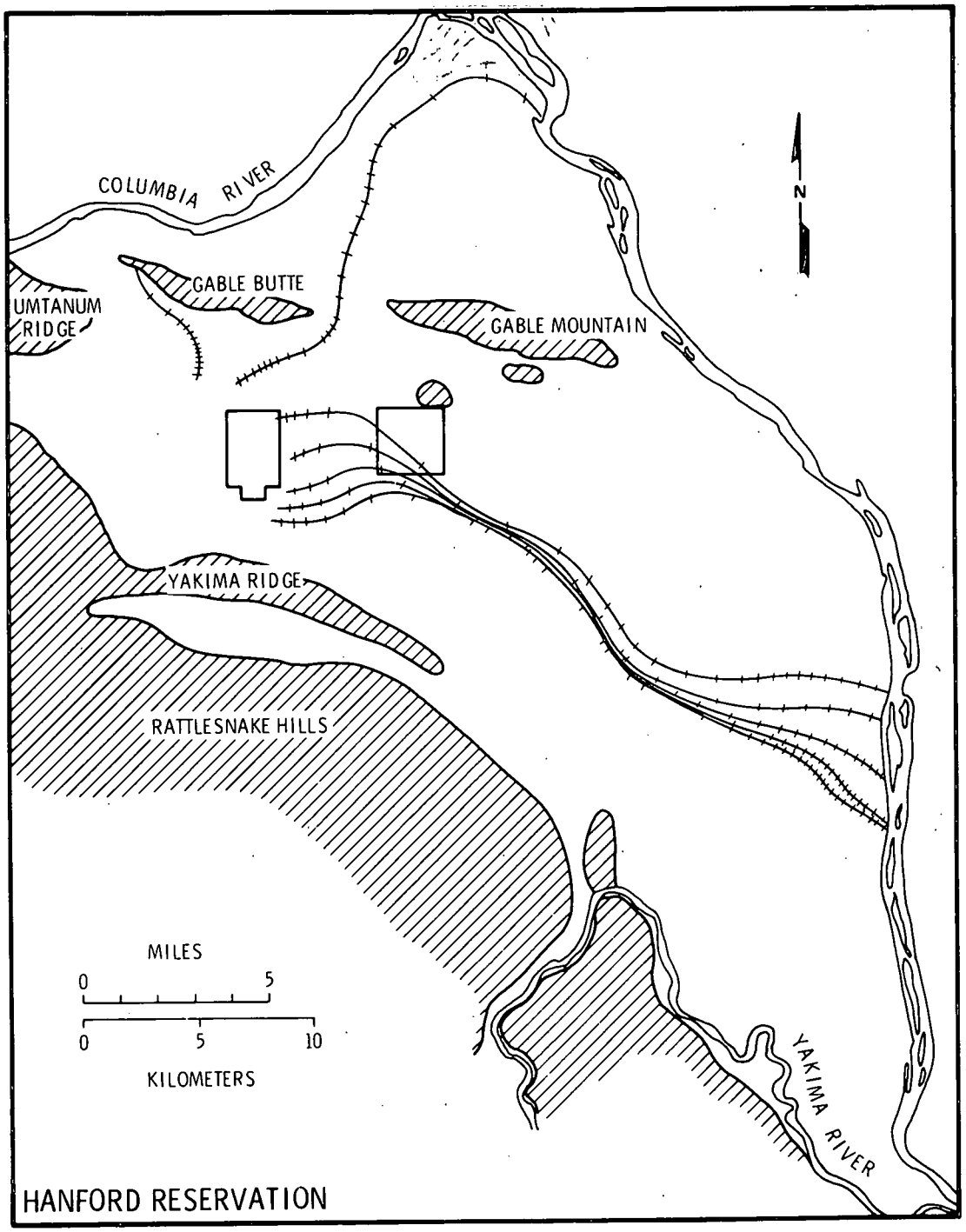

FIGURE E-5

PLOT OF THE STREAMLINES FOR 200 WEST AREA
ON THE 1995 POTENTIAL SURFACE

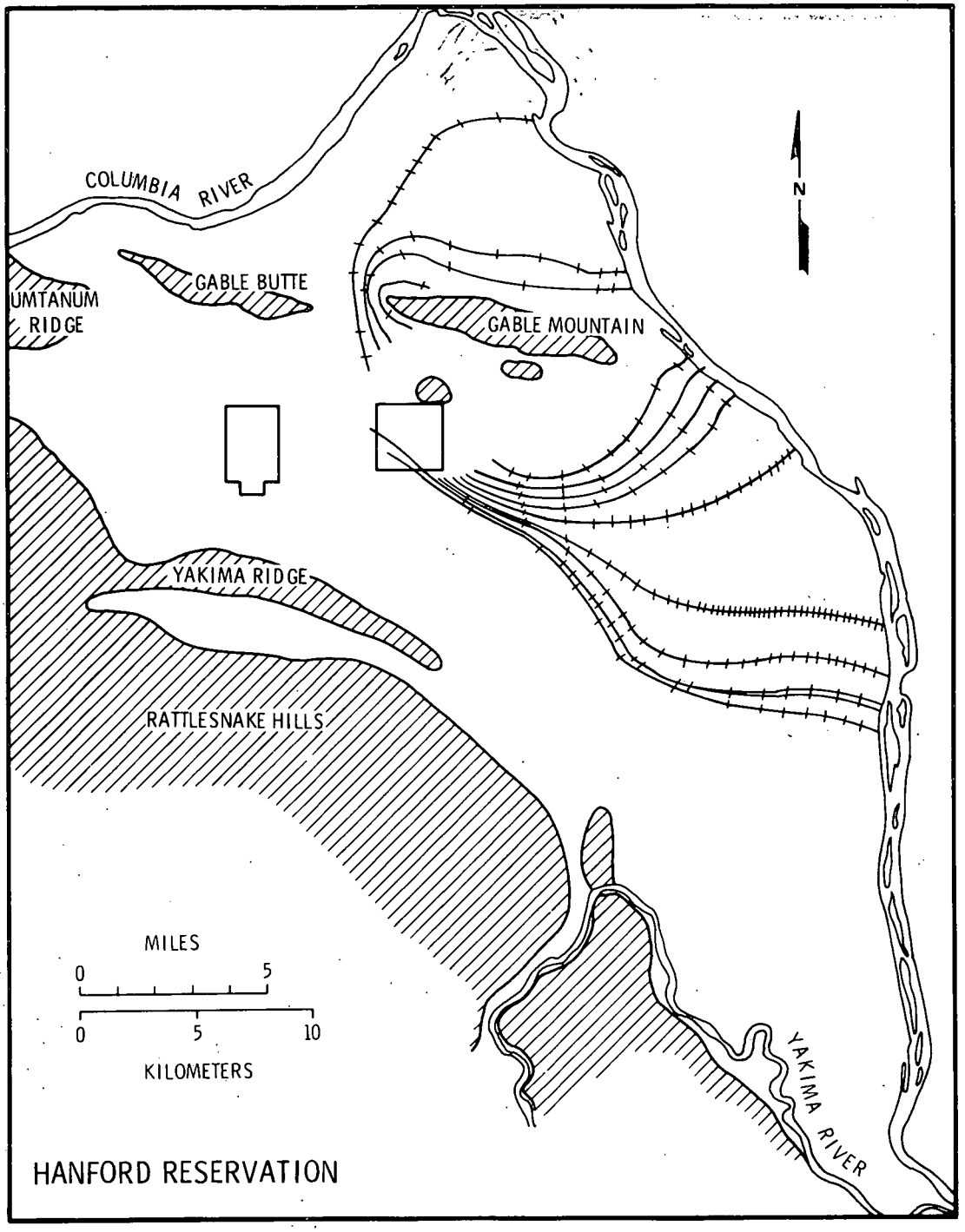

FIGURE E-6

PLOT OF THE STREAMLINES FOR 200 EAST AREA ON THE 1975 POTENTIAL SURFACE

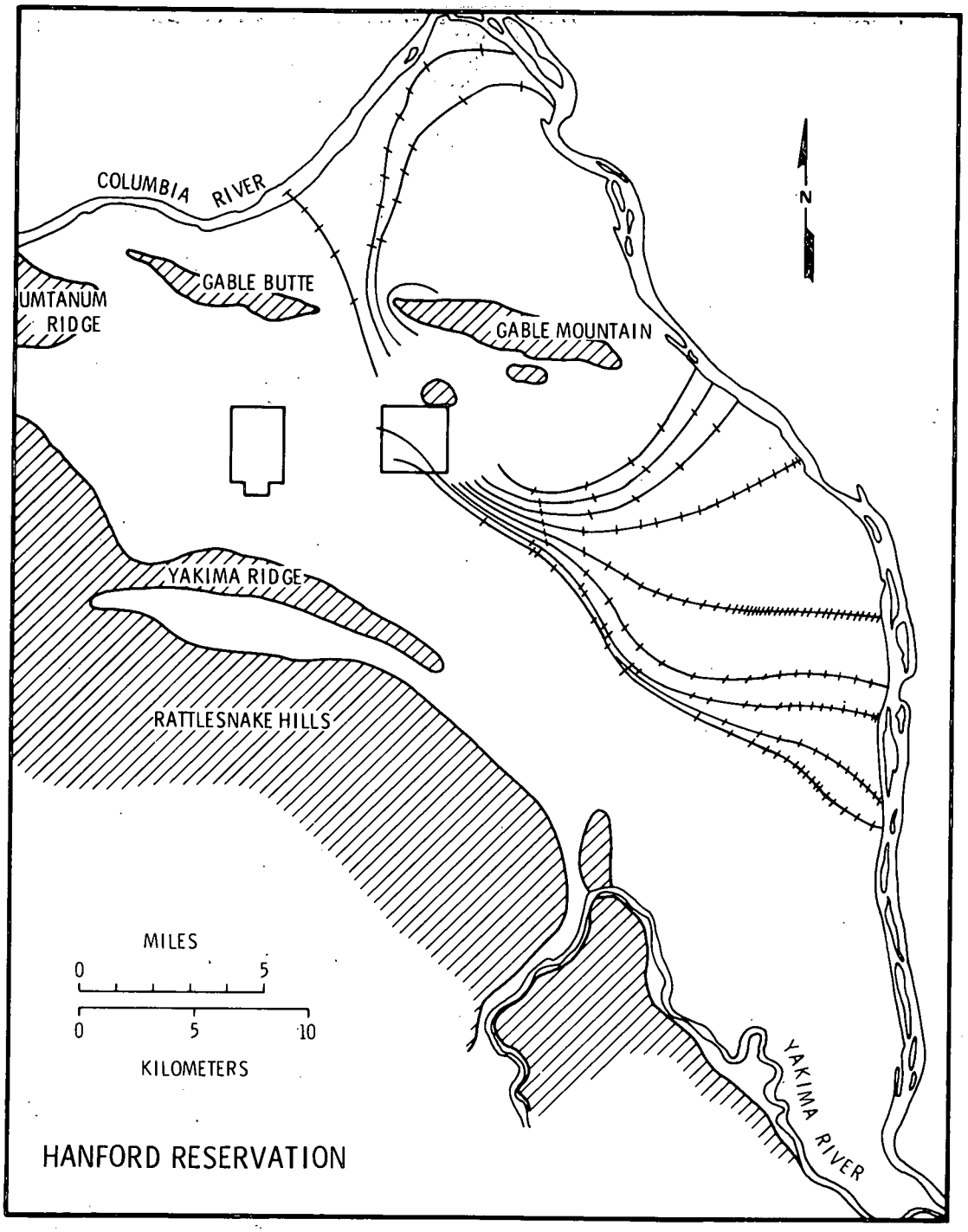

FIGURE E-7

PLOT OF THE STREAMLINES FOR 200 EAST AREA ON THE 1980 POTENTIAL SURFACE

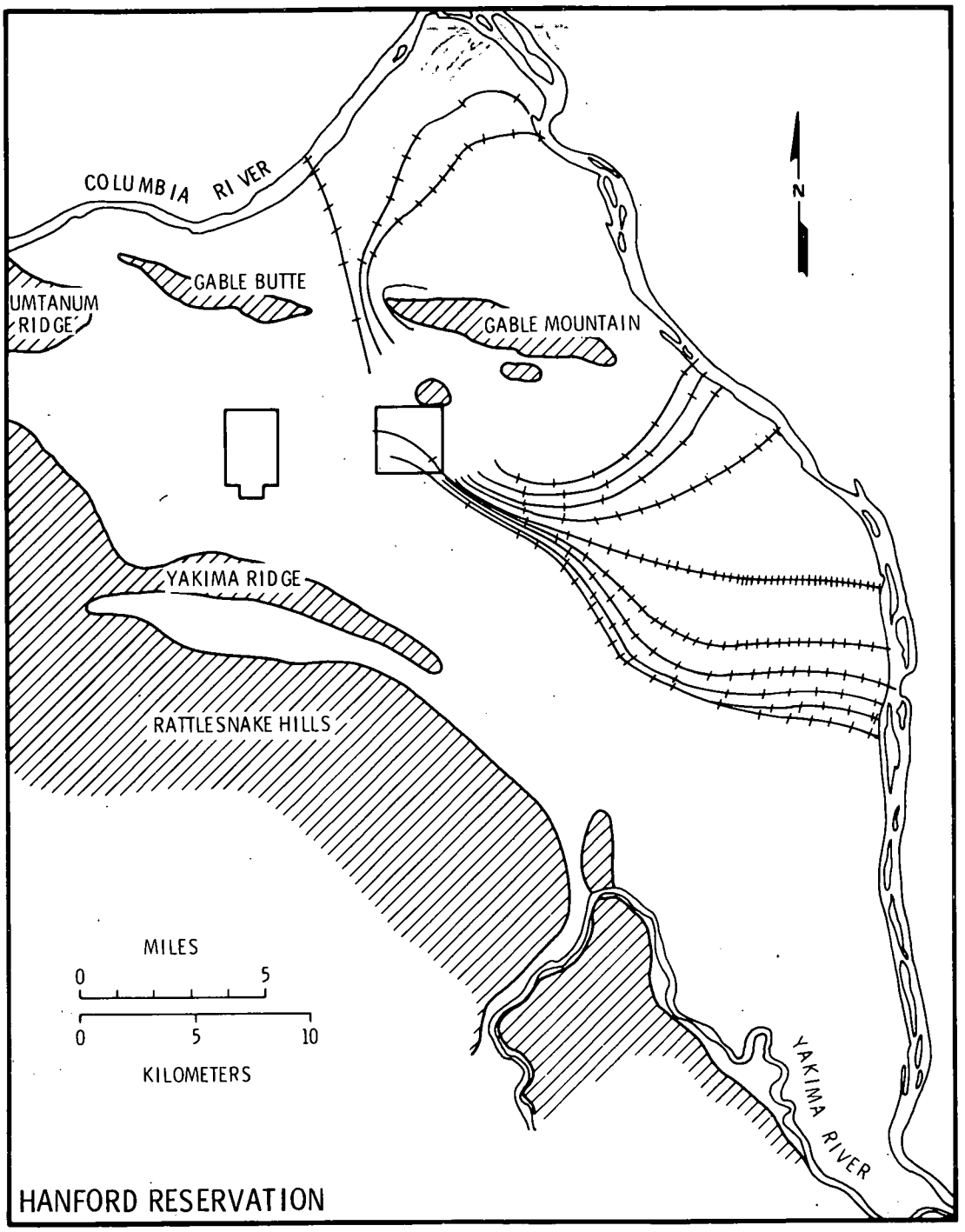

FIGURE E-8

PLOT OF THE STREAMLINES FOR 200 EAST AREA
ON THE 1985 POTENTIAL SURFACE

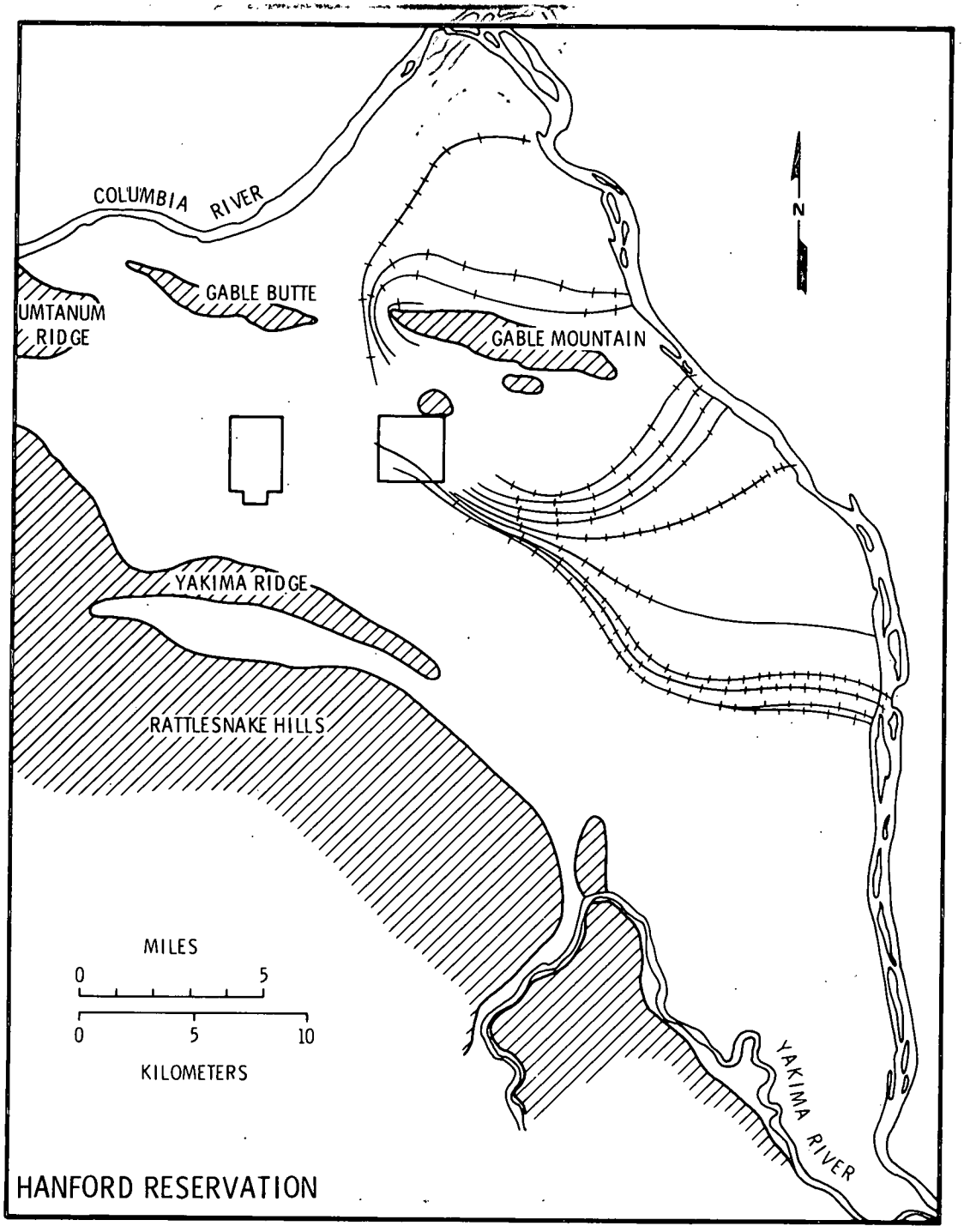

FIGURE E-9

PLOT OF THE STREAMLINES FOR 200 EAST AREA
ON THE 1990 POTENTIAL SURFACE

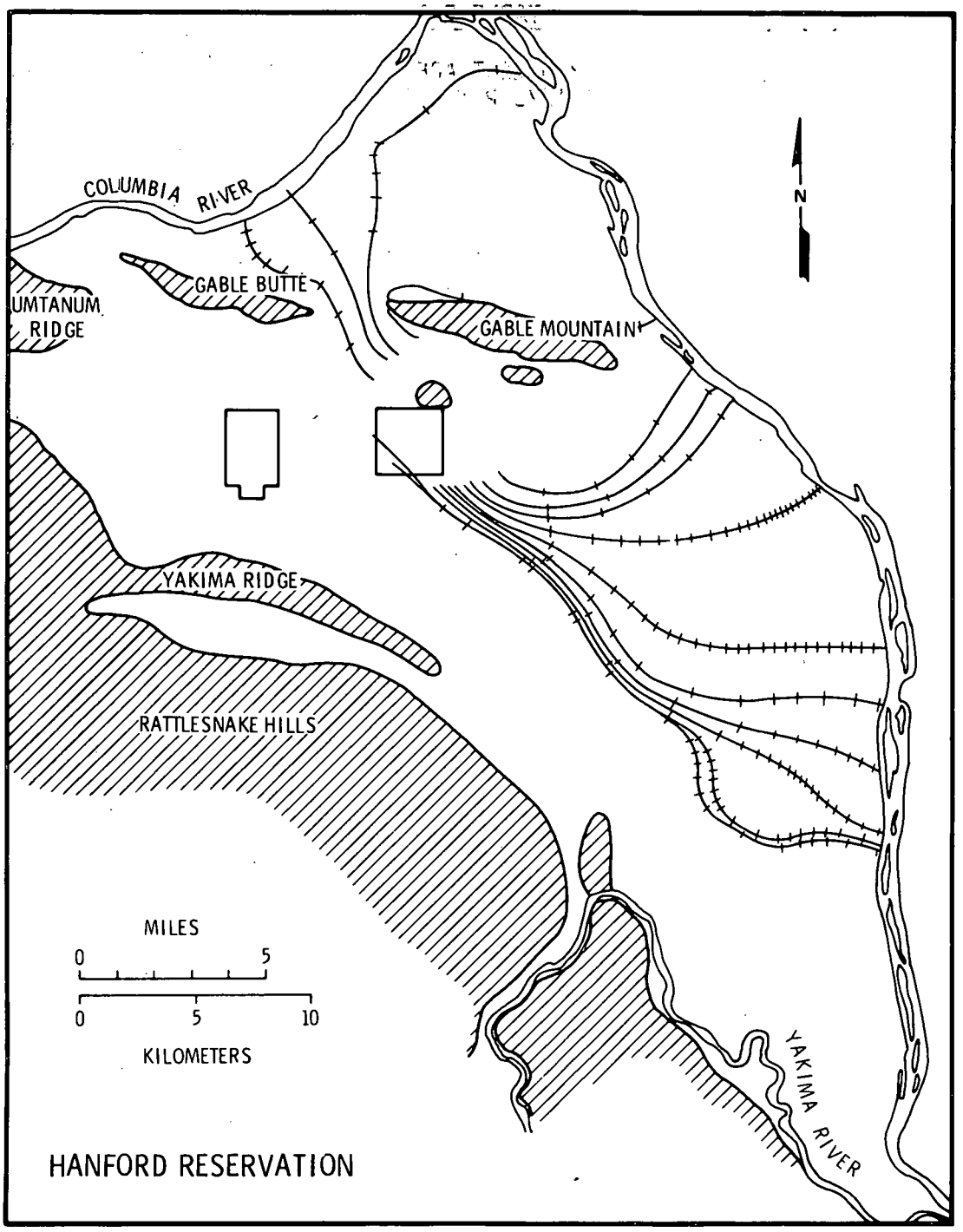

FIGURE E-10

PLOT OF THE STREAMLINES FOR 200 EAST AREA
ON THE 1995 POTENTIAL SURFACE

TABLE E-1

SUMMARY OF THE 200 WEST AREA STREAMLINE DATA
USING THE 1975 POTENTIAL SURFACE

Path-Streamline Number	Total Distance in Ft	Total Time in Days
1	112,630	33,410
2	111,834	29,810
3	111,362	34,220
4	110,935	44,300
5	112,048	68,780
6	15,043	19,900
7	17,239	25,660

Average Distance = 84,584
Average Time = 36,582

TABLE E-2

SUMMARY OF THE 200 WEST AREA STREAMLINE DATA
USING THE 1980 POTENTIAL SURFACE

Path-Streamline Number	Total Distance in Ft	Total Time in Days
1	111,958	36,830
2	109,975	58,160
3	104,574	42,608
4	101,583	31,520
5	42,991	24,690
6	15,285	17,740
7	16,986	23,500

Average Distance = 71,907
Average Time = 33,588

TABLE E-3

SUMMARY OF THE 200 WEST AREA STREAMLINE DATA
USING THE 1985 POTENTIAL SURFACE

Path-Streamline Number	Total Distance in Ft	Total Time in Days
1	106,284	57,980
2	104,750	49,610
3	99,244	29,360
4	97,120	61,130
5	46,551	22,970
6	36,718	35,920
7	17,715	23,770

Average Distance = 72,626
Average Time = 40,105

TABLE E-4

SUMMARY OF THE 200 WEST AREA STREAMLINE DATA
USING THE 1990 POTENTIAL SURFACE

Path-Streamline Number	Total Distance in Ft	Total Time in Days
1	115,691	59,240
2	100,358	38,000
3	98,119	32,150
4	99,325	45,740
5	84,028	89,930
6	70,672	51,310
7	17,462	26,200

Average Distance = 82,237
Average Time = 48,938

TABLE E-5

SUMMARY OF THE 200 WEST AREA STREAMLINE DATA
USING THE 1995 POTENTIAL SURFACE

Path-Streamline Number	Total Distance in Ft	Total Time in Days
1	105,712	60,500
2	104,369	55,550
3	100,554	43,490
4	98,303	32,330
5	102,977	48,440
6	71,795	54,010
7	17,590	28,540

Average Distance = 85,900
Average Time = 46,122

TABLE E-6

SUMMARY OF THE 200 EAST STREAMLINE DATA
FOR STREAMLINES USING THE 1975 POTENTIAL SURFACE

Path-Streamline Number	Total Distance in Ft	Total Time in Days
1	46,983	8,110
2	53,977	13,420
3	28,657	6,130
4	32,016	18,020
5	99,225	41,230
6	95,255	33,040
7	82,195	38,800
8	77,076	23,410
9	75,072	21,070
10	68,847	47,620
11	54,043	52,840
12	45,380	9,910
13	41,710	7,570
14	38,187	10,000

Average Distance = 59,902
Average Time = 23,655

TABLE E-7

SUMMARY OF THE 200 EAST STREAMLINE DATA
FOR STREAMLINES USING THE 1980 POTENTIAL SURFACE

Path-Streamline Number	Total Distance in Ft	Total Time in Days
1	15,982	1,630
2	53,664	12,430
3	55,035	15,310
4	29,850	9,190
5	87,363	20,620
6	89,003	39,340
7	80,115	31,960
8	75,231	18,550
9	74,154	33,760
10	64,899	59,680
11	51,412	28,900
12	44,387	10,360
13	41,600	8,110
14	38,438	9,820

Average Distance = 57,224
Average Time = 21,404

TABLE E-8

SUMMARY OF THE 200 EAST STREAMLINE DATA
FOR STREAMLINES USING THE 1985 POTENTIAL SURFACE

Path-Streamline Number	Total Distance in Ft	Total Time in Days
1	13,472	1,720
2	45,295	20,980
3	52,358	15,760
4	31,879	12,880
5	84,659	56,170
6	83,129	22,780
7	77,040	23,680
8	74,961	22,600
9	74,461	37,000
10	63,868	82,900
11	50,332	26,830
12	44,334	11,350
13	41,160	10,180
14	38,206	12,070

Average Distance = 55,368
Average Time = 25,492

TABLE E-9

SUMMARY OF THE 200 EAST STREAMLINE DATA
FOR STREAMLINES USING THE 1990 POTENTIAL SURFACE

Path-Streamline Number	Total Distance in Ft	Total Time in Days
1	12,211	2,440
2	47,763	10,090
3	50,997	16,120
4	50,644	22,330
5	86,701	46,180
6	82,609	25,030
7	76,238	24,490
8	75,839	36,010
9	66,118	69,760
10	52,507	38,440
11	45,759	14,230
12	42,907	11,620
13	40,751	11,530
14	37,596	16,210

Average Distance = 54,903
Average Time = 24,605

TABLE E-10

SUMMARY OF THE 200 EAST STREAMLINE DATA
FOR STREAMLINES USING THE 1995 POTENTIAL SURFACE

Path-Streamline Number	Total Distance in Ft	Total Time in Days
1	16,411	3,790
2	48,211	11,890
3	51,547	17,650
4	50,328	25,120
5	86,735	25,300
6	83,267	26,200
7	75,950	23,680
8	74,953	45,100
9	66,562	69,490
10	52,170	40,330
11	45,895	15,400
12	42,833	11,260
13	40,423	11,260
14	37,333	17,920

Average Distance = 55,187
Average Time = 24,599

DISTRIBUTION

No. of Copies

OFFSITE

UNITED STATES

J. Dieckouer
ERDA Division of Waste Management and Reprocessing Production
Washington, DC 20545

R. K. Heussar
ERDA Division of Waste Management and Reprocessing Production
Washington, DC 20545

D. E. Saire
ERDA Division of Waste Management and Reprocessing Production
Washington, DC 20545

A. H. Dahl
Chief, Environmental Science Branch
Energy Research and Development Administration
Idaho Falls, ID 83401

225 ERDA Technical Information Center

Y. Bachmat
Project Director
Holcomb Research Institute
Butler University
Indianapolis, IN 46208

T. F. Malone
Director
Holcomb Research Institute
Butler University
Indianapolis, IN 46208

No. of Copies

D. B. McWhorter
Department of Agricultural Engineering
Colorado State University
Fort Collins, CO 80523

W. H. Brutsaert
Cornell University
School of Civil Engineering
B22 Bailey Hall
Ithaca, NY 14850

M. R. Dusbabek
Fluor Engineers and Constructors, Inc.
Southern California Division
P. O. Box 11977
Santa Ana, CA 92711

K. Cartwright
Geologist and Head
Hydrogeology and Geophysics Section
Illinois State Geological Survey
Urbana, IL 61801

T. A. Prickett
Engineer
Illinois State Water Survey
Box 232
Urbana, IL 61801

R. B. Lantz
Executive Vice-President
Intera Environmental Consultants
1201 Dairy Ashford, Suite 200
Houston, TX 77079

No. of Copies

M. Wheeler
Division H8
Environmental Studies
Los Alamos Scientific Laboratory
Los Alamos, NM

J. Wilson
Parsons Laboratory for Water Resources and Hydrodynamics
Department of Civil Engineering
Building 48-209
Massachusetts Institute of Technology
Cambridge, MA 02139

L. Heindl
Executive Secretary
National Academy of Science
U.S. National Committee for the IHD
2101 Constitution Avenue
Washington, DC 20418

Technical Secretary
National Academy of Science
Committee on Radioactive Waste Management
National Research Council
2101 Constitution Avenue
Washington, DC 20418

F. N. Frenkiel
Computation and Mathematics Department
Naval Ship Research and Development Center
Bethesda, MD 20084

P. J. Wierenga
New Mexico State University
Department of Agronomy
P. O. Box 30
Las Cruces, NM 88001

No. of Copies

R. L. Bullard
Chief, Environmental Specialist Branch
Nuclear Regulatory Commission
Directorate of Regulation
7920 Norfolk Avenue
Bethesda, MD 20014

W. Gamill
Chief, Site Analysis Branch
Nuclear Regulatory Commission
Directorate of Regulation
7920 Norfolk Avenue
Bethesda, MD 20014

G. F. Pinder
Princeton University
Department of Civil and Geological Engineering
Princeton, NJ 08540

J. W. Keely
Chief, Subsurface Environmental Research Branch
Robert S. Kerr Research Lab
P. O. 1198
Ada, OK 74820

I. Remson
Professor of Geology
Stanford University
Stanford, CA 94305

C. Wheeler
State Engineer
State of Oregon
516 Public Service Bldg.
Salem, OR 97310

E. Wallace
Supervisor Water Resources Division
State of Washington
Department of Ecology
Olympia, WA 98501

No. of Copies

D. L. Shaeffer
Environmental Sciences Division
Union Carbide Corporation
Oak Ridge National Laboratory
Oak Ridge, TN 37830

L. F. Konikow
U.S. Geological Survey
Mail Stop 413
P. O. Box 25046
Federal Center
Denver, CO 80225

G. Debuchananne
Director
U.S. Geological Survey
2100 M. Street
Washington, DC 20037

J. D. Bredehoeft
U.S. Geological Survey
Water Resources Division
Reston, VA 22092

S. P. Neuman
Hydrology and Water Resources Department
University of Arizona
Rucson, AR 85721

P. A. Witherspoon
Department of Civil Engineering
University of California
Berkeley, CA 94720

J. N. Luthin
University of California, Davis
Department of Water Sciences and Engineering
Davis, CA 95616

J. Milliman
Department of Economics
University of Florida
Gainesville, FL 32601

No. of Copies

P. Domenico
Department of Geology
University of Illinois
Urbana, IL 61801

V. Te Chow
Hydrosystems Laboratories
University of Illinois
Urbana, IL 61801

F. L. Parker
Vanderbilt University
Nashville, TN 37203

D. S. Desai
Professor
Department of Civil Engineering
V.P.I. and S.U.
Blacksburg, VA 24061

J. Crosby
Geologist
Washington State Water Research Center
Pullman, WA 99163

FOREIGN

J. P. Philip, Chief
Division of Environmental Mechanics - CSIRO
P. O. Box 821
Canberra City A.C.T. 2601
Australia

T. Munn
Atmospheric Environment Service
4905 Dufferin Street
Downsview, Ontario
Canada N3H 5T4

F. W. Schwartz
Department of Geology
University of Alberta
Edmonton, Canada

No. of Copies

R. A. Freeze
Department of Geology
University of British Columbia
Vancouver, B.C.
Canada

E. O. Frind
Department of Earth Sciences
University of Waterloo
Waterloo, Ontario
Canada

Ghislain de Marsily
Directeur de Centre
d'Informatique
Geologique
Ecole National Superieure
des Mines de Paris
35, Rue Saint-Honore
77305 Fontainebleau
France

Jehoshua Schwarz
Tahal - Consulting Engineering
Ltd.
P. O. Box 11170
Tel Aviv, Israel

Jacob Bear
Professor, Vice President for
Academic Affairs
Department of Civil Engineering
Technion, Israel Inst. of
Technology
Haifa, Israel

R. G. Thomas
Senior Officer (Water Resources)
Land and Water Development
Division
Food and Agriculture
Organization of the
United Nations
Via delle Terme di Caracalla
00100 - Rome
Italy

No. of Copies

Tatsuo Shibaskai
Consulting Geologist
Group Leader of Research Group
for Water Balance
182 Fujigane
Tsurugashima, Saitama 350-02
Japan

German E. Figueroa Vega
Director de Aguas Subterraneas
Y Superficiales
Comision de Aguas del Valle
de Mexico
Balderas 55
Mexico, D.F.

Luis Lopez Garcia
INTECSA
Apartado 13104
Condesa de Venadito 1
Madrid 27, Sapin

ONSITE

Rockwell Hanford Operations

4 R. C. Arnett
H. Babad
R. G. Baca
G. S. Barney
D. J. Brown
D. J. Cockeram
R. A. Deju
R. D. Fox
R. E. Gephart
R. J. Gimera
D. R. Gustavson
R. E. Isaacson
A. G. Law
R. Y. Lyon
C. W. Manry
P. F. Mercier
J. V. Panesko
W. H. Price
I. E. Reep

No. of Copies

B. H. Richards
F. A. Spane
D. D. Wodrich
6 Rockwell Document Control

DOE Richland Operations Office
O. J. Elgert
J. A. Fernandez
R. E. Gerton
R. B. Goranson
M. W. Tiernan

Battelle-Northwest
H. C. Burkholder
D. B. Cearlock
C. R. Cole
J. R. Eliason
4 D. R. Friedrichs
D. A. Myers
J. R. Raymond
A. E. Reisenauer

United Nuclear Industries, Inc.
1 A. L. Cucchiara

Westinghouse Hanford Company
1 R. B. Hall

Boeing Computer Services, Richland
1 R. W. Nelson